Department of Precision and Microsystems Engineering
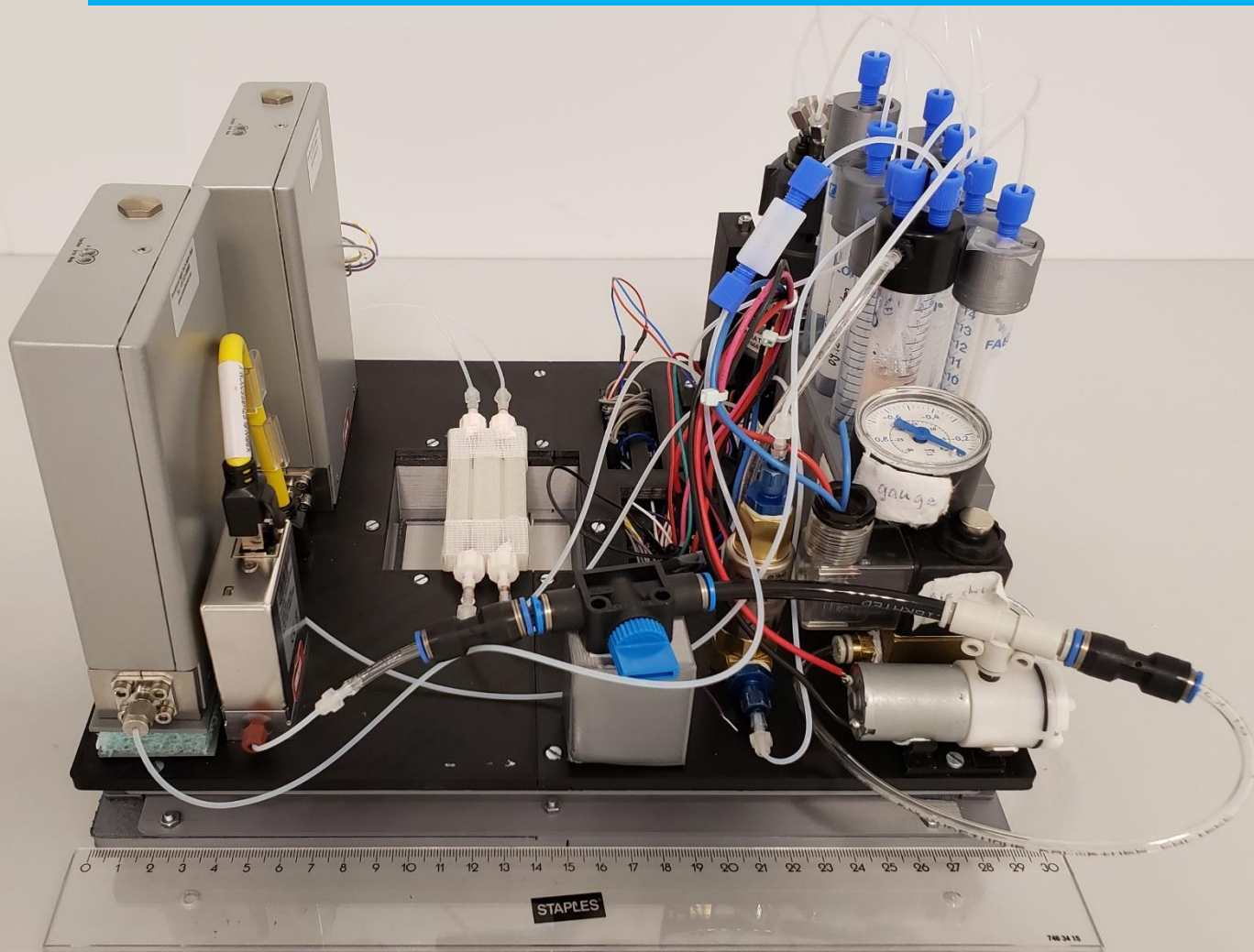
Portable and Integrated Organ-On-Chip Platform Using Off-the-shelf Components

Haoyu Zhu

TU**Delft** Delft University of Technology

Challenge the future

Portable and Integrated Organ-On-Chip Platform Using Off-the-shelf Components

Master's Thesis

by

Haoyu Zhu

in partial fulfilment of the requirements for the degree of

Master of Science
in Mechanical Enginnering

at the Delft University of Technology

Student number:	4861272	
Supervisor:	Dr. Murali K Ghatkesar,	TU Delft
Daily Supervisor:	Ir. Gürhan Özkayar,	TU Delft
Chair:	Prof.Dr.Ir. Joost Lötters,	TU Delft
External:	Dr. Ir. Massimo Mastrangeli,	TU Delft
	Dr. Ir. Pouyan Boukany,	TU Delft

Date of submission: September 8, 2020

TUDelft

Contents

List of Figures

List of Tables

1

Introduction

Organ-On-Chip is a biomimetic system that can mimic the environment of a physiological organ, by regulating key parameters including concentration gradients, shear force, cell patterning, tissue-boundaries, and tissue–organ interactions. As a vital branch of micro-technology, Organ-On-Chip (OOC) has been regarded as one of the most potential research field for its revolutionary contribution in biomedical field[1]. Microfluidic technology plays a vital role in the development of OOC, which is an important factor to distinguish OOC from conventional cell culture system. Among various advantages (Physiological environment, precise manipulation of cells, better integration with microdevices, low consumption of media, generating mechanical signals, etc.) created by microfluidic technology, the flow rate plays a significant role since they may create precise physiologic factors such as shear stress which is important for cell culture[2–4]. In other words, microflows that do not meet the experimental requirements, such as pulsed flow or flows with bubbles or plugs may influence the output of experiments, even cause damage and death of cells[5, 6]. Thus, providing a suitable flow for OOC experiments is closely related to the success of the experiment.
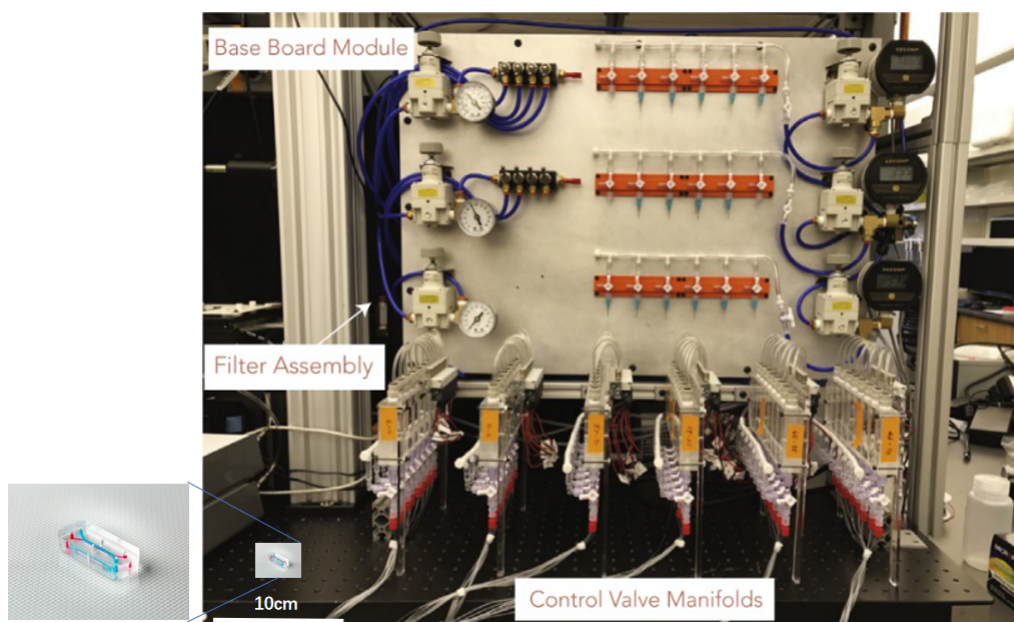
Figure 1.1: A microfluidic control system consisting of flow network and control components[7]. Additionally there are pumps that are not shown in the figure. Inset on the bottom left shows the actual microfluidic chip size compared to the external fluid control peripheral system.

In microfluidic applications, an OOC platform can be understood as a flow control system with integrated OOC interconnections which has the capacity to generate flows used for OOC experiments. It

is not easy as imagine to provide microflow with high accuracy and support OOC experiments. Pumps, valves, sensors are mandatory components that should be involved in a flow control system while most of them have large foot-print[7]. See Figure 1.1 for the comparison between the control system and microfluidic chip itself. It is not hard to imagine how bulky flow control systems bring inconvenience to OOC experiments. Not only is the location of the experiment fixed, but for different types of experiments, the modification of equipment has become a tough work.

To sum up, the general problems in flow control system for OOC applications are:

• Bulky off-the-shelf components and incompact design lead to inconvenient experiments and large reagent consumption [7–10].

• Quality of flows generated by instrument is not high enough to support OOC experiments [11, 12].

• Because of their fixed functions, it is difficult for the same system to be applied to different Organ-On-Chip models.

• Incompatibility of microscopes and incubators leads to the tedious process of chip disassembly and reassembly during experiments which risks the introduction of bubbles.

In general, there are several possible factors that lead to the bulky problem of conventional flow control systems: bulky components, duplicate modules, incompact architecture, lumpish control and monitor system. All of these can be solved by design, selection, architecture of a microfluidic handling system. Thus, designing and fabricating a portable, multi-functional flow control system with high flow control performance is significant to the development of OOC technology.

In this report, the literature survey and design proposal of Organ-On-Chips and their fluidic handling systems will be introduced in chapter 2. In chapter 3, a paper related to the topic is presented to show the construction and performance of the entire system. Next, the conclusion is made in chapter 4 based on results shown in chapter 3. The details of the author's personal scientific pursuit while executing this thesis work is presented in chapter 5 which is also regarded as a reflection chapter. The supplementary materials which are important for research in next phases are listed in the Appendix.

2

Literature Survey on Organ-On-Chip Platforms

This chapter consists of an exploration of existing literature regarding Organ-on-chip technology, microfluidic platforms and off-the-shelf microfluidic components and attempts to find a research gap that can be answered in a subsequent thesis.

2.1. Organ-On-Chip

Over the last thirty years, microfluidic technology has rapidly developed and created great opportunities in biomedical and biotechnology fields[14]. One of the most significant application is Organ-On-a-Chip (OOC), which simulates physiological functions of organs or organ systems by inhabiting living cells in microchannels and providing continuous flow for cell culture[15]. The contribution of on-chip organs to bio-medicine is mainly concentrated in *in vitro* drug experiments. Unlike *in vivo* experiments, OOCs can realize high-efficiency tests of drugs, and simultaneously avoid deviation caused by biological differences in animal experiments. For instance, as shown in Figure 2.1, when observing and detecting the effect of drugs on cancer cell metastasis, researchers apply *in vivo* tests by introducing pathogens and nanosensors into mice to obtain a series of physiological response characteristics in lymph node, lung, etc.. This not only consumes a lot of resources but also makes it difficult to verify the accuracy of the results due to the difference between physiological environment of animal and human. With the help of OOC, human cells can be cultured in microchannels and microfluidic technology can create a physiological environment closer to the human body environment.

Furthermore, with the assistance of microfluidic technology, OOC can better simulate the physiological environment of human beings. Compared with conventional cell culture technologies such as 2D and 3D culture, microfluidic cell culture system has various advantages. First, microchannels and micro flows allow more precise manipulation of cells, even of single cells, which cannot be realized by conventional culture technologies[16]. Second, microfluidic platform can provide better simulation of physiology environment in human bodies with micro flows and cyclic strains created by vacuum chambers[17]. Third, since flow at micro-level intends to perform a laminar behavior, it is more convenient to precisely control the parameters of physiological environment[18]. Last, culturing several types of cells in one single chip with different channels is realistic, which means organ systems can be created by connecting several "organs". This can not only increase the throughput of bio-experiments but also realize some physiology systems such as "Human-On-a-Chip" that cannot be imagined in the past[19].

2.1.1. Significant OOC implementation

Due to the development of Organ-On-Chip technology, researchers have not been satisfied with simulating only the fluid environment in the body, but have promoted the types of organs that can be simulated by mimicking the mechanical environment[18]. Furthermore, in order to simulate special organs such as heart and brain, researchers have integrated microelectrodes into the chip to make pacing or create electric signals[20, 21].
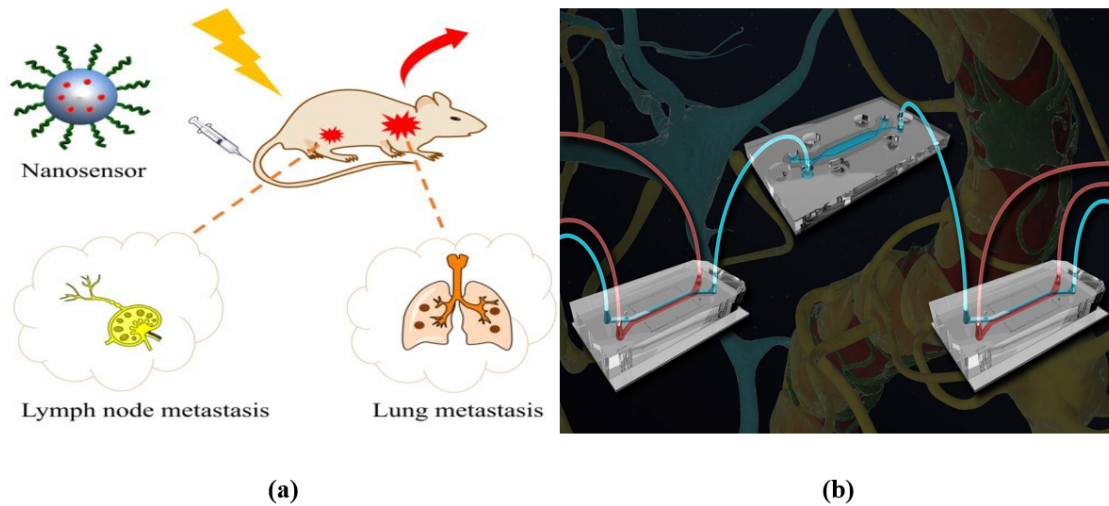
Figure 2.1: *In vivo* to *in vitro*: The application of OOC[13]. (a) The *In vivo* drug experiment is to annotate the sample in mice, and observe its reaction with nanosensors. (b) Organs-On-Chip can be realized by connecting different Organ-On-Chip models orderly, which can be regarded as the latest *in vitro* technology with great perspective

Thus, the OOC platforms involved in these existing or prospective experiments should not only provide accurate flow, but also integrate unconventional functions to satisfy state-of-the-art research in biomedical fields. Before analyzing the flow and function requirements of OOC experiments, it is necessary to have an overview of the development in this field and get the insight of both conventional and unconventional, representative designs.

In brief, there is a general trend of development in OOC field, which is 'Simplified organ, Physiological organ, Complicated organ system'. The first two categories can be classified into 'single-organ system' while complicated organ system is also called 'multi-organ system'[22].

The research of OOC usually starts with the simplest cell culture, pharmacology and pathology tests. Therefore, the early *in vitro* culture models of OOC are mostly composed of simple structure and relatively simpler functions. Figure 2.2(a) illustrates a Liver-On-Chip model built by Amedeo Carraro, et al.(2008)[23] The model mimics the *in vitro* physiological environment of hepatic cells by introducing a number of intrinsic microvascular-based channels. The breakthrough of this novel design is the application of microvascular channels which better mimics the *in vivo* vascular environment compared to other designs. The device can culture both primary rat hepatocytes and human hepatoma cells by providing *in vitro* medium continuously, which allows proliferation and maintaining hepatic functions such as metabolism and serum protein synthesis on the basis bi-layer design by introducing a porous membrane to protect cells from large shear stress. This model can be regarded as a single-organ system.

Figure 2.2(b) shows a typical example of a multi-organ system, which is used for PK/PD modeling. This model is based on a mathematical pharmacokinetics (PK) model[24, 25] and it is widely used in the study of adsorption, distribution, metabolism, elimination and toxicity (ADMET) of chemicals *in vitro* rather than *in vivo* at present[26–28]. In this model, multiple culture chambers representing different organs (e.g., liver, lung, fat, tumor, marrow) are connected and integrated on a single chip in an order that simulates the physiological and systematic environment *in vivo*. Nevertheless, this device has two drawbacks. First, The chambers are close to each other which does not occur in real organ systems with long blood flow path. Second, the cells on chambers may not fully differentiate, which will influence the experimental results[29]. Thus, one of the most potential directions of OOC device is creating 'Human-On-Chip(HOC)' that better mimics the physiological environment in human bodies.

2.1.2. Experimental requirements of Organ-On-Chip

In most OOC experiments, smooth flow is always more popular. Thus, conventional peristaltic pumps are not acceptable in OOC research[30]. Furthermore, More functions are introduced to OOC devices to fulfill physiological behavior such as breathing. Since the cell types varies a lot in present research, the study of flow types are also significant.
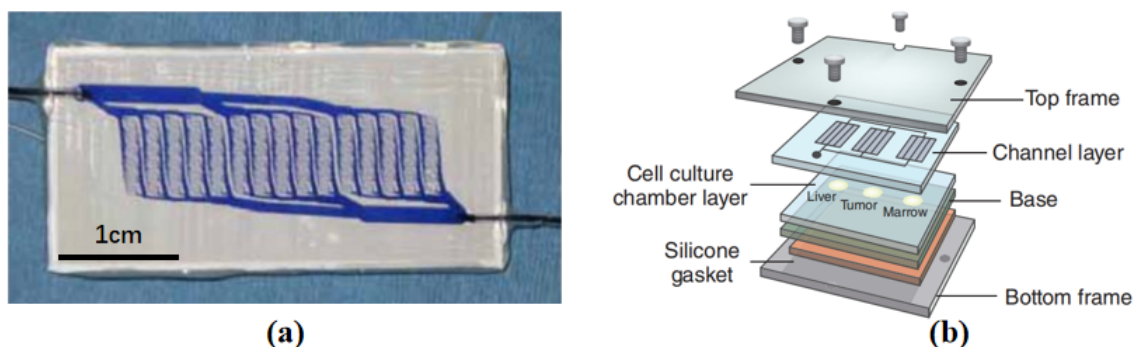
Figure 2.2: (a) Liver-on-chip model with microvascular channels[23], (b) Microfluidic chip based on pharmacokinetics and pharmacodynamics model[24, 25].

A. Flow type requirements

The most widely used flow in Organ-On-Chip research is growth media. They can be divided into six categories: Cultural media, Minimal media, Selective media, Differential media, Transport media and Indicator media, which contain nutrients needed by cells[31]. The second kind of liquid flow involved in OOC is artificial blood made from serum and other required nutrients, which is used to closer mimic the physiologic environment in human body[32]. Bacterium or drugs might also be added if some pathological and pharmacological analysis are needed. Although there are a large amount of growth media that involved in OOC experiments, it is lucky that most of them have similar flow characteristics and can be driven by most common pumping systems. However, since the viscosity factor widely ranges among these media, some pumping systems may not have the capacity to drive them in high flow rate, which should be a criterion for scheme selection in the following chapters.

In addition to liquid flow, gas flow is also more and more introduced into OOC experiments in new generation. With the increase of simulated organ types, simulation of some cells exposed to air is also particularly significant. The interaction behavior between liquid and air surfaces also aroused the interest of researchers. Divya D. et al. have developed a Lung-On-Chip device for lung-specific functional studies at the air-liquid interface[33]. As Figure 2.3(a) shows, the device is composed of two culture wells and one liquid channel, providing an air interface by combining microfluidic and suspended membrane culture systems. The device can be used to compare the efficacy of the hybrid system and the conventional platform by analyzing the function and integrity of A549 alveolar epithelial cell monolayer culture. During the experiment, flow is sent from inlet to outlet through the microchannels beneath two wells. Since wells have the capacity to accumulate culture media, a liquid-gas interface can be formed around the cells on membrane. In order to support such an experiment, single-channel liquid transportation is essential.

The third kind of flow is vacuum, which becomes more popular in recent OOC research due to its ability to create deflection or strains on soft materials. The mechanical signal created by vacuum can create novel functions for different types of cells to intermittently combine and separate to achieve non-interfering cultivation and interactive work of different cells in the same device[34].

Another novel application of vacuum is simulating physiological movement of alveoli. Figure 2.3(b) shows a Lung-On-Chip device (Huh, et al. 2010) mimicking the alveolar motion while breathing which can be used to obtain more accurate pharmacological and pathological conclusions in the Lung-On-Chip experiments due to cyclic strain created by periodic vacuum conditions[35, 36]. There are three kinds of inlets and outlets integrated on this chip, transporting culture media, gas and creating vacuum respectively. In the middle part of the cross-section, the upper channel contains gas while the lower one contains liquid, which simulates two sides of alveolar epithelium and endothelial cells. The middle porous membrane can be stretched by vacuum application on channels at two sides and the stretching frequency is similar to the frequency of human breathing (0.2Hz). In order to support this experiment, not only gas and liquid delivery system should be integrated, but also components (such as syringes) creating vacuum need to be added.

It is worth noticing that both liquid and air flows are introduced into this device, which indicates the representativeness of this device in OOC field.
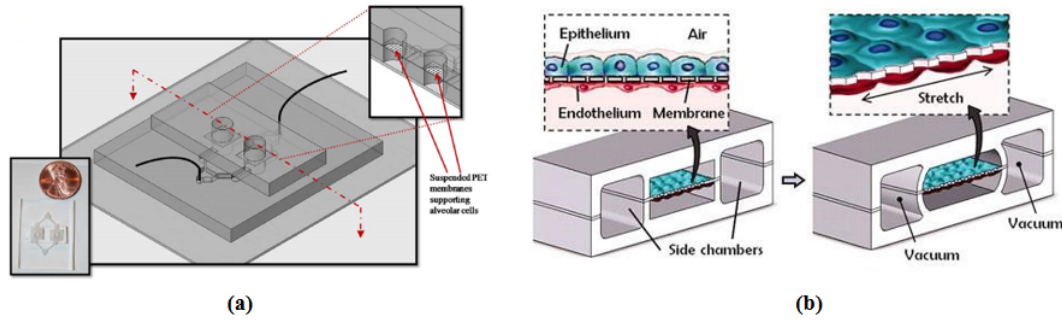
Figure 2.3: OOC models: (a) Study of air-liquid interface[33]. Live cells are deposited on the upper side of the membrane to form a similar physiological environment of alveolus. (b) Breathing Lung-On-Chip[35]. Cyclic vacuum is applied to the side chamber to mimic the breathing motion by stretching the middle membrane deposited with alveolus cells under a certain frequency ($\approx$0.2 Hz).

Table 2.1: Flow rates involved in distinguished OOC experiments

OOC category	Lung-On-Chip	Gut-On-Chip	Liver-On-Chip	Kidney-On-Chip
Flow rate[μL/min]	0.1-8.33	0.17-15	0.17-500	0.12-12
	[5, 43–45]	[46–49]	[23, 50–54]	[55–57]
OOC category	Vessel-on-chip	Multi-organ system	Bio-microfluidics	
Flow rate [μL/min]	0.0045-50	0.51-200	2-12000	
	[58–61]	[42, 54, 58, 62–64]	[65–67]	

B. Flow rate requirements

The flow rate provided by the microfluidic platform is one of the most fundamental characteristics. Wide flow range means that the instrument can be applied to more types of OOC experiments.

There are lots of evidence about the flow rate applied in OOC experiments in literature. In order to get an estimation of flow range required from our platform, several factors affecting flow rate in organ on chip research are extracted and summarized.

Shear stress is the most important factor caused by flow rate. Since most flow involved in OOC research can be regarded as laminar flow, shear stress at the wall can be calculated by using Newton's second law, $\tau_w = -\eta(\frac{du}{dz})$, where τ_w [dyn cm^{-2}] is the shear stress at the wall, u is the flow velocity, and z is the position within the height of the microchannel[37]. If the microchannel is designed with a high aspect ratio, which means $h << w$, the relation between flow rate and shear stress at the wall can be simplified as[38, 39]:

$$\tau_w \approx \frac{h}{2}\frac{\Delta p}{L} = \frac{6\eta Q}{wh^2} \tag{2.1}$$

It is apparent that shear stress is proportional to flow rate and is inversely proportional to the square of the height and width of the flow channel.

Shear stress caused by laminar flow in microchannels has a high correlation with cell differentiation, cell adhesion and live-dead ratio of cells. Some studies have shown that higher shear stress is beneficial to cell differentiation on the premise of ensuring that cells will not die due to excessive shear stress[40]. Lower flow rate can form a better physiological environment for cell adhesion[41]. The experiment from a Liver-On-Chip model built by Carraro, et al. (2008)[23] revealed that a flow rate of 8 μL/min led to best live-dead ratio of hepatic cells cultured in organ chip. In addition to shear stress on cells, flow rate also has significant impact on compound mixing and saving samples used for following procedures[42]. Furthermore, lower flow rate is also beneficial to chemical penetration in pharmacological analysis.

In order to analyze the flow rate that the OOC platform needs to provide more comprehensively and

rigorously, different flow rate data are extracted from several typical OOC experiments. Haan, et al. developed a digestion system on chip by integrating mouth, stomach, intestine models in one system. The lowest flow rate applied in the system was 1μL/min (Sample) while highest flow rate was 12 μL/min (Duodenal Duice), as shown in Figure 2.4[42]. Benam, et al. applied 1μL/min flow to the analysis of organ-level lung pathophysiology *in vitro* in 2016[68]. Dongeun Huh et al.(2017) used 0.25μL/min - 0.42μL/min flow for cellular-level lung injury analysis[5]. Shanshan Wang, et al.(2013) developed a 3D microfluidic model to Study invadopodia formation for lung carcinoma invasion. In the experiment, drug solution and culture media were perfused in a rate of 0.1 μL/min by a syringe pumping system[43].

Since the desired OOC platform should satisfy as many as OOC experiments at present or in the future, most distinguished literature about OOC research has been screened out and the flow rate involved in these experiments has been collected in Table 2.1.
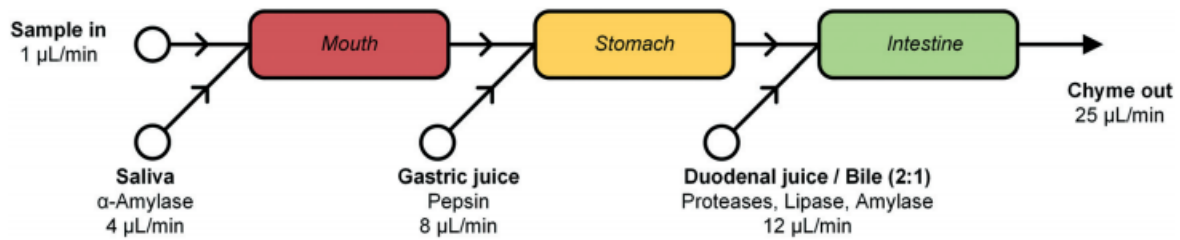
Figure 2.4: Schematic representation of the cell-free miniaturized digestive system[42]. Flow rate of the samples input into the device varies from 1 to 12 μL/min.
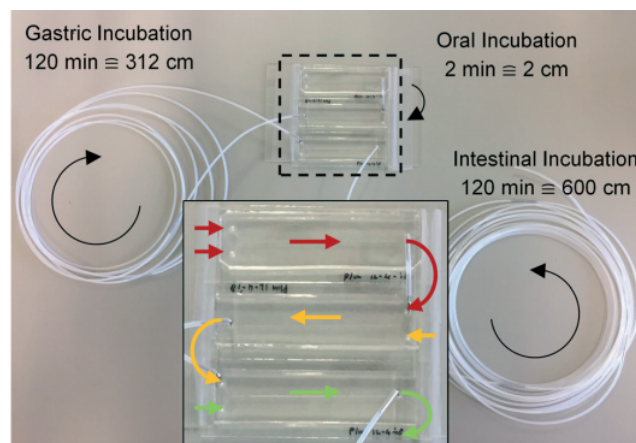
Figure 2.5: Photograph of the three micromixers[42]. Three square chambers represent the 'Mouth', 'Stomach', 'Intestine' respectively. Red and yellow arrows illustrate the flow direction of samples and the long tubings are used to provide enough time for organic incubation.

Table 2.1 illustrates following significant information:

• More than 90 percent of OOC experiments use liquid flow rates below 100μL/min, and the most popular flow rate range is 1μL/min ～ 50μL/min.

• Liver-on-chip includes the most complicated experimental types and therefore has the widest flow demand.

• The biomicrofludics experiments in the last category is considered as a comparing group. Since the platform built in this project is targeted to OOC experiments, the requirements of non-OOC microfluidic experiments do not need to be all satisfied. It is apparent that the flow range is much harder to reach if we expand the application scope to the whole microfluidic field.

• Around 15 percent of experiments apply a flow rate below 1 μL/min, which is a challenge for off-the-shelf components (sensors and controllers) to reach.

To sum up, the ideal flow rate that should be provided by our OOC platform is 0.1 μL/min - 500 μL/min, while a more realistic flow rate range can be set to 1 μL/min - 50 μL/min. It is worth noticing that wider flow rate range is always better than narrow range, which means that the flow rate range provided by our instrument should be as wide as possible.

C. Other Requirements

Fluctuation is one of the challenges in OOC studies, since the flow fluctuation may seriously change the microfluidic characteristics and then influence the result of experiments. In droplet generation research, fluctuating flow will definitely affect the quality of droplets[69], which could even be devastating trouble for the whole experiment. Therefore, smooth flow with even no fluctuation is one of the most important requirements in this project.

Bubble creation is also a critical obstacle in OOC research. They may harm cells and disrupt experiments by spoiling cell viability, rupturing cell membrane or even washing away cells[5]. Dongeun Huh et al. implemented an experiment about cellular-level lung injury induced by fluid mechanical stresses in 2017, which also illustrates that the flow plug in microchannels may cause extremely high stress on cells and lead to cell damage[6].

Unfortunately, due to the micro-scale of tubes and channels, air bubbles can be very difficult to be removed, which is detrimental for OOC experiments[70]. There are several factors that lead to the formation of bubbles in microfluidic platforms, including changing temperature, channel geometry, property of PDMS, configuration of connectors and valves, gas dissolution[71].

The last requirement of the microfluidic platform, growth media recirculation, could be regarded as a flexible condition. Introducing flow recirculation is significant if no pumping systems are included[72]. It can also reduce costs if the growth media and drugs are expensive. No waste will be created by the system since 'waste' becomes sources in recirculation system. On the other hand, the recirculated waste may contaminate the flow, since by-products generated by the primary reaction cannot be removed in time. Moreover, some characteristics of flow may change as well since by-products could influence the PH, viscosity, etc.

2.1.3. Architecture requirements

Since the goal is to develop a portable flow control system, the size should be one of the priorities when designing. Considering the height of mini-CORI FLOW (137mm) and the number of components we are going to use, the limit of size is set to 400mm ×250mm ×150mm. The weight should allow a single person to carry the platform in lab, thus, 5 kg is selected as the target maximum weight of the entire instrument.

Internal volume (swept volume + dead volume) is one of the urgent problems in flow control systems. Large internal volume introduces three disadvantages into the system[73]:

- The time for a full replacement of the liquid can be longer than expected.

- A long transfer time of the fluid along the tube

- A large consumption of sample

Considering the internal volume in state-of-the-art OOC platforms and the normal tubing sizes, the limit is set at 3mL and should be designed as low as possible.

Because the system is small, uninterrupted experiments in different locations are possible. Even if the chip needs to be moved to other laboratories, it can be transported together with the platform. It means a standard interconnection device needs to be integrated into the platform to accommodate various kinds of chips. Up to now, a large number of microfluidic interconnection sockets have been developed, but most are not able to deal with the connection for all OOC chips[74, 75]. In Figure 2.6(a), a Luer-lock solution is designed to deal with the sealing and parallelization problem in microfluidic interconnections. But due to the size of screw-shaped connections, it is hard to deal with close on-chip holes. In Figure 2.6(b), Ball joint interconnection blocks are used to connect tubes with chips but they can only be applied on chips with female connectors. In this project, designing and fabricating a novel socket is not a focus, however, it is the design goal of this project to improve the application range of equipment on the basis of realizing basic functions. Therefore, if commercial sockets cannot meet the requirements, designing a better socket is a choice as well.
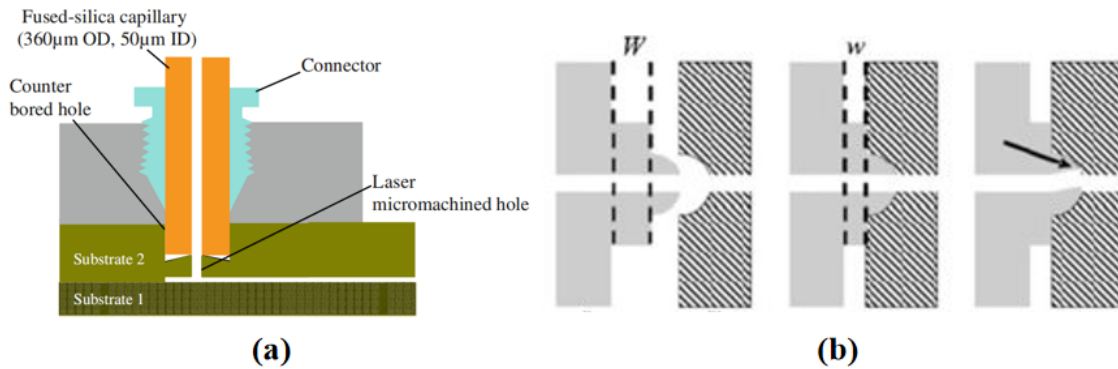
Figure 2.6: Interconnection solutions in literature (a) Luer-lock solution that cannot deal with close inlets[74]. The laser micro-machined hole is well parallelized with the 6/32 thread and fused-silica capillary with no leakage, and the burst pressure is 3.8 bar. (b) Ball joint interconnection blocks (BJIB)[75]. The subfigures from left to right represent the unconnected BJIB, ideally connected BJIB under a pressure from left, misaligned BJIB respectively. The interconnection is made of PDMS and there is no dead volume in this design.

2.1.4. Control requirements

Control is a mandatory part of an OOC platform since the flow needs to be controlled and stabilized at a desired level during the entire experiment. At present, Arduino microcontroller is going to be used to control the system and the control algorithm can influence the performance of system in a significant way. Due to the limitation of project theme and time, the problems of control algorithm and system performance will not be investigated in detail. Instead, some automatic control processes suitable for Organ-On-Chip experiments will be developed and some control parameters will be optimized to a certain extent.

Compared with early OOC experiments, the latest studies always involve multiple sub-experiments or processes and different flows should be introduced into the chip during the entire experiment[45, 53]. Different flow rates need to be applied step by step for the study of the influence of flow rates to cell behaviors as well[63, 65].Thus, the basic function to be realized by the control system is defined as step-by-step generation of flow with 0.1 μL/min, 1 μL/min, 10 μL/min, and 100 μL/min flow rate.

General parameters used to identify the performance of a flow control system are resolution, settling time and stability. However, some parameters cannot be quantified in this phase since they differ greatly from flow control systems based on different principles. In other words, it is hard to find an index to limit all flow control systems. For instance, the settling time is much longer in pressure based system since the pressure in reservoir needs to be accumulated. It also means that the settling time significantly depends on not only the optimization of control algorithm but also the choice of components. Data show that the settling time of typical valve flow control system is 0.6s, while that of typical pump flow control system is 0.7s[76]. As explained earlier, this cannot be used as a strict evaluation standard for equipment. However, based on most Organ-On-Chip literature, it is not difficult to find that 5 s is a reasonable upper limit.

Resolution is a vital factor for microfluidic systems since small value difference in flow rate may lead to extremely different physiological environment. According to most Organ-On-Chip experiments, while different flow rates are required, the differences between the flows are generally not less than 1 μL/min.

Stability depends on both control algorithm and performance of the components. Thus, it can be a factor to select suitable components for an OOC platform. In order to optimize our system to reach a good performance, the upper limit of our system is set to 0.5% RSD, For most OOC applications involving flow rates around 10 μL/min, the fluctuation is limited to around 500pL/min, which is negligible value in most OOC experiments.

Settling time could be another factor to identify the performance of OOC platform since it has standard consideration in most devices, and affects their capacity to prevent from disturbances.

2.2. State-of-the-art Organ-On-Chip Platforms

After 30 years' development, a large amount of OOC flow control systems have been developed to satisfy OOC experiments. These platforms can be classified into two types: Commercial instruments and Self-built experimental platforms.

2.2.1. Commercial instruments

There are lots of OOC platforms or devices that have been developed by commercial companies all over the world. These companies mostly focus on designing not only pumping systems but also microfluidic components such as single pumps, valves, sensors, etc. The most popular companies in this field are *Elveflow, Fluigent, Micronit, Corsolution,* etc.

A microfluidic pressure source designed by *Elveflow* is shown in Figure 2.7(a)[8]. The instrument has the capacity to provide pressure ranging from -900mbar to 6000mbar and the response time is only 9ms. One advantage of pressure source is that they can provide most smooth flow under extremely low flow rate. Nevertheless, since the instrument does not integrate any flow sensor, the error between pressure and flow rate cannot be displayed and collected to better control the OOC experiment, which means that in order to satisfy the design requirement in my study, various extra components such as flow sensors and valves should be added and make the platform bulkier. Similar problems also take place in a pressure source from *Fluigent* (Figure 2.7(b))[9]. The size of this instrument is smaller than that from *Elveflow* but several components need to be lined up to satisfy multi-channel situations.

Some companies are working on the integration of the pumping mechanisms to build a compact platform that satisfies requirements of OOC research. Figure 2.7(c) shows a microfluidic platform designed by *Micronit*[10]. The applications include but are not limited to *Neural or Cardio-vascular Networks-On-Chip, Gut-On-Chip, Liver-On-Chip, Skin-On-Chip, Lung-On-Chip, Mesenchymal stem cells (MSC) or Bone Marrow-On-Chip, ESC or iPSC-derived stem cells (ESC/iPSC)-on-a-chip*. The flow range of this platform is from 75nL/min to 5mL/min and it is worth noticing that the system is built on a stainless steel breadboard by using a pressure source form *Fluigent.* Since one of the most significant advantages of pressure source in OOC applications is fluctuation-free flow[30], this platform has the capacity to deliver extremely smooth flow without fluctuation. Furthermore, a microfluidic interconnection solution is integrated in this platform even though it is still difficult to solve the problem of packaging standardization of microfluidic technology. One of the weaknesses of this platform is that the size of this instrument is $450 \times 450 \times 280mm^3$ and the weight is over 5kg, which is still bulky and cannot be carried easily by a single person. In addition, since no sensors and controllers are integrated, Its function is not comprehensive enough and its stability is in fact questionable.
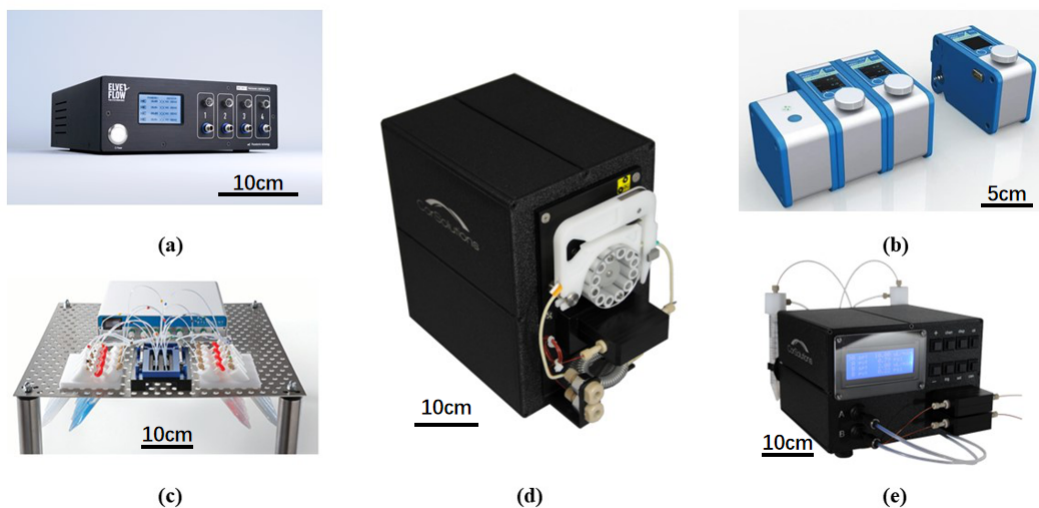
Figure 2.7: Commercial OOC devices (a) Elveflow OB1 MK3 pressure controller[8], (b) LineUP™ Series[9], (c) *Micronit* platform solution[10], (d) *Corsolution* PeriWave Pump[77], (e) *Corsolution* PneuWave Pump[78]

The most successful microfluidic device is designed by *Corsolution*, an American company focusing on developing microfluidic components and systems. Figure 2.7(d) shows a pumping system designed

on the basis of peristaltic pumps[77]. The flow range of this instrument is from 20nL/min to 5mL/min, and it supports flow recirculation. The size is around $300 \times 200 \times 300$mm^3 thus it is still bulkier than our expectation. Although the instructions indicate that the product can produce non-fluctuating flow, the description is not credible due to the characteristics of peristaltic pump itself since no damping components are included according to the schematic diagram shown in Figure 2.8(a). Another instrument created by *Corsolution* is based on pressure source, which is also called pneumatic pump (Figure 2.7(e), 2.8(b))[78]. This version has the capacity to deliver free-fluctuation flow, however, no recirculation functions are integrated and the size is similar to peristaltic version. Due to the positive pressure principle, gas may be dissolved in the sample which could cause bubbles on the chip. Both versions have integrated flow sensors and the basic functions of the microfluidic platform have been almost completely realized. Nevertheless, it is worth mentioning that both versions are not compatible with microscopes and are not able to integrate microfluidic chips, specifically organ chips in the entire system and create a standard packaging scheme for these chips, which could be a limitation since chips are not allowed to be assembled with tubings without any auxiliary connectors.

(a)   (b)
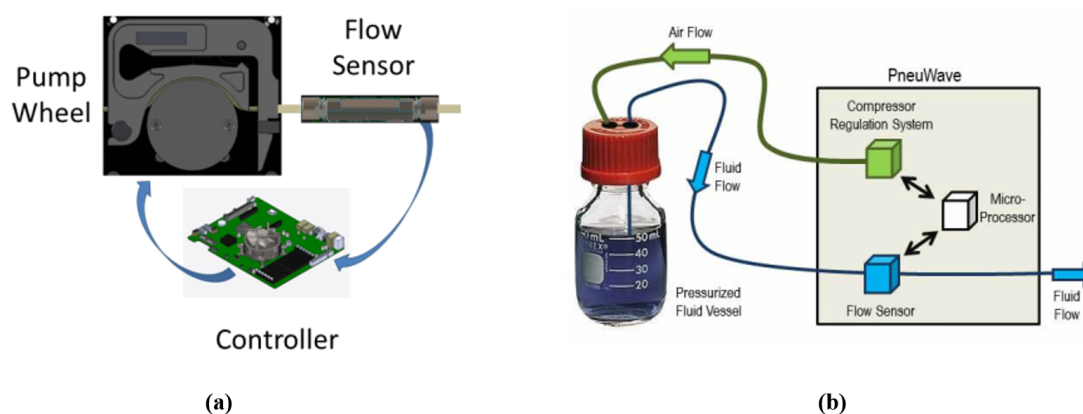
Figure 2.8: The internal composition and principle of the instrument from *Corsolution* (a) PeriWave Pump[77] (b) PneuWave Pump[78]

2.2.2. Microfluidic platforms in the literature

Most OOC researchers choose to build their own experimental platform for microfluidic supply due to the tedious implement steps, unstable conditions and irregular chip connection schemes of commercial OOC platforms. Many non-commercial OOC platforms that have better performances have also been made public in literature for the same reason.

Figure 2.9(a) shows a self-built setup for its specific OOC application. Noticing that a switch valve and a primer syringe are integrated for clearing the gas inside tubes and pumping systems in advance. A pressure monitor is also added for accurate observation and control of experimental parameters[23]. Compared to buying a platform from companies, introducing self-built platform can reduce costs, add components freely and improve the performance of experimental equipment in a targeted way. Figure 2.9(b) shows a demo from *Bürkert*. It is a microfluidic control system solution and consists of pumps, valves, microcontrollers and reservoirs. A transparent plate is used for accommodating tubings and PCBs. Since this scheme does not involve any connector and adaptors to fit tubes with different sizes, dead volume can be minimized. It is worth noticing that the 2D layout of the design indicates a equivalent design in micro-scale, which represents the development of a new generation of highly integrated microfluidic chips.

Three distinguished microfluidic platforms are illustrated in Figure 2.9(c)(d)(e) respectively. In Figure 2.9(c), An open-source, programmable pneumatic setup for automated control of microfluidic devices is shown. It has 48 control lines and 18 individually-addressable flow lines[7]. The response time of valves is excellent and remote control can be realized. Nevertheless, the setup is extremely bulky and costly, and no flow sensors or extra sensors are involved, which means this platform is too general but not specific in terms of OOC experiments. Figure 2.9(d) shows a portable microfluidic platform with extremely small size and it has relatively perfect pneumatic execution and detection components[79].
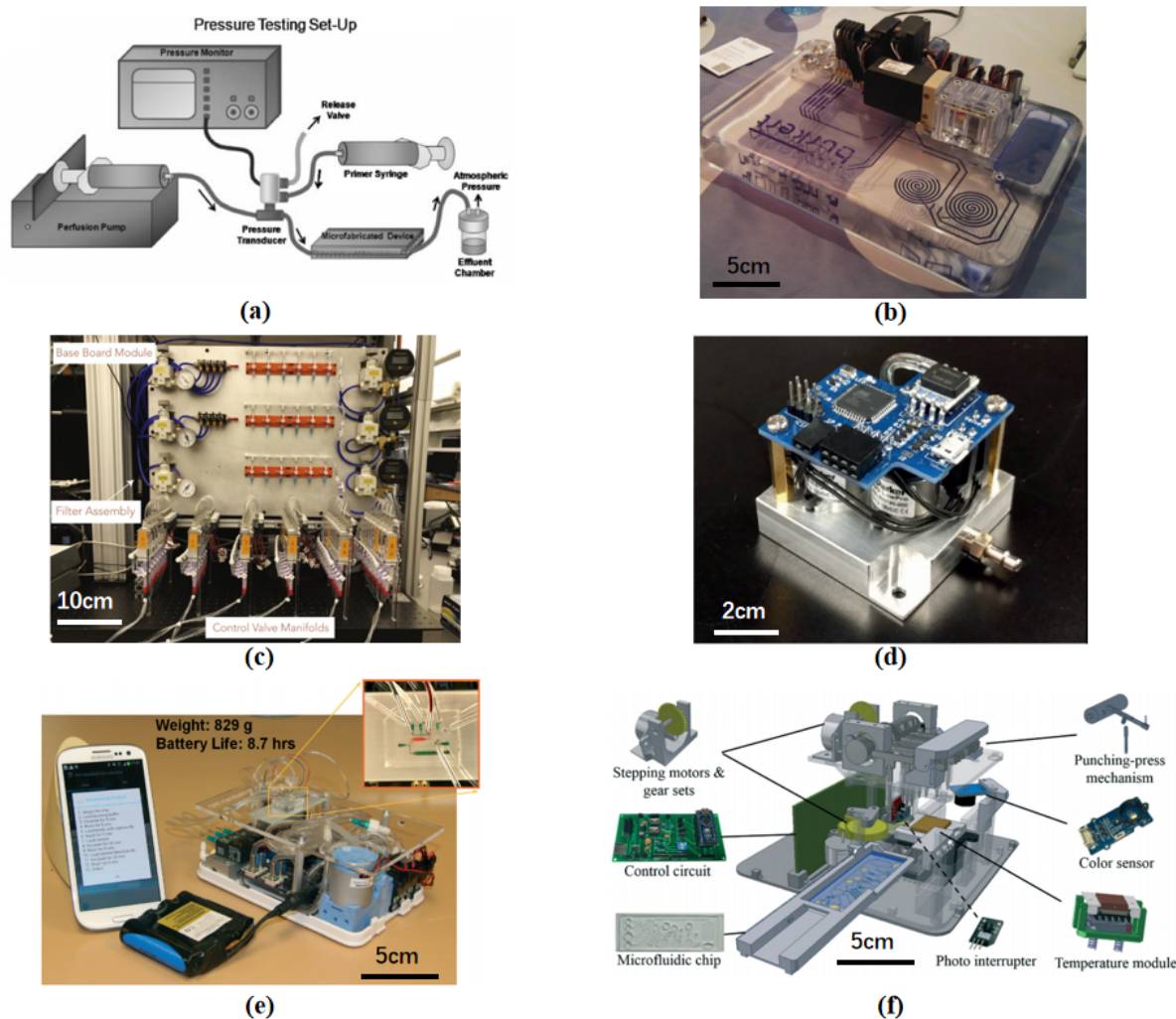
Figure 2.9: OOC platforms in the literature (a)Self built platform for liver-on-chip experiments[23], (b) Microfluidic control system from *Bürkert*, (c) A bulky microfluidic setup[7], (d) All-in-one automated microfluidics control system[79], (e) A smartphone controlled handheld microfluidic system[80], (f) A sample-to-answer platform for rapid detection of pathogens[81].

However, no flow sensors, reservoirs and chip connections are integrated, which makes it more like a pneumatic pumping system (similar to pumps in *Corsolution*)but not a complete OOC device. Figure 2.9(e) contains a most distinguished microfluidic platform that covers most of the requirements of the proposals in this project, including small size, integrated reservoir and chip connections and wide flow range[80]. Nevertheless, it is still facing some general problems that almost all microfluidic/OOC platforms are suffering from as well. First, positive air pressure causes bubbles in the sample fluid, which may cause extreme cell death in OOC experiments. Second, vacuum created by peristaltic pumps may still generate fluctuations in vacuum tanks, which will cause fluctuations(not severe) in flows as well. Third, no flow sensors are integrated thus there is no intuitive flow rate output. Last but not least, flow recirculation is impossible for this compact setup.

Portable devices used in digital microfluidics have developed for several years. A sample-to-answer platform for rapid detection of pathogens is shown in Figure 2.9(f)[81]. It is highly integrated and involves comprehensive functions in pathogen detection. The novel design ideas are the use of capillary pump, punching press mechanism (acting as valves to control sample mixing), integration with smartphone interface. Even though these ideas cannot satisfy our requirement for OOC experiments, the design concept of this highly integrated instruments is still worthy of reference.

| Pump | → | Valve | → | Sensor | → | Microfluidic Chip |

Figure 2.10: General design scheme of an OOC platform. Location of each component is flexible.

Table 2.2: Applicability of different pump systems to OOC experiments

Requirements	Gravity	Surface tension	Osmosis	Syringe
Flow type	-	-	-	++
Flow range	-	-	-	+
Smooth flow	++	-	++	+
Bubble generation	++	++	+	-
System complexity	-	+	+	++
Summation	+	0	++	+++++
Requirements	Peristaltic	Gas pressure	Electric	Centrifugal
Flow type	++	++	+	-
Flow range	++	++	-	+
Smooth flow	-	++	++	++
Bubble generation	++	+	-	++
System complexity	++	+	-	-
Summation	+++++++	++++++++	0	+++

++: Completely satisfied, +: Basically satisfied, -:Not satisfied, 0: Neutral

2.3. Microfluidic Handling Principles
2.3.1. General scheme
A complete flow control system should have at least three components: pump, valve, sensor. By combining with an Organ-On-Chip model, a general scheme of an OOC platform can be developed, which is shown in Figure 2.10.

Mostly, valves can be divided into two categories: switch valve and proportional control valve which have the capacity to switch on/off the flow and linearly control the flow rate respectively. Although valves can be divided into more categories according to the principle, different kinds of valves, such as diaphragm valves and solenoid valves, are similar in nature, so there is little difference in their effects on fluids. Category of pumps is more complicated since they can be classified into 'current source' and 'voltage source', and each classification contents multiple pumps based on different principles. Different pumps based on various principles may have large effect difference, thus, it is worth discussing in the following paragraphs.

2.3.2. Selection of pumping principle
In general, pumping systems used in microfluidic experiments can be classified into eight categories: Gravity-driven pump, Osmosis-driven pump, Surface tension-driven pump, syringe pump, peristaltic pump, gas pressure pump, Electrokinetic and electroosmotic pump, Centrifugal pump[11]. In order to screen out the schemes used in this design more efficiently, Table 2.2 is made and includes the advantages and disadvantages based on the requirements of OOC experiments.

Figure 2.11 covers the working principle and flow characteristics of several common pumping systems which are widely used in engineering and scientific research. Gravity-driven pump is a kind of pump working on the basis of gravitational potential energy. In order to generate a constant flow, hori-
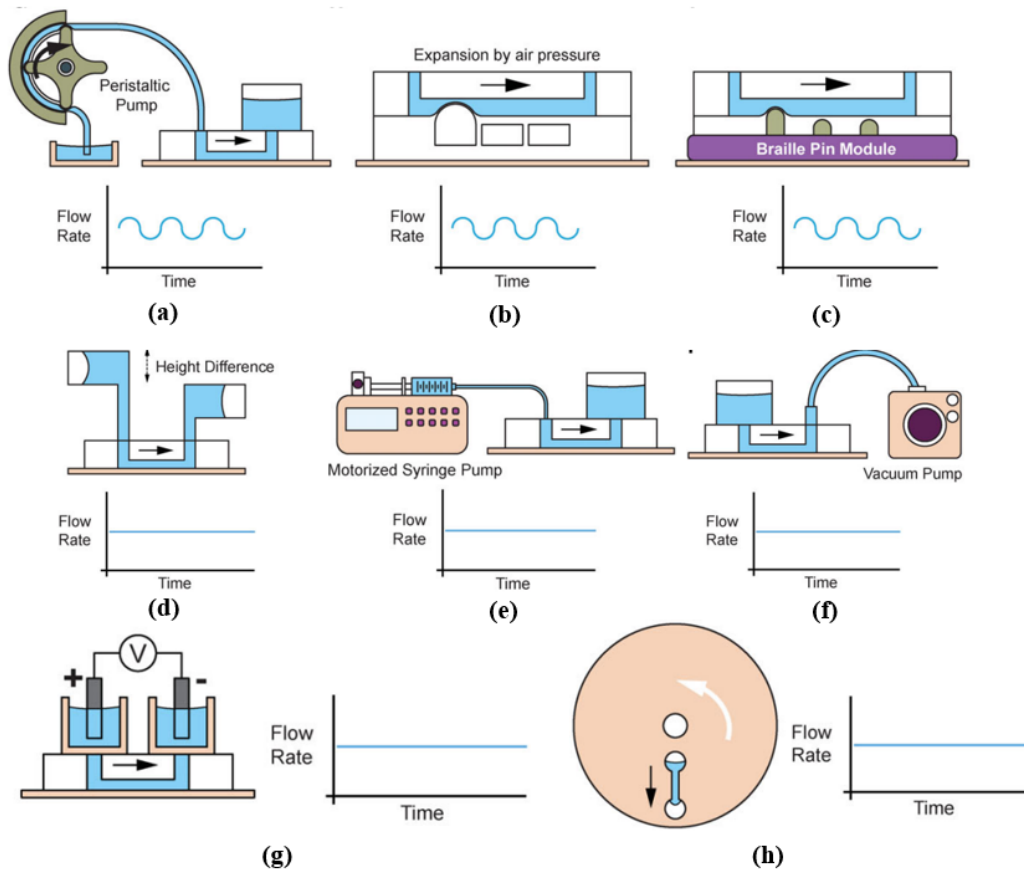
Figure 2.11: Schematic diagrams of pumping systems[11] (a) Conventional peristaltic pump, (b) Pneumatic peristaltic pump, (c) Braille pin based peristaltic pump, (d) Gravity-driven pump, (e) Syringe Pump, (f) Vacuum pump, (g) Electroosmotic pump, (h) Centrifugal pump
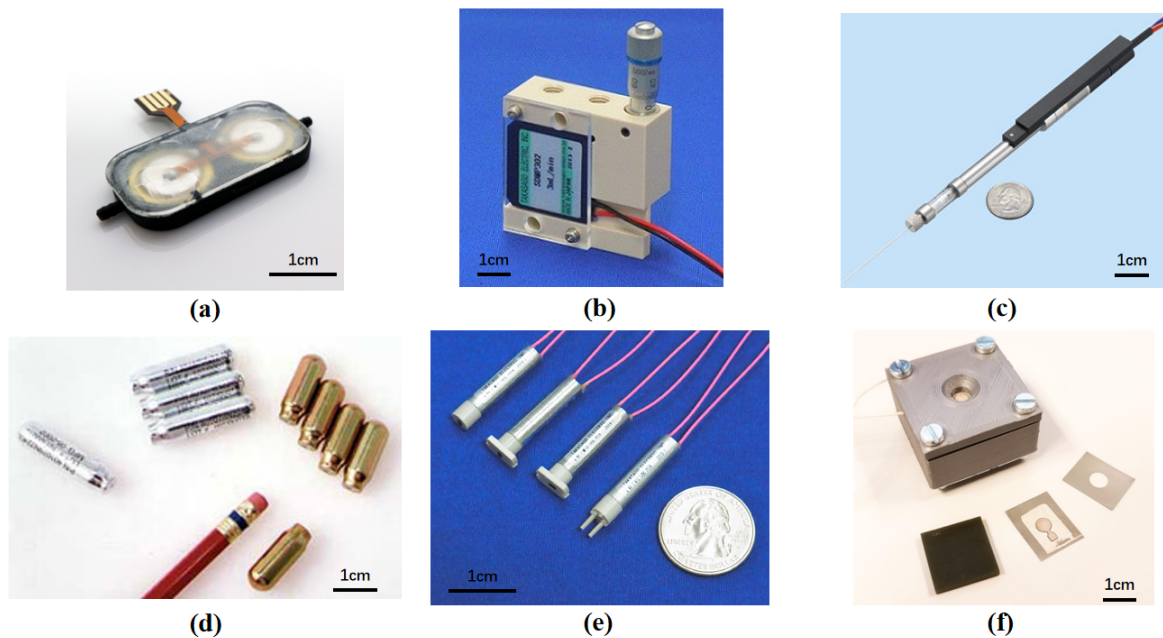
Figure 2.12: Other components that could be integrated in an OOC platform (a) *Bartels* peristaltic pump[82], (b) *Takasago* needle valve[83], (c) *Takasago* pen-type syringe [84], (d) *Leland* mini gas cylinder[85], (e) *Takasago* shut-off valve[86], (f) A control valve designed by Gunda *et.al*[87]

Table 2.3: Significant data of *Bronkhorst* flow sensor

	Flow range	Size (mm^3)	Precision	Principle
μ-FLOW	min. 5...100 mg/h max. 0.1...2 g/h	$98 \times 25 \times 118$	$\pm 2\%$ FS*	CTA*/CPA*
mini CORI-FLOW	min. 0.05...5 g/h max. 2...200 kg/h	$120 \times 31.75 \times 137$	liquid: $\pm 0.2\%$ of rate gas: $\pm 0.5\%$ of rate	Coriolis

FS: Full Scale, CTA: Constant Temperature Anemometry principle, CPA: Constant Power Anemometry principle

zontal reservoirs can be placed at both ends of the system, as shown in Figure 2.11(d)[88]. Peristaltic pumps can be realized by various methods, as shown in Figure 2.11(a)(b)(c)[89–91]. These pumps work on the principle of periodic pressure difference between both sides of rotor thus will always create periodic fluctuations in flows. Syringe pump is the most widely used pumping system on OOC applications (Figure 2.11(e))[92]. The sample in reservoir is pushed by a piston driven by a step motor to tubes and chips. Gas pressure pump category includes gas tank pumping system and vacuum pumping system whose working principles are shown in Figure 2.11(f)[11]. Other pumping systems such as electric pumps(Figure 2.11(g)) do not need any mechanical parts[11] but are based on electrical and chemical properties thus may have various side effects on samples in OOC applications. Centrifugal pumps (Figure 2.11(h)) consist of a rotating plate to accommodate the main part of flow, which may greatly increase the volume and complexity of the system.

Table 2.2 illustrates the applicability of Different Pump Systems to OOC Experiments. Since we are focusing on the flow requirements of OOC systems, five factors are taken into account, which are flow type, flow range, smooth flow, bubble generation and system complexity. It is worth mentioning that even though recirculation is one of the requirements analyzed in the second chapter, it should not be included since it is a soft requirement. Because one unsatisfied factor may have catastrophic influence on the design, '-' should be counted as minus point in the summation of grade.

2.4. Off-the-shelf Components

Pumps, valves, sensors, etc. are all necessary components to form a OOC platform. Since only the *Bronkhorst* flow sensors can satisfy the precision requirement in this project, The sensor selection has been fixed. On the contrary, other components should be selected carefully so that an optimized OOC platform could be designed.

2.4.1. Flow sensor

Bronkhorst flow sensors are supposed to be used in this project for its distinguished precision and stability. According to the flow requirements in OOC experiments, not all sensors from *Bronkhorst* satisfies our need and two versions have been selected after consideration, which are μ-FLOW (can only be used for liquid sensing) and mini Cori-FLOW (can work under both liquid and gas situation).

Table 2.3 illustrates the technical data that are useful for our design. It is worth mentioning that mini Cori-FLOW has a drawback since the lowest flow rate it can reach is 0.05g/h(0.83mg/min). Using the equation below, it can be shown that the volumetric flow rate is around 0.83μL/min (water), which barely satisfies our minimum flow rate requirement (1-50 μ/min) discussed in chapter 2, but still cannot satisfy the experiments with lower flow rate requirements. In contrast, the lowest flow rate of μ-FLOW is around 0.083μL/min (water), which almost covers the requirement of more Organ-On-Chip models. mini Cori-FLOW can always handle gas flow sensing in a low-flow situation since the density is thousands of times lower than liquid.

$$Q_V = \frac{Q_M}{\rho} = \frac{50mg/h}{1000mg/mL} = 0.05mL/h \approx 0.83\mu L/min \qquad (2.2)$$

Nevertheless, μ-FLOW is based on the principle of thermal detection which has the operating temperature from 5 to 50 degrees and it can only detect liquid. It means the cells which can only survive
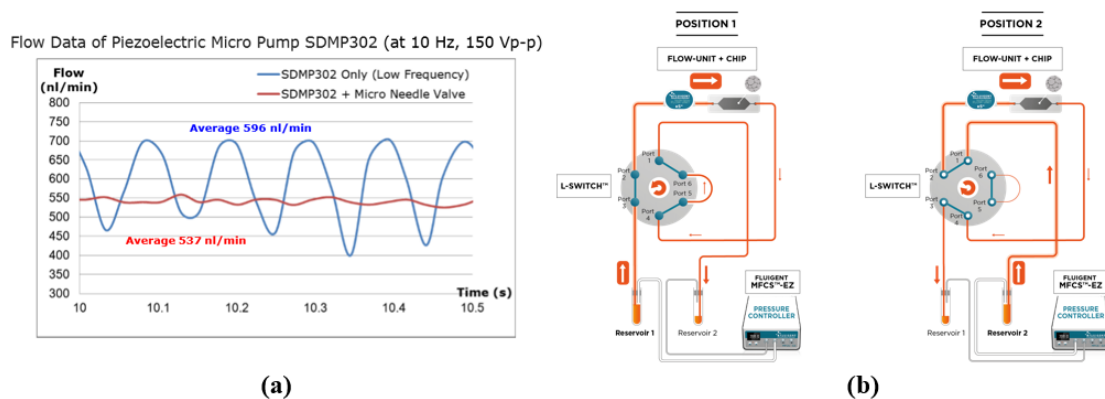
Figure 2.13: (a) Image of flow changes with time with the support from Takasago needle valve[83], (b) Recirculation loop formed by L-switch[93]

Table 2.4: Data of direct fluid-actucation pumps

Brand	Model	Size [mm^3]	Flow rate	Flow type	Principle
Bartels	mp6-hyb	$30 \times 15 \times 3.8$	0.01-10 mL/min(liquid) 8 mL/min(gas)*	gas & liquid	diaphragm
Clark	RP-Q1	$15 \times 25 \times 30$	max. 0.45 mL/min	liquid	rotor
Takasago	SDMP-Standard	$25 \times 25 \times 4.8$	3 or 7 mL/min*	-	diaphragm
	Ultra-small	$11 \times 37 \times 12$	15 μL/min*	liquid	rotor
	RP-TX Series	$33 \times 12 \times 21.5$	0.3-40 μL/min$\pm$20%	liquid	rotor

*: Typical flow rate, -: Unknown

below 37 degrees will be damaged after the sensed flow. Some solutions such as adding micro-coolers are reasonable but may increase the size of the system. In addition, the precision of μ-FLOW is ten times lower than mini Cori-FLOW, which is another drawback of this device. Thus, we need to make a trade-off between flow range and principle practicability.

2.4.2. Pump

Peristaltic pumps are one of the most conventional pumps in flow control systems. They can be used in multiple ways such as liquid actuation, positive pressure and vacuum generation. All the methods can actuate microfluids but have different performances. In microfluidic field, diaphragm peristaltic pumps is popular since they can be made in extremely small size, as shown in Figure 2.12(a)[82]. Nevertheless, most off-the-shelf micropumps cannot satisfy the minimum flow rate, and they still create large flow fluctuations due to the pressure variation among diaphragms. Table 2.4 illustrates the data of certain microfluidic peristaltic pumps for direct fluid actuation and Table 2.5 shows the data of several mini pressure generation pumps on sale.

In order to solve the problem of fluctuation in peristaltic pumps, a needle valve from *Takasago* can be integrated as shown in Figure 2.12(b)[83]. With the flow restriction from needle valve, fluctuation can be limited since flow with large rate cannot go through the narrow path with a needle. The effect is shown in Figure 2.13(a)[83] and it is worth noticing that the pump used to integrate with needle valve has a typical flow rate of 3mL/min, which means the needle valve may limit the upper bound of flow range and it will be difficult for the system to reach high flow rate.

Commercial syringe pumps are mostly integrated with sensors and actuators thus are bulky. Figure 2.12(c) shows a microsyringe pump from *Takasago*[84], of which length is 170mm while the minimum flow rate is 10.5nL/min. If only significant factors are taken into consideration, the syringe pump could

Table 2.5: Data of pressure-generation pumps

Brand	Model	Size [mm^3]	Pressure range	Flow rate*	Principle
Bartels	mp6-gas+	$30 \times 15 \times 3.8$	0.85-1.15(bar)	20 ml/min	diaphragm
SURGEFLO	-	$60 \times 25 \times 25$	0.42-1(bar)	1.2 L/min	DC motor
Nitto Kohki	VP0125 230V CE	$50 \times 48 \times 62$	0.67-1(bar)	7 L/min	Piston
	DP0110-Y1	$45 \times 50 \times 30$	0.67-2.5(bar)	7.5 L/min	DC motor

*: Flow rate of gas in the device when vacuum is generated

Table 2.6: Data of *Leland* gas cylinders [Figure 3.3(d)]

Gas	Capacity(ml)	Weight(g)	Diameter(mm)	Length(mm)
N$_2$	20	75	19.68	69.29
N$_2$	1	0.123	3.75	10
Air	74	18	15	45
Air	97	30.2	15.75	56.3

be a good choice for its compact design and low flow rate it can reach.

As for pressure based pumping system, since no bulky pressure controllers can be taken into account, small gas cylinders are the best choices as shown in Figure 2.12(d)[85]. Most cylinders in this company are compact and dependable, which could be a good choice for this project with a combination of pressure regulators. Nevertheless, the compact design may lead to safety problems which will be discussed in the next section. Data of gas cylinders from *Leland* containing different gases are shown in Table 2.6.

2.4.3. Valve

Valves are also important components in a microfluidic system. They can be devided in switch valves, shut-off valves and proportional control valves. Shut-off valves should always be fixed with the flow sensor for zeroing the instrument[94]. A check valve from *Takasago* can deal with the problem with an extremely short length of 27mm[86]. Switch valves can be used to change input samples from different reservoirs while another application is recirculation, as shown in Figure 2.13(b)[93]. With the assistance of a multi-switch valve, the source and waste reservoir can be swapped while the direction of the flow in OOC chip does not change.

Proportional control valves are vital components in pneumatic systems since they are used for controlling flows provided to chips with a pressure difference between two ends. Figure 2.12(f) shows a proportional control valve from Gunda et al[87]. The size is $5 \times 5 \times 1.8$cm^3 and the resolution is 0.2μL/min under a pressure difference of 500mbar, which is acceptable and even has a potential to get lower flow rate under lower pressure difference. Nevertheless, this valve does not have the capacity to deal with gas flow, thus bounds the thinking of design. A better choice could be a commercial proportional control valve from *Bürkert*[95], with a size of $20 \times 20 \times 60$mm^3. It can deal with both neutral gases and liquids with a maximum flow rate of 1mL/min (orifice size = 0.05mm).

Bronkhorst High-Tech B.V. also has flow controllers consisting of a sensor and a control valve. This is another choice since it not only satisfies the requirements of component selection, but also provides an off-the-shelf feedback control system and reduces unnecessary workload.

2.4.4. Optional components

In addition to the mandatory components shown above, some devices could be added to improve the performance of our OOC platform, such as oxygen sensor, temperature sensor, strain sensor,
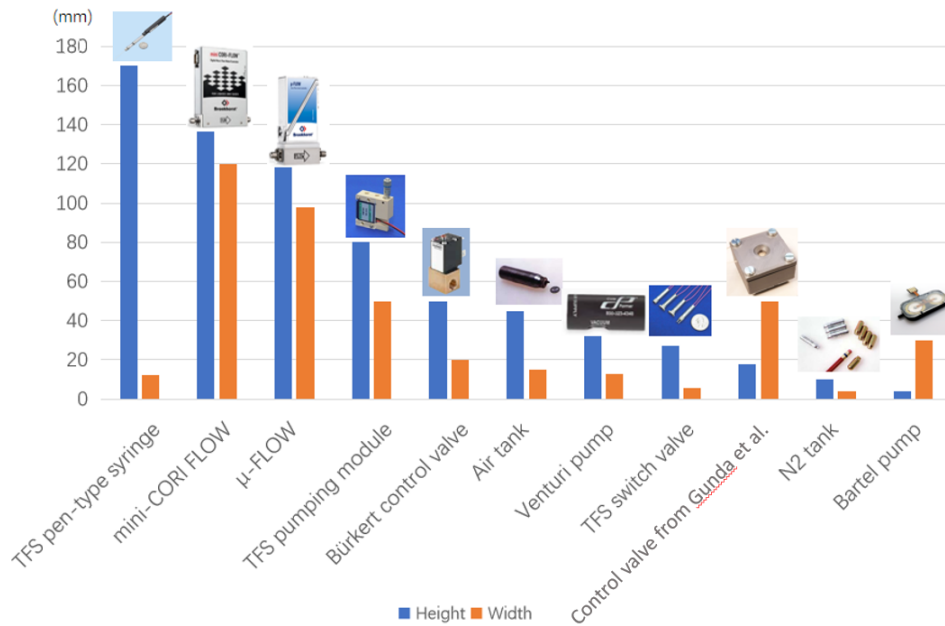
Figure 2.14: Size comparison of microfluidic components
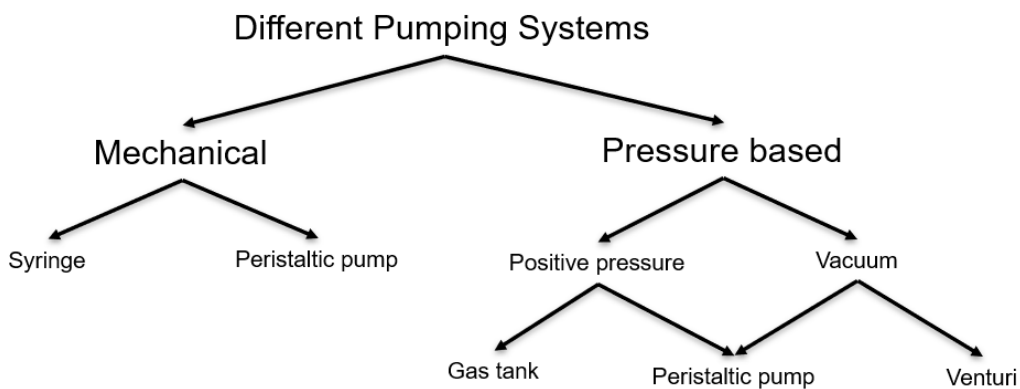
Figure 2.15: Classification of different pumping methods.

bubble trapper, etc. As this equipment is in the preliminary design stage and focuses on realizing the target requirements, the research on these components would be arranged after the preliminary design and verification.

In order to better illustrate the size of different components discussed above, a histogram (Figure 2.14) is made based on the height of them.

2.5. Design Schemes

According to the selection of pumping system for OOC application in Table 2.2, four schemes have been designed and classified into 2 categories, as shown in tree diagram 2.15. Among these systems, 'syringe system','peristaltic pumping system' and 'positive pressure system' are based on the principle of positive displacement, while 'vacuum system' is driven by a negative source. In the pressure based category, both positive and negative pressure can be classified further based on the principle to create the pressure difference. Using a principle without any mechanical parts such as gas tank and Venturi pump can completely eliminate the fluctuation in flow including pressure generated by the source. Nevertheless, Peristaltic pumps will cause little pressure fluctuation while they are used to generate pressure difference in a buffer tank since air is highly compressible which will cause large damping inside the vacuum container[12].

①	sample reservoir	⑤	flow sensor
②	microcontroller	⑥	microfluidic chip
③	pressure tank with regulator	⑦	switch valve
④	Venturi tube	⑧	control valve
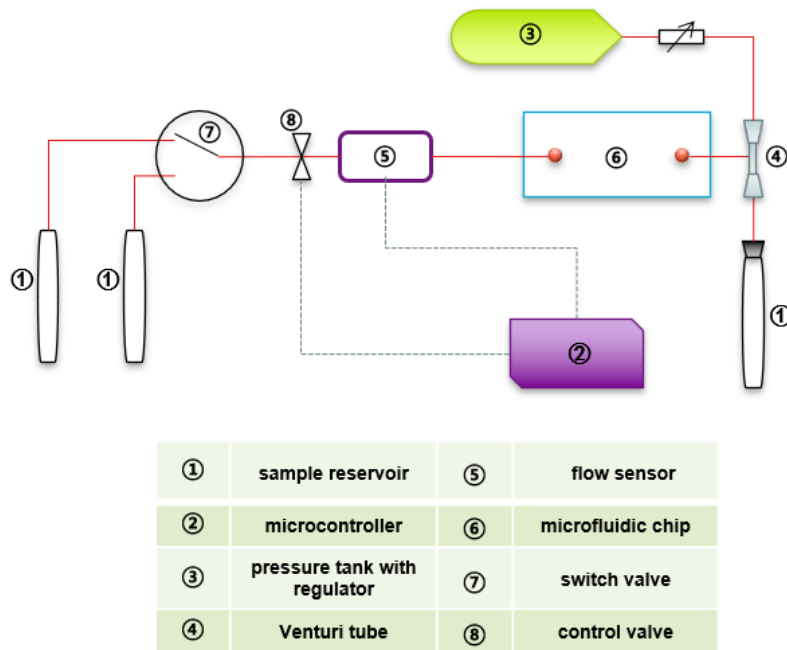
Figure 2.16: Peripheral connection scheme based on the venturi pumping method at the outlet. The under pressure at the outlet (4) is generated by connecting it to a venturi tube (4). The main drawback of the system is that it requires continuous supply of large amounts of pressurized air (3).

2.5.1. Scheme selection

In this section, a design scheme is screened out by analyzing the potential advantages and disadvantages. Compared to mechanical and positive pressure systems, vacuum-based system stands out since there is no pressure increase at the source of flow lines thus no gas will be pressed into the liquid and forms bubbles while pressure drops. Among vacuum systems, Venturi system is regarded as a novel design since no mechanical parts will be introduced into the system thus there is no potential fluctuations and mechanical vibrations. The scheme is shown in Figure 2.16.

In this figure, a gas cylinder should be integrated to create large gas flows for actuating the Venturi pump. Then, a pressure difference should be created at the vacuum port on pump which should 'pull' the fluids from source reservoirs to the waste reservoir by applying a pressure difference. Even though Venturi system has lots of benefits, it creates large noise and needs large gas cylinders for long-term experiments. This is a serious deficiency so vacuum systems based on peristaltic pumping principles have been introduced for comparison.

Figure 2.17 illustrates the schematic design of a flow control system with alternative channels based on a peristaltic vacuum pump. The solid line represents the fluid connection, while the dashed line represents the interaction of electronic control system. A peristaltic vacuum pump is placed at the end of the system, generate a stable vacuum environment inside the waste reservoir and then 'suck' the flow from source reservoirs which are exposed to atmospheric pressure. Microcontroller is electrically connected to the control valve and the flow sensor which can be used for feedforward and feedback control. Since the electrical connection depends on the component selection, the specific circuit connection needs to be further explored, so it is not shown in detail in the schematic diagram. Compared to the Venturi system, this vacuum system has several drawbacks such as vibrations and potential fluctuations, however, it can support long-term experiments and the size can also be suppressed if mini-pumps are introduced into the system.

It is worth mentioning that vacuum systems always requires perfect air tightness to prevent any bubbles in the flow since even an unconspicuous leakage could 'such' air into the liquid flow and form bubbles and damage cells.

To sum up, advantages and disadvantages of all pumping systems introduced above are recorded in Table 2.7 which shows that vacuum system based on peristaltic pumping principle stands out due to its advantages with great potential and least limitations.

Table 2.7: Potential advantages and disadvantages of different pumping systems used in the peripheral connection.

	Potential advantages	Potential disadvantages
Syringe system	•Extremely low flow rate •Easy connection •Intuitive operation and control •Short settling time (fast)	•Pulsation •Bubble creation •Short term •No recirculation •Bulky
Peristaltic system	•Easy recirculation •Easy connection •Intuitive operation and control •Short settling time (fast) •Long term •Easy recirculation	•Fluctuation •Contamination •Narrow flow range •Vibration and noise
Positive pressure system	•Smooth flow •Wide flow range	•Micro-bubble creation •Complex connection •Feed back control is needed. •Long settling time (slow)
Venturi system	•Smooth flow •Low flow rate •Less dissolved air •Less dead volume •Easy recirculation	•Narrow flow range •Feed back control is needed •Extreme short term •Noisy •Influence the circumstance •Strict air tightness requirements
Peristaltic vacuum pump system	•Smooth flow •Low flow rate •Less dissolved air •Long term •Easy connection •Less dead volume •Easy recirculation	•Narrow flow range •Feed back control is needed •Vibration and noise •Strict air tightness requirements
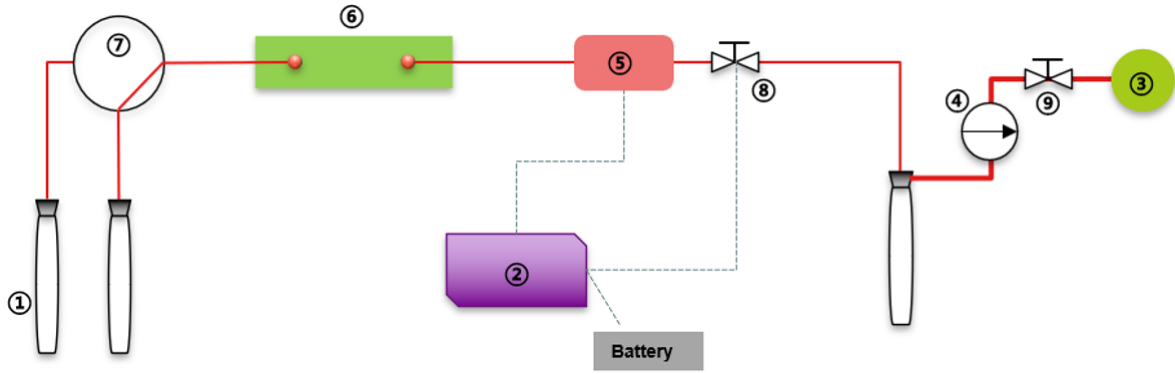
Figure 2.17: Peripheral connection scheme based on the vacuum pump at the outlet. The under pressure is created at the outlet reservoir due to the vacuum pump (3).
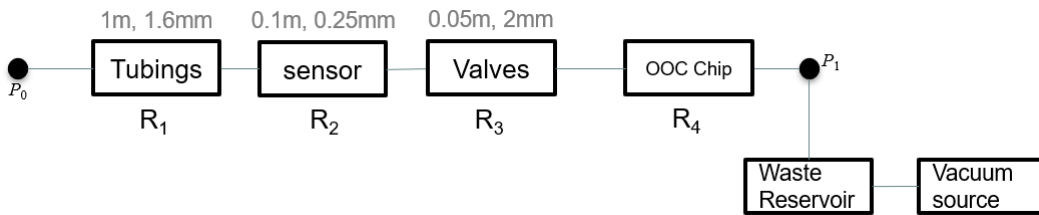
Figure 2.18: Fluidic resistance from different sub-systems that contribute to the flow rate. Grey numbers above the blocks represents the estimated length and inner diameter of channels of the components

2.5.2. Phased verification

A significant potential limitation of vacuum system is the flow range it can provide. Since most off-the-shelf mini vacuum pumps can only generate quasi-vacuum environment, there are worries about the largest flow rate it can generate based on the pressure difference. In order to judge whether vacuum system has the capacity to meet the needs of most OOC experiments, circuit analog method[96] has been introduced and used to calculate the maximum flow rate in several Organ-On-Chip models.

Figure 2.18 illustrates a schematic diagram of a peristaltic vacuum pump system used to calculate the flow rate based on the estimated channel width and length in different components. The pressure difference between two joints can be analog as voltage in circuits while flow resistances in flow path are similar to electrical resistances. According to the diagram and the investigation of off-the-shelf vacuum pumps, the flow path can be considered as a circuit in series, where $V_0 = 1000 mbar, V_1 = 150 mbar$. Then, the flow rate in the system can be evaluated based on the data of components as below:

$$R_0 = R_{rec} = \frac{12\eta L}{wh^3} \tag{2.3}$$

$$R_i = R_{cir} = \frac{8\eta L}{\pi r^4} \tag{2.4}$$

$$Q = \frac{\Delta V}{R_{tot}} = \frac{V_0 - V_1}{R_1 + R_2 + R_3 + R_0} \tag{2.5}$$

Table 2.8: Flow rate evaluation in Venturi system

Fluid type	Dynamic viscosity [Pa s]	Resistance [Pa s/m^3]		Flow rate [μL/min]	
		Lung-On-Chip	Kidney-On-Chip	Lung-On-Chip	Kidney-On-Chip
DI water	8.9×10^{-4}	3.382×10^{12}	2.154×10^{12}	1508	2368
DMEM	7.8×10^{-4}	3.217×10^{12}	2.141×10^{12}	1585	2382
RPMI-1640	10.6×10^{-4}	3.637×10^{12}	2.174×10^{12}	1402	2346

Here, the length and diameter of tubes are equivalent to 1m and 1/8" respectively. The length of the tube in the flow sensor is approximately 0.1m while the diameter is set to a minimum value (0.25mm) to ensure the feasibility. Internal length and diameter of valves are 0.05m and 8mm. Noticing that the resistance of valves and flow sensors is much larger than tubes, thus, the overall value of the resistance is the summation of resistance from sensors, valves and microchip. Using the data above, the resistances of components can be determined in equation (2.6).

$$
\begin{cases}
R_1 \approx \frac{8}{\pi} \times \frac{10^{12}}{1.6^4} = 3.9 \times 10^{11}\eta \\
R_2 \approx \frac{8}{\pi} \times \frac{0.1 \times 10^{12}}{0.125^4} = 1.0 \times 10^{15}\eta \\
R_3 \approx \frac{8}{\pi} \times \frac{0.05 \times 10^{12}}{0.1^4} = 1.3 \times 10^{15}\eta
\end{cases}
\tag{2.6}
$$

In terms of all data provided above, the flow rate of the system applied to two OOC models is calculated as shown in Table 2.8. The data of microchannels in OOC models are extracted from Lung-On-Chip[35] and Kidney-On-Chip[55]. The result shows that the maximum flow rate could reach over 1mL/min, which is hundreds of times higher than the requirement. Nevertheless, since resistances of OOC models differ a lot from each other, we need to further verify this conclusion in the following experiments and tests involving as many different OOC chips as possible.

2.5.3. Uniqueness
A large number of OOC platforms have been designed while almost all of them are based on positive displacement pumps. Compared to Ventri system, Persistaltic pumping based vacuum system becomes our target since it can create potential to develop a compact flow control system with high performance and long duration while it has no negative influence on circumstance environment. The uniqueness of this system could be:

- bubble-free and fluctuation-free

- possibility to deal with multi-channel flows with a single pump

- decrease the internal volume from reservoir to chip since no pump is involved

2.6. V-model and Target Specifications
A V-model that can illustrate our design process is shown in Figure 2.19. This model has been modified to fit the plan of this project and the processes in the orange dash line are the focus. Blue arrows in this model represent a sub-cycle and the later operation depends on the change of the previous operation. The design cannot proceed to the next step until the results of the previous cycle are completely determined.

According to V-model, system integration and architecture will be the focus and challenge in this project, and no components design will be involved unless there are no suitable off-the-shelf components to choose from.

Design specifications are illustrated in Table 2.9. It is divided into three categories including all important specifications regarding the requirements analysis in Section 2.1.

Design challenges below are summarized according to the survey about OOC applications and state-of-the-art OOC platforms.
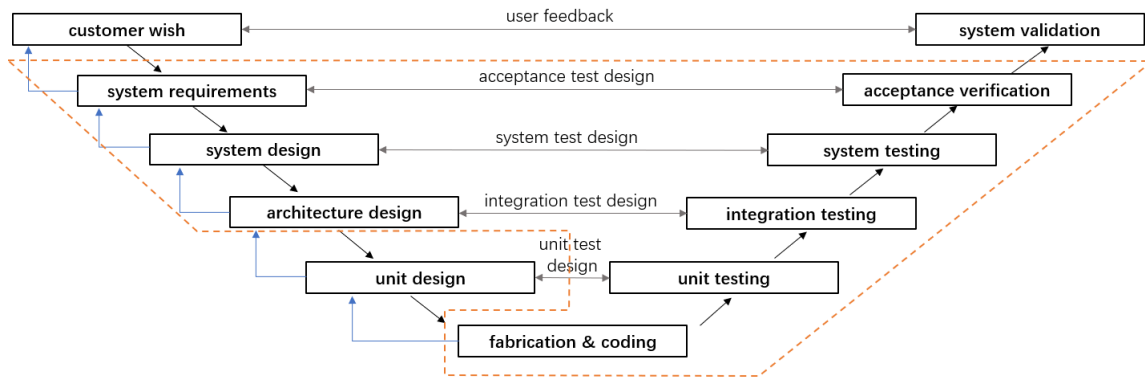
Figure 2.19: V-model, orange dash line represents the design focus[97].

Table 2.9: Target specifications of Organ-On-Chip platform

Category	Variety	Target specifications
Application	Number of channel	Min. 1
	Flow type	Liquid,gas,vacuum
	Volumetric flow range	1 – 50 µL/min
	Other	Bubble-free,fluctuation-free
Architecture	Size	400 × 250 × 150 mm
	Internal volume	3 mL
	Weight	5 kg
Control	Function	Stepped automatic control
	Input-output relation	Linear
	Resolution	1 µL/min
	Flow stability	Min. 0.5% RSD
	Settling time	<5 s

- To choose/design relevant compatible components to satisfy the specs.

- To develop a scheme for a portable, compact system compatible to use under an optical microscope, and fit inside an incubator for OOC experiments.

- To provide interconnections (fluidic and electrical) for various components.

- To design circuits and automatically control the required flow rate precisely.

3

Portable and Integrated Organ-On-Chip Platform Using Off-the-shelf Components

Portable and Integrated Organ-On-Chip Plaform Using Off-the-shelf Components[†]

Abstract-Due to the developments of microfluidics, Organ-On-Chip (OOC) technology is developing rapidly in recent years. Microflow plays a vital role in OOC applications, thus a microfluidic platform that can generate high-quality flow is always needed. However, the exisiting OOC systems contain bulky peripheral components, incompact design and low-quality fluid flow (bubbles and fluctuations). To deal with these issues, a portable and integrated OOC flow control platform system has been developed. The platform is designed for three kinds of popular Organ-On-Chip models: Lung-On-Chip, Gut-On-Chip and Tissue-On-Chip,and is able to change the fluid (both liquid and gas) automatically and control their flow rate on the chip. The fluid actuation is based on a stable vacuum tank and therefore can create high-quality flow without fluctuations. PID flow controllers are used to maintain the desired flow rate under a constant pressure difference created by the vacuum pump. By integrating with other predetermined off-the-shelf components with small footprints, the platform realized is 290mm long, 240mm wide and 220mm tall, and weighs 4.8 kg in total. The system is highly modular with capability to exchange the necessary components, and can be placed under the optical microscope (upright or inverted) to monitor inside the microfludic chip without having to disconnect. It can also be placed inside an incubator for continuous controlled fluid flow in the OOC. The system works on a rechargeable battery that can be easily changed to support long-term cell culture. The setup consumes a minimum of 7.2W and a maximum of 11.5W power.

1 Introduction

Organ-On-Chip(OOC) technology has become a vital branch of *In vitro* biomedical tests recently.[1] Microfluidic technology plays a significant role on OOC research in recent years for its irreplaceable advantages such as better simulation of real physiological environment[2], easier manipulation of single cells[3], capacity to control more parameters accurately due to laminar flow[4], etc.

Although microfluidic technology brings significant benefits to OOC research, challenges arose due to requirements of precise flow, automatic control and compatibility of advanced experimental instruments such as microscopes and incubators. One of the important challenges is the lack of portable microflow-generation device which is applicable to most OOC experiments.[5] Researchers mostly chose to assemble commercial off-the-shelf devices to make a dedicated experimental setup for typical microfluidic chips.[6,7] It is not only inefficient but also not portable, movable and wasteful of experimental resources. Most of these dedicated systems can be classified into four categories based on pumping principles, which are syringe pumping system, peristaltic pumping system and pressure-based system. Syringe pumps are widely used in low-flow situations for the stability of generated flow and extremely low flow range which can satisfy most OOC experiments.[8] Nevertheless, the pressure from piston could press gas into liquid and form large number of bubbles in flow, which will create serious damage to cells or even kill them.[9] Peristaltic pumps can be easily purchased, integrated and controlled for microflow generation but will create severe fluctuation in flow which is unwanted in OOC experiments as well.[10-12] Positive pressure becomes more popular in recent OOC studies since the flow is stable and bubble-free property is better than syringe pumping systems . Nevertheless, gas could still dissolve in liquid under positive pressure[13] and system portability will be decreased since most commercial controllers need huge tanks to create pressure. Even though drawbacks appear in pressure based
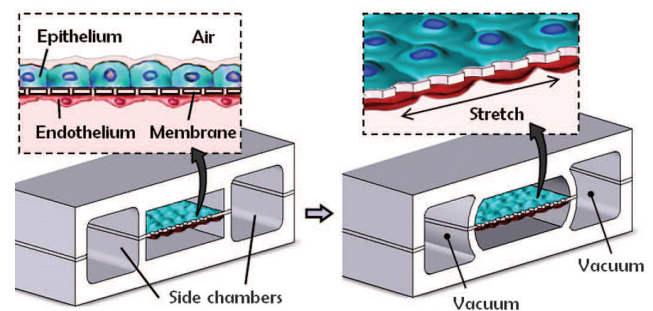
Fig. 1 Micro-manufactured Lung-On-Chip model with two fluid channels in the middle and two side vacuum channels.[16] Stretch of the middle membrane is created by the collapse of thin wall of vacuum chamber, which can mimic breathing motion of alveolus with deposited lung cells on both sides of membrane. Depending on different applications, upper channel allows both liquid and gas flow while lower channel always contains liquid flow.

systems, its capacity to create low rate, high precision flow is still attractive. In 2014, Li *et al.* has developed a smartphone-controlled handheld microfluidic handling system for single-layer pressure-driven systems and multilayer elastomeric microfluidics. It uses pressure difference to drive flows so that the flow perfused into the chip is fluctuation-free. However, since no flow controller is integrated, precision control of microflow becomes a problem when using this system in most OOC applications.[14] Nowadays, with the help of flow controllers from Bronkhorst High-Tech B.V., low rate flow can be controlled with high precision under certain pressure differences inside flow path.[15] Furthermore, there is a possibility that bubble-free flow can be created by a vacuum pump locating at the end of the flow path and the bulky gas tank can be eliminated as well.

In 2010, Huh *et al.* developed a new kind of OOC model, consisting of two flow channels and a middle membrane in a sandwich structure. Besides, two side chambers are constructed beside flow channels and separated by a thin wall structure. This novel design allows a stretch effect on the middle membrane by applying vacuum in side chambers, which can be used to mimic physiological motions of human organs.[16] Then, a large num-

ber of studies followed this idea and other OOC models such as Gut-On-Chip also referred to this design.[17] Therefore, a microfluidic handling device that can be used in this new type of OOC model has broad application prospects.

In this paper, an integrated OOC platform has been designed, implemented and characterized. The system is not only portable and compatible with microscopes and incubators, but is also able to generate high-performance flow both for gas and liquids and take over popular OOC experiments automatically. Compared to conventionally using peristaltic pumps or syringe pumps, the experimental process will be more convenient, the possibility of sample contamination will be reduced, and the high-quality fluid flow could make the experimental results more accurate.

2 Materials and Methods

2.1 Materials

Most functional components used in the setup are off-the-shelf. The names, brands and model keys of core components are listed in Table 1. Rest of the accessories such as electronics and connectors are listed in supplementary material.

Table 1 List of the functional components in the platform.

Name	Brand	Model Key
Vacuum pump	SURGEFLO	-
Shut-off valve	-	-
Vacuum gauge	Festo	VAM-63-V1/0-R1/4-EN
Manual valve	Festo	HE-2-QS-6
Switch valve	IDEX	MHP7970-500-4
3-way valve	SMC	VDW-250-1-G-2-01F-A-Q
Flow controller	Bronkhorst	ML120V21-BAD-CC-K-S-DA-A0V
Pressure controller	Bronkhorst	IQP-600C-1K5A-AAD-00-V-A

2.2 Methods

This OOC platform consists of a fluidic handling system, an electronic system and a mechanical system. Among them, the fluidic handling system contains a stable vacuum subsystem, a cyclic vacuum subsystem and a flow control subsystem. The first step to develop the entire platform was designing and prototyping the fluid handling system, second step was to systematically integrate electronic system, and the last step was finalizing the development by designing the layout and fabricating a base to support all components. In order to test the applicability and performance on handling microfluid, a protocol of Lung-On-Chip experiment was created and several tests has been carried out.

2.2.1 Stable vacuum subsystem

The stable vacuum subsystem is one of the most important part in the platform since it is the only factor to drive microflow. In this paper, the vacuum pressure level is expressed as a negative value lower than the atmospheric pressure. Different from normal vacuum system, this system can create an extremely stable vacuum by added a shut-off valve and waste reservoir (regarded as a vacuum tank) before the peristaltic vacuum pump in the flow path. All attempts aim to create a stable vacuum environment in a close container which is disconnected to the vacuum pump after closing the shut-off valve. The complete logic and timeline are shown as follows.

(1) 0th second: Turn on shut-off valve. The shut-off valve is

a solenoid valve and can be held on by applying 24 V_{DC} from the battery.

(2) 2nd second: Turn on vacuum pump and suck the air in waste reservoir for 5 seconds. This procedure ensures a maximum vacuum (-610mbar) according to the performance of vacuum pump.

(3) 7th second: Turn off shut-off valve to seal off the vacuum inside waste reservoir.

(4) 8th second: Turn off vacuum pump. Vacuum fluctuations, vibration, noises and power consumption will all be eliminated. The reason why shut-off valve is turned off 1 second before turning off the vacuum pump is to prevent vacuum leakage while they are turned off at the same time. In some cases, the vacuum pump will not be turned off but supplied by an alternative power source which has a voltage drop from 12 V to 5 V. This is mainly used to maintain a vacuum for cyclic vacuum channel with low power consumption, noise and vibration.

Due to the flow from source reservoir, the vacuum will slowly drop to atmosphere level after some while. The time to maintain a suitable vacuum is dependent on the flow rate and fluid type applied to both channels. In most Organ-On-Chip applications, low flow rate is used for liquid, which can always ensure the vacuum level for over 10 minutes. As long as the vacuum level drop to certain levels that are lower than the requirement, the vacuum creation procedure will be automatically restarted to prevent any drift of flow rate. The time gap of the restart can be set by the end-user, but it is supposed to restart the procedure every 10 minutes in order to fit into most situations. In some cases that gas flow is necessary, it is supposed to set the gas flow rate to a lowest value (1.3 mL/min) and set the time interval for vacuum generation to 5 minutes or keep the shut-off valve on and allow the vacuum pump (supplied by 5 V Power) to suck gas continuously from the waste reservoir since gas flow could exhaust the vacuum fast. Since the vibration and noise of the vacuum pump powered by 5 V is negligible, the performance of the flow would not be influenced.

2.2.2 Cyclic vacuum subsystem

Typically, cyclic vacuum is widely used to support the displacement of soft on-chip structures, which can be used to mimic real motion in human organs. For instance, popular Lung-On-Chip[16] models have side channels connected to vacuum source and can stretch the middle membrane under a certain frequency ($\approx$0.2 Hz) in order to mimic the breathing motion of alveolus.

Although it is not difficult to develop a cyclic vacuum system without footprint and complexity restrictions, most schemes are not applicable in a portable system since it is better to use fewer components to realize cyclic vacuum. Based on the stable vacuum system used to realize flow actuation, several restrictions appear while designing the cyclic vacuum system. Some tricks are used as well to solve problems under the restrictions.

(1) No extra pumps should be involved in the system. Therefore, cyclic vacuum system should be connected between the vacuum pump and shut-off valve so that it does not influence the vacuum level created in waste reservoir for the flow control subsystem. a manual shut-off valve should be added in the path of cyclic vacuum subsystem as well since a large leakage may appear during the stable vacuum is being created. After the stable vacuum is created, the voltage of power supplying
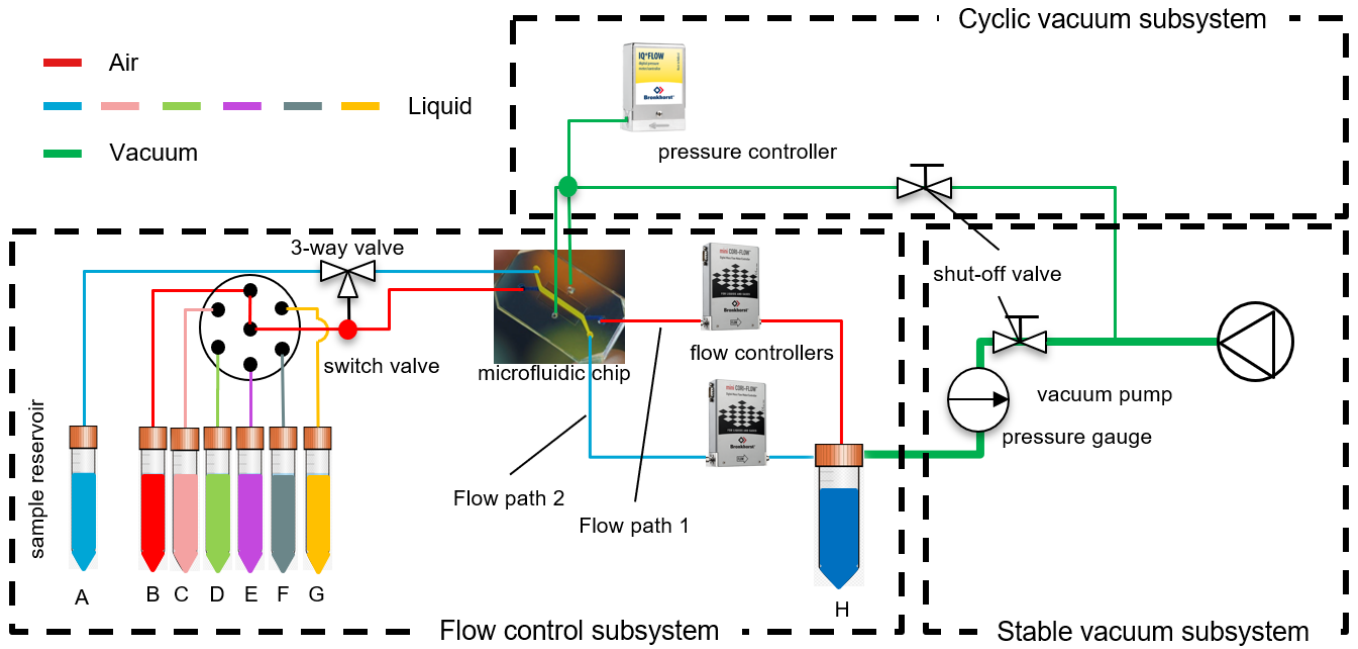
Fig. 2 Schematic diagram of fluidic handling system. It contains three subsystems, including a stable vacuum subsystem, a cyclic vacuum subsystem and a flow control subsystem. A stable vacuum created at the end can suck samples in different reservoirs to waste reservoir passing through switch valves, microfluidic chip and flow controllers. Flow rate of both flow paths can be controlled separately by controlling the valve in the flow controllers. A switch valve and a 3-way valve are used to change media for both channels automatically. After a stable vacuum is created in waste reservoir H, the shut-off valve will be closed and the vacuum pump will continue working under a power saving mode (5 V power supply) to create vacuum for cyclic vacuum system. By controlling the valve in pressure controller, vacuum level in on-chip vacuum chamber can be cyclically controlled at desired vacuum level and frequency. The system is highly modular and can be used for Organ-On-Chip models without vacuum requirement or with single channel as well by simply disconnecting and blocking certain channels.

vacuum pump should be switched from 12 V to 5 V to reduce power consumption, vibration and noise.

(2) Only one pressure controller is allowed, and the vacuum created by the pump is always fixed. One critical requirement of cyclic vacuum used in Organ-On-Chip situation is that the vacuum should be applied and realized in the second level, which means a port for supplying new air is always needed. In most cases, two controllers should be added separately at inlet and outlet of a vacuum container so that the air can be supplied or sucked out regularly by controlling the airflow volume at both inlet and outlet.[18] However, it is also realistic to use one pressure controller to cyclically control the vacuum level in a close space. According to Figure 2, the on-chip vacuum chamber is connected to both vacuum pump and atmosphere with a T-junction. A pressure controller is integrated between the vacuum chamber and atmosphere, which can detect the vacuum level near chamber and control it at a desired value. If a high vacuum is needed, solenoid valve in the controller will be nearly closed so that the vacuum level in chamber becomes close to the level created by the vacuum pump. If a low vacuum is required, the valve can be opened up more to allow more air to enter the vacuum chamber, so that the vacuum level in the chamber will be decreased. By using feedback control in the pressure controller, vacuum level can be cyclically changed with a cyclic setpoint programmed in the microcontroller.

(3) Vacuum level should be applicable for Organ-On-Chip applications. In other words, the vacuum level should be in the range from -100 mbar to -280 mbar. Since the pump can always create a vacuum over -500 mbar, the maximum vacuum in chamber can always satisfy the requirements. Nevertheless, low vacuum could be restricted by the size of orifice in pres-

sure controller since a vacuum can always appear even though the valve in controller is fully opened if the orifice is too small. This will be discussed in next section based on the results of performance tests.

2.2.3 Flow control subsystem

The principle of flow control of the platform is described in equation (1).

$$Q = \frac{\Delta P}{R_{flow}} \tag{1}$$

Q represents the volumetric flow rate in flow path. ΔP is the pressure difference between the beginning and end of the flow path. R_{flow} can be regarded as the total hydrodynamic resistance in the flow path.

According to the scheme in Figure 2, equation (1) can be converted to

$$Q = \frac{\Delta P_{Const}}{R_{Tubing} + R_{Switch} + R_{Splitter} + R_{Chip} + R_{Controller}} \tag{2}$$

Here, ΔP_{const} is a fixed vacuum in waste reservoir created by the vacuum pump. Among all hydrodynamic resistances, only the one from flow controller is adjustable but it is enough to tune the flow rate Q by changing only one kind of hydrodynamic resistance.[19]

The off-the-shelf flow controller used in this platform is Cori-FLOW controller from Bronkhorst. It consists of a flow sensor and a piezoelectric valve. The sensor in controller is based on Coriolis principle[20] and can detect the flow rate 10 times more precisely than conventional temperature method. Since it is a mass-flow controller, detected mass flow rate should be converted to volumetric flow rate if necessary for better com-

prehension, which means, for different fluids with various density, same mass flow rate may represents different volumetric flow rates. As for the controller in flow path 1, both liquid and gas should be sensed and controlled. Thus, the volumetric flow rate should be higher than liquid due to lower density. The integrated valve is made from piezoelectric material, thus applying different voltages to the material can create displacement, which can be used to proportionally control the hydrodynamic resistance in valve channel, and then control the flow rate in the entire flow path. Feedback control technology is used here to reach desired flow rate, prevent outside disturbances and maintain flow rate under a changing pressure difference. By programming the setpoint in Arduino Mega 2560 microcontroller, a signal representing desired flow rate can be input into the flow controller and an output signal can be read by the microcontroller after the process of PID algorithm in the flow controllers. The performance of the flow rate control is dependent on the PID settings in flow controller, which will be discussed in the next section.

Another novel design in flow control subsystem is integration of switch valve and 3-way valve for multi-sample manipulation. The switch valve used in this instrument is a 7-port valve from IDEX including 6 inlet ports and 1 outlet port. Each inlet port is connected to a source reservoir containing typical samples. By applying 4-line BCD control signals, stepper motor in the valve can rotate to desired position. Additionally, a sensor is integrated in switch valve to detect the open port and send feedback signal to Arduino microcontroller to tell users the number of the open port and the status of the valve. Based on this method, different samples can be changed and perfused into the chip automatically. A problem appears regarding a double-channel system since only one switch valve is allowed in a portable Organ-On-Chip platform. Therefore, a 3-way valve is integrated into flow path 2 to allow the samples from flow path 1 flowing into both channels. For instance, DI water and ethanol can enter both channels by switching 3-way valve from reservoir A to switch valve so that both flow paths can be conditioned at the same time. It is also allowed to perfuse different samples to flow path 2 while path 1 is closed. Nevertheless, sample contained in flow path 1 should always be the same one in flow path 2 if path 1 is working, except sample in reservoir A is perfused.

2.2.4 Arduino-based electronic system

Arduino Mega 2560 is selected as the microcontroller of the Organ-On-Chip platform. There are two reasons for this selection: (1) The platform should automatically work in incubator, which means no connection from outside controller such as laptop is allowed. (2) It is easy to program and can be easily comprehended by end-user. A dedicated 9 V battery is used to supply power for the microcontroller.

Seven off-the-shelf devices are being controlled logically and powered by typical voltage levels, including the vacuum pump, shut-off valve, 3-way valve, switch valve, two flow controllers and one pressure controller. Except for vacuum pump, other devices are supplied by 24 V power. Vacuum pump can be powered under 12 V or 5 V depending on its application so that power consumption, noise and vibration can be reduced. A relay is integrated to switch between 12 V and 5 V voltage and is triggered by the digital signal (0/5 V) from microcontroller.
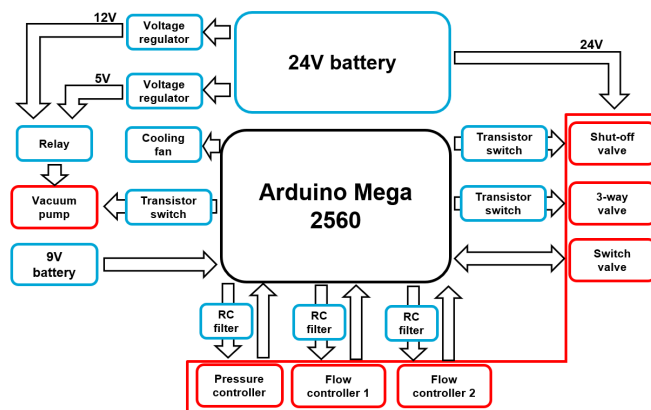
Fig. 3 Schematic diagram of Arduino-based electronic system. Blue blocks represents electronics while read blocks represents flow control components. Shut-off valve, 3-way valve and switch vacuum pump are controlled by transistor switches while transistors are triggered by Arduino digital ports. RC filters are used to create pure analog setpoints for controllers. Vacuum pump can be supplied by 12 V or 5 V power switched by a relay. Apart from vacuum pump, all other devices are powered by 24 V voltage. For convenience of illustration, other components except vacuum pump are wrapped by red 'L'-shaped area, which means that they are all driven by 24 V voltage.

A 24 V battery is used to supply power for all other devices except microcontroller and cooling fan. Two voltage regulators are integrated to convert 24 V voltage to 12 V and 5 V voltage. Cooling fan is used to cool down the regulators since the temperature may exceed the limit value while cyclic vacuum is being implemented.

Two flow controllers are connected by a 9-pin D sub connector to self-designed PCB. Among 9 pins of each connector, 6 pins are used including three ground pins, one +24 V pin, one setpoint pin and one readout pin. The readout pin is connected directly to analog input ports of microcontroller to read the sensed flow rate from flow controller, while setpoint pin should be connected to a RC filter before it goes to analog output port of microcontroller. This is because Arduino microcontroller can only send out PWM signals from analog output ports, which is not suitable for the controller with AD converters since it should be controlled by pure analog signal.

Three transistor switches are integrated to logically control the shut-off valve, vacuum pump and 3-way valve. Each switch consists of a transistor and a resistor. Since the transistor can be triggered by a 5 V signal from microcontroller, 24 V power can be selectively power the devices. The regulators, RC filters and transistor switches are integrated on a general purpose PCB board.

The switch valve is controlled by 4-line BCD control technology and is connected with the microcontroller by a 12-pin Molex connector. 11 pins are being used including four signal input pins (digitally control the motor), four position readout pins, two error detection pins and one ground pin. All digital control methods are based on binary algorithm and can be easily manipulated in the Arduino program.

2.2.5 System architecture

One uniqueness of this platform is the compatibility with microscopes and incubators. Since there are always enough space and no extra structure inside incubators, a portable system with a footprint of $290 \times 240 \times 220$ mm is able to fit into most in-
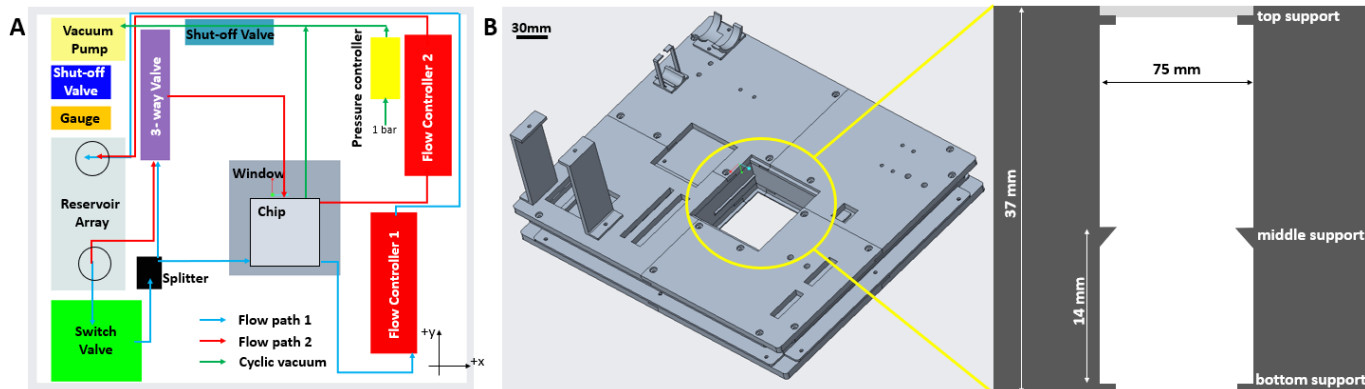
Fig. 4 Architecture of the platform. (A) Layout of the off-the-shelf components including tubings and flow path. (B) CAD model of the base. The footprint is 290 × 240 × 115 mm. Three frames on the top layer are used to fix the switch valve, gauge and vacuum pump from down to up respectively. Zoom-in view: Cross-section of the window showing how the chip can be mounted at different depths to allow focusing in the optical microscope (both inverted and up-right microscope). Three supports are designed from top to down while the top support is distributed vertically in the horizontal plane with the other two supports. The middle support is 14 mm higher than the bottom support and the footprint of the window is 75 × 75 × 37 mm.

cubators in laboratories. Nevertheless, compatibility of microscopes becomes a problem due to following factors that should be considered: (1) The platform looks neat and the footprint should be limited within a laptop size. (2) The system should be weight-balanced to reduce the risk of tipping over from the support of microscopes. (3) There should be enough space around the window which is used to accommodate chips. Otherwise, the lenses or other structures of microscopes may conflict with the components on the platform. (4) A microfluidic chip can be studied both under inverted and upright microscopes, and there should always be enough distance for focusing. (5) The layout should be considered to make the flow path as simple as possible to reduce the bending and internal volume of tubings.

Figure 4A shows the layout of the platform from the top. The base of the platform is designed to a sandwich structure where electronics including batteries, microcontroller, PCB board and most wires are placed neatly inside. Since the base is not transparent, only the PCB board is exposed to the outside world for cooling and connection of off-the-shelf components through a window. Based on this design, electronics and fluidic handling system can be separated and the platform looks neater.

According to the balance requirement, the weight of negative versus positive on x-axis, and y-axis, should be close to each other. Considering each controller is 0.9 kilogram, all other components except pressure and flow controllers are located on one side while controllers are placed on the other side. Battery, as the second heaviest component weighing 0.7 kilograms are placed at the middle part on the positive y-axis, which is balanced by a 0.45 kg switch valve at the negative side. Although there is still some weight difference between different parts on platform, it is stable enough to place it on a microscope without slip risks.

Structure compatibility is another factor that should be considered during layout design. Due to the L-shape pillar of microscope lenses, a square-shape space should be designed to accommodate any possible structures from microscopes without conflict with components on the platform. A transparent window is designed at the middle of platform so that chip can be put on top of 75 × 25 mm glass slides in window and be studied under both inverted and upright microscopes. Since

the base has a thickness of 37mm, it is not possible for inverted microscope to focus on the microfluidic chip if the chip is placed on the top surface of the base. Thus, two supports are designed in window both on the top surface and bottom surface so that the chip can be placed on alternative surface dependent on the type of microscope being used, as sub-figure (1) and (3) in Figure 4B shows. Sub-figure (2) shows that an extra support is designed at 1.4mm height from bottom to avoid insufficient focusing distance from top view due to stroke limitation of microscope platform in Z direction if chip is placed on the top surface.

In terms of the schematic diagram of fluidic handling system, flow path 1 should start from a source reservoir, pass through the switch valve, splitter, chip, flow controller 1 and reach waste reservoir at last while flow path 2 starts from a source reservoir, pass through the 3-way valve, chip, flow controller 2 and ends at the same waste reservoir. According to Fig.4A, both flow paths are extended around the central window, and the pipeline has almost no redundant bending and overlapping, which has achieved the goal of neatness and small internal volume as much as possible. A T-junction is added in cyclic vacuum subsystem to split the flow paths to chip and pressure controller respectively. A 40 mm-height block is added to support the manual shut-off valve to avoid large stress on the thick tubing connected to vacuum pump.

2.2.6 Base plate and microfluidic chip model

The base of the platform has a sandwich structure with space for accommodation of electronics in the middle. Due to the limited stroke of 3D printer, each layer should be printed separately in 4 pieces and use overlapping structures with M3 screws to combine into one complete layer. The top layer is supported by four pillars with horizontal side grooves so that some space around the base can be used to accommodate fingers while carrying the platform by hand. The window in the middle can also be regarded as a square-shape pillar which supports the top layer. The second support for placing glass slides is fabricated on this component as well.

Theoretically, it is not supposed to fix both controllers at a same base due to severe crosstalk between each other. In order to avoid it, a vibration isolation support has been fabricated

Table 2 Protocol of Lung-On-Chip experiments using Organ-On-Chip platform

Step	Process	Type of fluid
1	Conditioning	Ethanol, DI water
2	Epithelial cell seeding	Culture medium with cells
3	Endothelial cell seeding	Culture medium with cells
4	Cell culture	Culture medium
5	Breathing lung simulation	Air, Culture medium

and fixed under flow controller 2. The support consists of a base plate (1.5 mm) and a upper plate (1.5 mm) with 4 mm foam in between. the upper plate has two through holes for fixing flow controller by M5 threads. The base plate is fixed on the top of the system base by double-sided types.

In most Organ-On-Chip experiments, large hydrodynamic resistance appears due to channels with small inner diameter. In order to imitate a similar flow environment for flow performance tests, a Lung-On-Chip-like chip is fabricated and integrated. The chip base contains two tracks to accommodate Tygon tubings which has an inner diameter of 200 μm. Both ends of Tygon tubings are inserted with a needle with 300 μm outer diameter and 200 μm inner diameter so that gas leak can be prevented due to the expansion of Tygon tubings. By using Luer-lock connectors, the needle can be gas tightly connected to PTFE tubings used in the main part of the platform.

2.2.7 Protocol of a Lung-On-Chip experiment

In order to illustrate how the platform is applied to Organ-On-Chip applications and why it is unique compared to conventional instruments, a protocol of Lung-On-Chip experiment is presented below with Table 2. Schematic diagram of each step and correlative timing diagram of components can be found in supplementary material.

In most cases, Lung-On-Chip model starts from the conditioning of the chip and flow control system. Depending on different requirements, one or several liquids should be perfused into both channels step by step including Ethanol, DI water and buffer medium. Switch valve should be switched to the condition media and the 3-way valve should be switched to combine both channels and cut the flow path to reservoir A before finishing vacuum creation. At the same time, valves in both flow controllers should be fully open to allow maximum flow rate in the conditioning process. In the second step, epithelial cells should be deposited on the membrane in one channel thus the valve in the controller should be closed to prevent flow in another channel. A similar situation happens in the third step while the 3-way valve should be switched to reservoir A (turned off) and the valve in the other controller should fully close but the one closed in the second step should be opened. In the fourth stage, both channels should be separated by the 3-way valve and two different culture media are perfused into the chip respectively and the low flow rate of fluids need to be kept. Noticing that the switch valve should be switched to a new reservoir at the beginning of each step. In the last stage, the switch valve should switch the upper channel to air and the cyclic vacuum subsystem should work for mimicking the breathing motion.

The system can take over most work during the process automatically, which is hardly realized for conventional microfluidic instruments.

2.2.8 System performance tests

System performance tests can be divided into four categories: liquid flow performance test, gas flow performance test, cyclic vacuum performance test, bubble and internal volume test, which are always necessary to ensure the precise control of high-performance flow in Organ-On-Chip applications. During the first three tests, four sub-tests were implemented.

(1) Voltage-range relation test. This can be also regarded as the calibration between input signal and output value. In this test, two points need to be highlight including the controllable range and linearity. A linear system is always easier to be controlled since output signal is more predictable.

(2) Stability test. Short-term stability and long-term stability were both considered since fluctuations and long-term drift are both not desired in Organ-On-Chip applications. Each long-term stability test lasted for 100 minutes so as to ensure that convincing data can be obtained efficiently in a limited time.

(3) Settling time test. This test is performed in the form of step response. The setpoint was selected from 10 μL/min to full range. This selection is for the prevention of 'cut-off' effect of the overshoot from large flow rate to low flow rate which leads to an unintelligible graph. The criteria to judge if the flow rate or vacuum level has reached the setpoint is an error of 5%.

(4) Resolution test. Resolution test is mainly set at low flow rate and low vacuum range since these are mostly applied in Organ-On-Chip applications and resolution is usually more important in the case of small values. The tests are carried out under a square wave response with 30-second period for liquid/gas tests and 10-second period for vacuum test. This is to avoid long settling time affecting the accuracy of the results.

Bubble test was done under a microscope to check if there are bubbles inside the channel of the equivalent chip through a 30-minute duration. Due to the duration limit of the video function from the microscope, the video is 3 minutes long and can be checked in the supplementary material. Since it is difficult to observe the flow of the fluid in the video from microscope, a real-time flow chart was displayed by the controller in order to 'monitor' the flow in microchannel. Internal volume was tested by perfusing DI water from the beginning to the end of each flow path by a syringe pump in a flow rate of 500 μL/min. During the tests, all controllers were fully opened to ensure an accurate result.

3 Results and discussion

3.1 Assembled system and power consumption

The assembled setup is shown in Figure 5A and 5B. It has the length of 290 mm, width of 240 mm and height of 220 mm, with the weight of 4.8 kg. It is portable enough to be held by a single person in lab and put into incubators. As Figure 5C shows, the system can also be placed stably under a microscope without any conflict between the structures.

The power consumption of the vacuum pump under 12 V power supply is 3.12 W, which can decrease to 0.55 W under a power supply of 5 V. Moreover, vibration and noise are greatly reduced and have negligible impact on the experiment. The maximum power consumption of the Switch valve shut-off valve, 3-way valve, flow controller and pressure controller is 0.5 W, 4.8 W, 3 W, 3 W and 1.5 W respectively. Powered by a 24 V, 2000 mAh battery, the working duration of the sys-
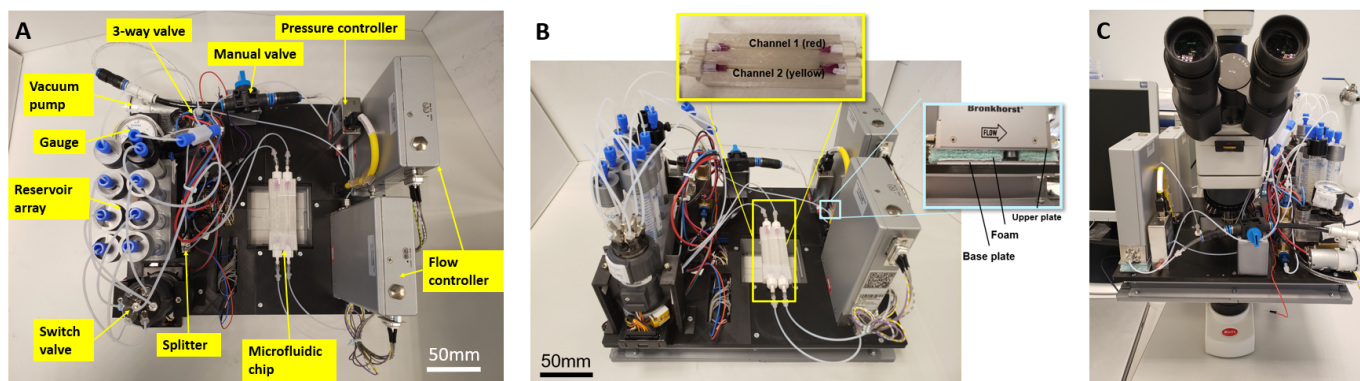
Fig. 5 Assembled platform. (A) Top view of the platform. Functional components are labelled around the image. (B) Image of the integrated Organ-On-Chip platform from a 45-degree sight. The footprint of this instrument is 290 × 240 × 220 mm while the weight is 4.8 kg. All fluidic components are placed on the top layer while electronics including the microcontroller and batteries are placed inside the base. Inset 1: self-made equivalent chip with two Tygon tubings with 200 m inner diameter mimicking real Organ-On-Chip models. Inset 2: Vibration isolation support used to avoid crosstalk of flow controllers. (C) Photo of the platform placed under a microscope (Motic, BA310Met-T Binocular). The movable plate of the microscope has 5-millimeter stroke in z direction. The platform can be placed on the plate stably without any conflict with the frame of the microscope.
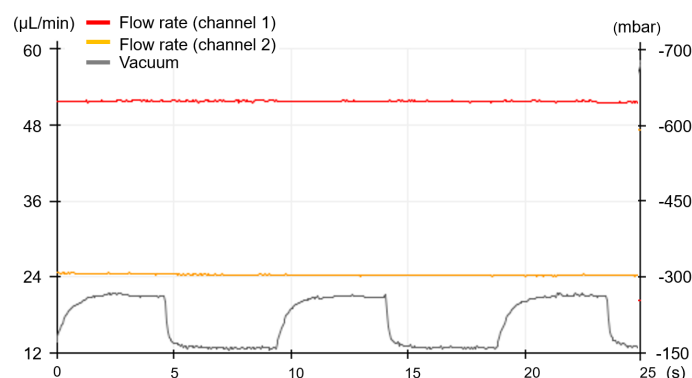

Fig. 6 Flow rate/vacuum display. The left scale shows the flow rate while the right y-axis scales the vacuum level. x-axis represents the timeline which can be expanded or shrunk by changing sampling interval. In this example, flow rate in flow path 1 is 51 μL/min while the flow rate in path 2 is 24 μL/min. Vacuum level in the cyclic vacuum subsystem is from -157 mbar to -280 mbar, which can be regarded as a popular vacuum range in Organ-On-Chip applications for mimicking organ movement.

tem varies from 3 to 10 hours based on different applications. Since the battery is easy to be replaced, theoretically, only two rechargeable batteries are enough to support experiments lasting for several days.

3.2 Display and end-user interface

When the system is connected to a computer with Arduino program, it is possible to monitor the flow rate and vacuum level in the same window, as shown in Fig. 6. The left scale shows the flow rate while the right y-axis scales the vacuum level. x-axis represents the timeline which can be expanded or shrunk by changing sampling interval. Since a window can show a fixed number of samples (500), if the sampling interval is 50 ms, the duration for each window will be 500 × 0.05, which is 25 s as shown in Fig. 6.

Other interfaces and software are still being developed. In the next phase, a Bluetooth modular may be integrated so that end-user can change parameters through the app in mobile phone and control the system without any connection between. Computer software for parameter control may also be developed in the next phase to get rid of changing parameters directly in Arduino program.

3.3 Stable vacuum generation

The maximum vacuum generated in the waste reservoir is -610 mbar when the manual valve is closed. In the case of mimicking lung breathing, the manual valve should be open to allow the following procedure of cyclic vacuum generation. Due to the increased volume of the close space and decreased gas tightness related to cyclic vacuum system, stable vacuum created in the waste reservoir becomes -420 mbar. The decreased value does not influence the flow performance of the flow control subsystem since the controller is PID based and can maintain a desired flow rate even though the pressure difference keeps dropping with time.

3.4 Liquid flow performance

Liquid flow is regarded as the most basic and important flow type in Organ-On-Chip applications. DI water, ethanol, PBS, different culture media are all in liquid form which has relatively higher viscosity, higher density, and incompressibility. As for some Organ-On-Chip applications such as Gut-On-Chip, both channels on chip should be perfused with liquid in most experiment stages. Thus, it is meaningful to test the liquid flow performance of the platform. Since both channels are controlled by the same type of flow controller and share the same vacuum source, it should not lead to obvious differences only because of the different valves integrated into each channel, which is also proved by testing both flow paths during experiments. In order to show the results more conveniently, results of flow path 1 was selected as an example in this paper.

3.4.1 Flow rate control with applied voltage

In the first stage, the relation between input voltage (setpoint) and output voltage (mass flow rate) was tested by collecting results with interval of 0.098 V of input voltage. Then, the position of each sampling point is drawn in the two-dimensional coordinate with x-axis as input voltage and y-axis as output flow, and each point is connected into a relation curve. For easier understanding, mass flow rate was converted into volu-
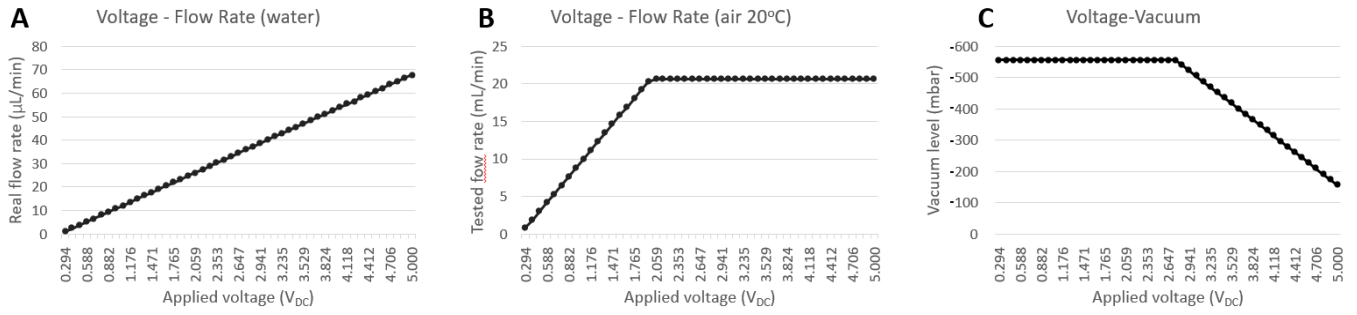
Fig. 7 Graphs showing relation between voltage and flow rate/vacuum. x-axis represents applied input voltage while y-axis scales the tested flow rate or vacuum level. (A) Linear relation between applied voltage and flow rate of DI water, which also illustrates a flow range from 1.5 to 68 μL/min. (B) Linear relation between applied voltage and flow rate of air, which also illustrates a flow range from 1.3 to 20.7 mL/min. Due to limited pressure difference, controllable range is from 0.33 to 1.96 V_{DC} in terms of input voltage. This is because the valve in controller has been fully opened while the input signal is 1.96 V_{DC}, which can also be regarded as the maximum gas flow rate this setup can reach due to the limited hydrodynamic resistance. (C) Linear relation between applied voltage and vacuum level, which also illustrates a vacuum range from -157 to -556 mbar. The controllable range is from 2.75 to 5 V_{DC} in terms of input voltage. The saturation in cyclic vacuum system is because of the maximum vacuum created by the vacuum pump, which means the valve in the pressure controller has been fully closed while input voltage is 2.75 V_{DC}.

metric flow rate by equation (3). This test can be considered as a calibration of the flow controllers in the platform. It is always needed to do this calibration since the fluidic and electrical environment are all much different than those during the tests before being sent out of the factory.

$$Q_V = \frac{1000 \times Q_M}{60 \times \rho} \quad (3)$$

Here, Q_M represents the mass flow rate and Q_V is the volumetric flow rate. ρ represents the density of the fluid. '1000' and '60' shows that there is a conversion between the unit of flow controller (g/h) and this platform (μL/min). The density of DI water used in the test is regarded as 1 g/cm^3.

From end-user's perspective, input voltage applied to flow controllers should be converted into a number that can be processed by Arduino microcontroller by equation (4).

$$V_{in} = \frac{5 \times N}{255} \quad (4)$$

V_{in} is the input voltage applied to flow controllers while N represents the number that should be set in Arduino program.

Fig. 7A shows the relation between input voltage from Arduino to controller and the volumetric flow rate reached in system after PID process. This is a linear relation which fits the function of the flow controller. In other words, the flow rate is easier to be controlled and more predictable based on the relation between the number input by users and the reached flow rate. Nevertheless, one issue appears in terms of the slope and flow range of this relation.

Regarding DI water as the liquid flowing into the system, the flow range should be 0.83-83 μL/min, which is larger than the range tested in reality (1.5-68 μL/min). Converted into input voltage and output voltage, it shows 5 V input voltage matching a 4.4 V output voltage after PID process. In order to eliminate the influence of self-designed circuit, flow controller was connected to an independent circuit. The ground wire and 0 V wires were connected to two different batteries. However, the experimental results did not change. Then, the equivalent chip and switch valve connected before the flow controller were removed, which means that only the flow controller was integrated in the flow path and the pressure difference between the inlet and outlet reached the maximum value (-610 mbar) of the

platform. In this condition, there was no change of the relation, which indicates that optimization of flow path and equipment cannot reduce the error in this vacuum environment. Based on the above tests, this may be due to the steady-state error caused by a smaller pressure difference (0.6 bar) compared to the test environment (10 bar) before leaving the factory. Some meaningful methods to do the troubleshooting in next phase are increasing the value of integrator or applying a large positive pressure difference into the system (ideally 10 bar). Fortunately, even if the controllable maximum value decreases, users can still accurately control the flow rate based on the calibrated line graph. Another issue is the minimum flow rate the platform can control. Since the flow rate in monitor drops to zero if the target flow rate is set lower than 1.5 μL/min for DI water, it is not difficult to deduce that there might be two possible facts behind this result. (1) The valve in the flow controller is fully closed if the setpoint is set below 0.33 V. (2) Flow rate is too small for the sensor to detect even though there are still fluid flows in the system. Thus, it is supposed to use another flow sensor to detect the flow rate while the setpoint is set lower than 0.33 V. The desired flow sensor used to test the flow rate could be μ-FLOW series from Bronkhorst[21] which can detect 10 times lower flow rate compared to Cori-FLOW series used in the platform.

3.4.2 Settling time, resolution, stability tests

Fig. 8A illustrates the settling time of liquid flow. The settling time is 4.5 seconds from low to high flow rate and more tests show that there is no great difference if the upper and lower bound changes. Although these data is barely acceptable in most applications, the following experimental results prove that it is meaningful to optimize the PID parameters of the system to improve its flow control performance in the next phase.

Fig. 8D shows the resolution of the liquid being controlled at minimum flow rate. The red thick lines are used to average the real flow rate in order to show the trend of flow rate change more clearly. The resolution is 0.6 μL/min due to the limitation of AD converter in Arduino microcontroller. In other words, the resolution is limited by the resolution of the value which can be input in Arduino program.

Long-term stability shows that there is no drift throughout a 100-minute test. Both long and short-term stability illustrate
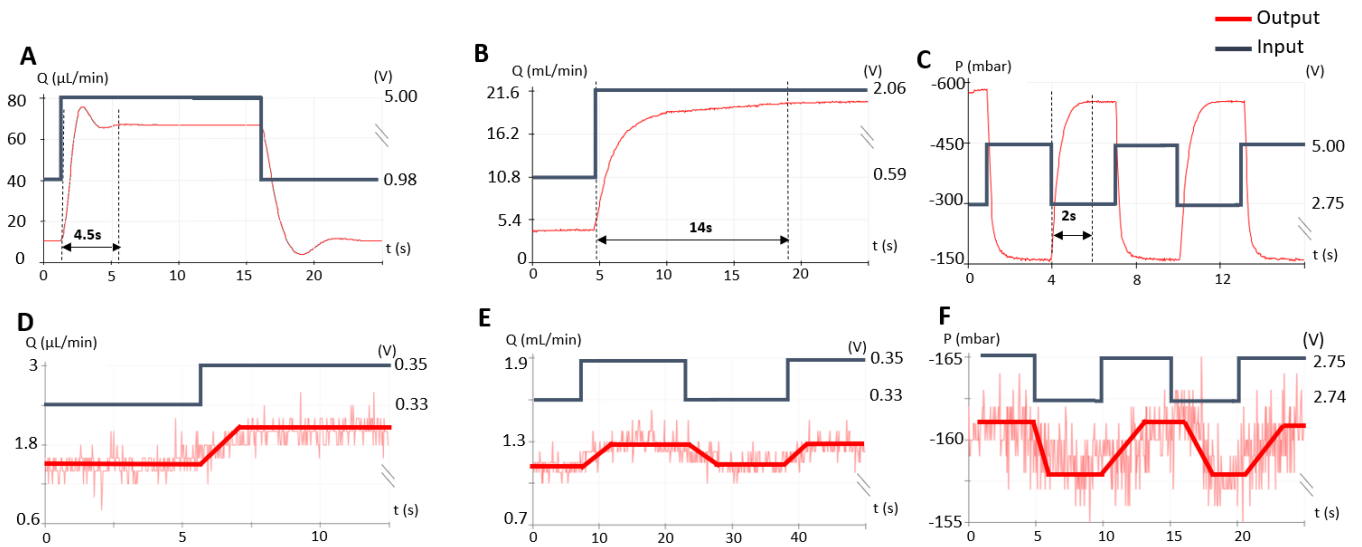
Fig. 8 Performance of the platform in terms of liquid flow, gas flow and cyclic vacuum. Purple line represents the input level while red line is the response from the system. In each graph, left y-axis represents the scale of output value (volumetric flow rate in subfigure (A)(B)(D)(E), vacuum level in subfigure (C)(F)) while input value (electrical signal) is scaled by y-axis at the right. The x-axis is the time scale with the unit of second. In graph (D)(E)(F), the red thick lines are used to average the real flow rate in order to show the trend of flow rate change more clearly. (A) Step response of liquid flow with settling time of 4.5 s. (B) Step response of gas flow with settling time of 14 s. (C) Step response of cyclic vacuum with settling time of 2 s. (D) Step response of liquid flow at minimum flow rate with a resolution of 0.6 μL/min. (E) Square wave response of gas flow at minimum flow rate with a resolution of 0.2 mL/min. (F) Square wave response of cyclic vacuum at minimum vacuum level with a resolution of 3 mbar.

that the minimum Relative Standard Derivative is 0.58%. It is worth mentioning that the accuracy of this result is limited by the AD converter located in Arduino microcontroller. Because the AD converter has only eight bits, the value which are smaller than converter resolution is approximately calculated, which means the actual stability is better than the current calculation result. In order to get more accurate results, it is recommended to use AD converters with a higher number of bits.

3.5 Gas flow performance

Voltage-flow rate relation, stability, resolution and settling time performances of gas flow were tested as well. Flow path 1 was tested since gas flow is only necessary for one channel.

According to Fig. 8B, controllable flow range of air in flow path 1 is from 1.3 to 20.7 mL/min, with input signal linearly increasing from 0.33 to 1.96 V_{DC}. A 'cut-off' effect appearing in the relation is due to limited pressure difference, which means the highest mass flow rate of airflow is 1.5 g/h. In other words, the proportional control valve in the controller is fully open at 1.96 V input signal. Thus, even if larger input signal is sent into the controller, the valve cannot be opened more and flow rate cannot be increased out of the controllable range. Similar to liquid flow, there is the same static error from output to input signal.

Settling time of gas flow is 14 s from 4 to 20.7 mL/min. Repeated tests show that not much difference appears if the upper and lower bound changes during the settling time test. The result is not satisfactory, because the system is too slow to prevent from outside disturbances. Compared to liquid flow, there is no overshoot in gas flow system which means the proportional factor should be tuned larger and more integrators should be added to decrease the static error and increase the speed. Nevertheless, there is a trade-off when tuning PID factors since better performance of gas flow may lead to extremely large over-

shoot of liquid flow or even cause instability. It is supposed to give more weight factor for liquid flow performance while optimizing the PID controller since liquid flow is wider used in Organ-On-Chip applications.

Resolution of gas flow is 0.2 mL/min which is limited by the resolution of setpoint signal from the microcontroller. Long-term stability shows that there is no drift for low rate airflow. Nevertheless, as for high rate flow, the vacuum in the waste reservoir could be consumed fast and a drift will always appear. Thus, it is supposed to apply a lowest gas flow rate (1.3 mL/min). If it is necessary to apply gas flow with a higher flow rate, please turn on the shut-off valve in stable vacuum system and supply vacuum pump by 5 V power so that a stable vacuum source can always be connected to the end of the flow path. Short-term stability shows a minimum relative standard derivative (RSD) of 0.56%, which is limited by the resolution of AD converter. This is similar to liquid flow situation.

3.6 Cyclic vacuum performance

In order to test the cyclic vacuum performance, the shut-off valve of stable vacuum system should keep closed and manual shut-off valve in cyclic vacuum subsystem was opened to form a clear flow path.

The voltage-vacuum relation shown in Fig. 7C illustrates a linear relation between input voltage and output vacuum. A cut-off effect similar to gas flow relation appears as well due to the limited vacuum created by the vacuum pump. Since the full range of pressure controller is 0.05 - 0.9 bar(a), and compared to vacuum range created by vacuum pump (0.44 - 1 bar(a)), it can detect a much higher vacuum which exceeds the capacity of vacuum pump. It indicates that the vacuum level cannot increase more since the valve in pressure controller has been fully closed at an input signal of 2.75 V_{DC}. Furthermore, the vacuum level is -157 mbar with a fully open valve in the pressure con-
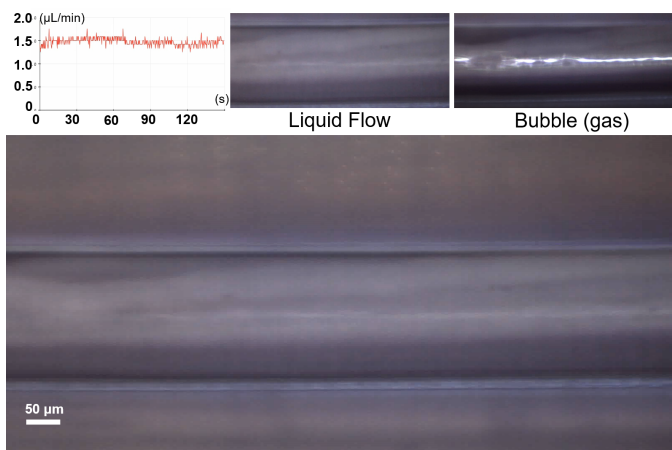
Fig. 9 Screenshot of the video of bubble test. The photo at bottom is the window to monitor bubbles in video. A comparison of liquid flow and bubble shown under microscope is placed at the upper right corner. It is apparent that bubble has more reflection and looks darker. The flow chart in the upper left corner is used to monitor the flow rate in the channel in real-time. Since it is difficult to observe the flow of the fluid in the complete video located in the supplementary material, it is meaningful to use the flow controller to monitor the flow rate in real-time. In next phase, microbeads can be added into the flow so that the flow rate can be efficiently monitored in real-time which is more intuitive.

troller. It is because of a 0.3 mm orifice diameter which limits the lowest vacuum in the chamber, and a larger orifice should decrease the lowest vacuum. It is worth mentioning that the pressure detected is not the same as that in on-chip vacuum chamber due to the T-junction in flow path and the hydrodynamic resistance between orifice and on-chip chamber, which can be optimized by connecting shorter and thicker tubings between the pressure controller and the chip.

Settling time of cyclic vacuum was tested by responding to square wave with a period of 6 seconds. The result shows that the settling time is 2 s from lowest to highest vacuum level, which is fast enough for mimicking lung breathing motion. Large overshoot was prevented by adding an extra step with $4\,V_{DC}$ setpoint for 10 ms, which is regarded as input shaping technology. Resolution of cyclic vacuum system is 3 mbar. It is limited by the resolution of setpoint as well. The flow stability of vacuum is 0.16% RSD with no drift in the long term.

3.7 Bubble and internal volume test

According to Fig. 9, gas shows a darker color with more reflection under microscope. During the entire 3-minute video, no macro bubbles and microbubbles appear in channel, which indicates the system is bubble-free if all connectors and components are gas-tight. It is worth mentioning that the vacuum-based system has higher requirements for air tightness than the positive pressure system. Since the connection between the chip and the platform is dedicated, the bubble-free performance is highly dependent on the connection of the chip even though other parts have excellent gas tightness.

The internal volume of flow path 1 is 2.1 mL while flow path 2 has 2.5 mL internal volume. The space in the tubings accounts for a large proportion of the internal volume in both flow paths. The reason why path 2 has more internal volume is due to the large volume in the 3-way valve which is based

Table 3 Specifications of the portable OOC platform

Category	Variety	Specifications
Application	Channel amount	2(flow)+1(vacuum)
	Flow type	Liquid,gas,vacuum
	Flow range/ Vacuum range	1.5 – 68 μL/min[1]
		1.3 – 20.7 mL/min[2]
		-157 – -556 mbar
	Other	Bubble-free,fluctuation-free
Architecture	Size	290 $\times$ 240 $\times$ 220 mm
	Internal volume	Channel 1: 2.1 mL
		Channel 2: 2.5 mL
	Weight	4.8 kg
Control	Function	Stepped automatic control
	Controllability	Linear
	Resolution	Liquid[1]: 0.6 μL/min
		Gas[2]: 0.2 mL/min
		Vacuum: 3 mbar
	Flow stability	Liquid[1]: min. 0.58% RSD
		Gas[2]: min. 0.56% RSD
		Vacuum: min. 0.16% RSD
	Settling time	Liquid[1]: 4.5 s
		Gas[2]: 14 s
		Vacuum: 2 s

1: DI water is the tested liquid. The value may change if the liquid changes.
2: The fluid is the air in a temperature of 20°C.

on solenoid working principle. Therefore, it is a meaningful attempt to try to replace it with a diaphragm valve with a smaller internal volume in next stage. It is worth mentioning that sample with lower volume can be used in this platform as well. For instance, a sample with 0.5 mL volume can still be perfused precisely into the chip if the following steps are taken place. (1) Flow PBS into the system. (2) Use switch valves and flow sample medium into the system. (3) Switch back to PBS to create a continuous flow which allows the reaction of the sample medium for a long time under a low flow rate situation.

4 Conclusions

A portable and integrated microfluidic handling system for Lung-On-Chip, Gut-On-Chip, Tissue-On-Chip applications has been designed, fabricated and characterized. Vacuum is used to generate pressure difference and Cori-FLOW controllers are integrated to precisely control low rate flow for both liquid and gas. Compared to existing designs, the system has the following uniqueness: (1) This platform is applicable for three kinds of popular Organ-On-Chip models including Lung-On-Chip, Gut-On-Chip and Tissue-On-Chip, where two liquid/gas channels and one vacuum channel are involved, which means a large amount of Organ-On-Chip experiments using similar chip models can be taken over by the platform. (2) A logically controlled vacuum pump and a shut-off valve are used to create stable vacuum inside a waste reservoir locating at the end of the flow path, which eliminates flow fluctuations, mechanical vibrations, power consumption and noises created by the vacuum pump. (3) Two Cori-FLOW Controllers from Bronkhorst High-Tech B.V. are integrated in order to precisely control liquid

flow at an extremely low flow rate (1.5 μL/min - 68 μL/min, DI water at 20°C) and flow rate can be tuned automatically by setting target flow rates at certain times in the program. (4) A 6-port switch valve (From IDEX HEALTH & SCIENCE) and a 3-way valve are used to automatically change input samples perfused into both channels. (5) Architecture of the platform is designed to be highly compatible with different microscopes and incubators. The footprint is 290 × 240 × 220 mm, and the weight is 4.8 kilograms therefore it is easy for a single person to carry this platform. (6) Arduino Mega 2560 microcontroller is used to automatically control all off-the-shelf components without connection with outside world devices such as laptops and monitors. (7) The platform can support long-term experiments with a large-volume rechargeable battery which can also be easily reassembled into the system. specifications of the setup are listed in Table 3.

Short-term future work to improve the system includes: (1) Flow controller troubleshooting of static error and optimization of the feedback control performance. (2) Adding temperature control into the system to sense and control the temperature in chip precisely. (3) GUI design (user interface) (4) System validation using real Organ-On-Chip models. (5) Improving the modularity of the system, and make it more convenient to increase or decrease the number of flow channels and specific functions. (The upgrading scheme of the platform on current stage is in the supplementary material). (6) Design and integration of a standard microchip packaging setup which can solve the risk of bubble generation from the root cause. Based on these improvements, shrinking the entire system into a microsystem with similar function and performance is highly attractively in long-term future, which could be realized by shrinking off-the-shelf components into micro-fabricated devices and integrating all electronics onto a microchip.

Notes and references

1 N. Convery and N. Gadegaard, *Micro and Nano Engineering*, 2019, **2**, 76 – 91.

2 J. E. Sosa-Hernández, A. M. Villalba-Rodríguez, K. D. Romero-Castillo, M. A. Aguilar-Aguila-Isaías, I. E. García-Reyes, A. Hernández-Antonio, I. Ahmed, A. Sharma, R. Parra-Saldívar and H. M. N. Iqbal, *Micromachines*, 2018, **9**, year.

3 T. Porkka-Heiskanen, *Current Opinion in Neurobiology*, 2013, **23**, 799 – 805.

4 A. U. R. Aziz, C. Geng, M. Fu, X. Yu, K. Qin and B. Liu, *Bioengineering (Basel, Switzerland)*, 2017, **4**, year.

5 C. D. Chin, V. Linder and S. K. Sia, *Lab Chip*, 2007, **7**, 41–57.

6 A. Carraro, W.-M. Hsu, K. M. Kulig, W. S. Cheung, M. L. Miller, E. J. Weinberg, E. F. Swart, M. Kaazempur-Mofrad, J. T. Borenstein, J. P. Vacanti and C. Neville, *Biomedical Microdevices*, 2008, **10**, 795–805.

7 P. de Haan, M. A. Ianovska, K. Mathwig, G. A. A. van Lieshout, V. Triantis, H. Bouwmeester and E. Verpoorte, *Lab Chip*, 2019, **19**, 1599–1609.

8 K. Kaarj and Yoon, *Micromachines*, 2019, **10**, 700.

9 W. Zheng, Z. Wang, W. Zhang and X. Jiang, *Lab Chip*, 2010, **10**, 2906–2910.

10 C. K. Byun, K. Abi-Samra, Y.-K. Cho and S. Takayama, *ELECTROPHORESIS*, 2014, **35**, 245–257.

11 A. Kalantarifard, E. A. Haghighi and C. Elbuken, *Chemical Engineering Science*, 2018, **178**, 238 – 247.

12 Fluigent, *Comparison between peristaltic, syringe and pressure pumps for microfluidic applications*, https://www.fluigent.com/microfluidic-expertise/advantages-of-pressure-based-microfluidic/system-comparison-for-microfluidic-applications/.

13 Y. Wang, D. Lee, L. Zhang, H. Jeon, J. Mendoza-Elias, T. Harvat, S. Hassan, A. Zhou, D. Eddington and J. Oberholzer, *Biomedical microdevices*, 2012, **14**, 419–26.

14 B. Li, L. Li, A. Guan, Q. Dong, K. Ruan, R. Hu and Z. Li, *Lab on a Chip*, 2014, **14**, 4085–4092.

15 Bronkhorst, in *Instruction Manual: mini CORI-FLOW ML120 (Ultra) Low Flow Coriolis Mass Flow Meters / Controllers*, 2018.

16 D. Huh, B. D. Matthews, A. Mammoto, M. Montoya-Zavala, H. Y. Hsin and D. E. Ingber, *Science*, 2010, **328**, 1662–1668.

17 H. Kim, D. Huh, G. Hamilton and D. Ingber, *Lab on a Chip*, 2012, **12**, 2165–2174.

18 Bronkhorst, in *Instruction Manual: EL-PRESS^{TM} series Digital Pressure Meters and Controllers*, 2020.

19 K. W. Oh, K. Lee, B. Ahn and E. P. Furlani, *Lab Chip*, 2012, **12**, 515–545.

20 A. Mehendale, *PhD thesis*, University of Twente, Netherlands, 2008.

21 Bronkhorst, *-FLOW MASS FLOW METERS AND CONTROLLERS FOR LIQUIDS*, https://www.bronkhorst.com/int/products/liquid-flow/mu-flow/.

4

Conclusion and Recommendations

4.1. Conclusion

Table 4.1: Obtained specifications of Organ-On-Chip platform

Category	Variety	Target specifications	Obtained specifications
Application	Number of channel	Min. 1	2(flow)+1(vacuum)
	Flow type	Liquid,gas,vacuum	Liquid,gas,vacuum
	Volumetric flow range/ Vacuum range	1 – 50 μL/min (DI water)	1.5 – 68 μL/min (DI water) 1.3 – 20.7 mL/min (air,°C) -157 – -556 mbar
	Other	Bubble-free,fluctuation-free	Bubble-free,fluctuation-free
Architecture	Size	400 × 250 × 150mm	290 × 240 × 220mm
	Internal volume	3 mL	Channel 1: 2.1 mL Channel 2: 2.5 mL
	Weight	5 kg	4.8 kg
Control	Function	Stepped automatic control	Stepped automatic control
	Input-output relation	Linear	Linear
	Resolution	1 μL/min (DI water)	Liquid: 0.6 μL/min (DI water) Gas: 0.2 mL/min (air,°C) Vacuum: 3 mbar
	Flow stability	Min. 0.5% RSD (DI water)	Liquid: min. 0.58% RSD (DI water) Gas: min. 0.56% RSD (air,°C) Vacuum: min. 0.16% RSD
	Settling time	<5 s (DI water)	Liquid: 4.5 s (DI water) Gas: 14 s (air,°C) Vacuum: 2 s

In this thesis, a portable and highly modular fluidic handling system for Lung-On-Chip, Gut-On-Chip, Tissue-On-Chip applications has been presented. The thesis contains literature research of commercial instruments and Organ-On-Chip devices, scheme design and selection, system architecture in mechanical and electrical domain to system performance tests and optimization schemes. By using

a stable vacuum source created by vacuum pump and precision flow controllers, fluctuation-free and bubble-free flow can be generated for Organ-On-Chip applications. Automatic sample replacement can be realized by switch valves and no disassemble procedure needs to be scheduled during experiments due to the compatibility with optical microscope and size fitting inside an incubator. The target and final specifications of the platform are shown in Table 4.1.

4.2. Recommendations and Future Work

According to the results of performance tests, main issue of the platform in this phase is the performance of the controllers, which have not been fully optimized for the specific environment of the vacuum system in the platform. According to the long settling time of airflow and large overshoot of liquid flow, a trade-off needs to be considered when balancing the performance of both flows (liquid and gas) using PID technology. Integration of a temperature controller also matches users' requirements since a typical physiological environment in human body can be simulated without putting the system in incubator and connections between computers and batteries can remain to support clear monitor and smoother experiments (without the changing battery). In order to provide a more convenient end-user interface, a GUI should be created both on computer and mobile phone so that all parameters can be manipulated in an intelligible software/app. A bluetooth module can be integrated to communicate with mobile devices. It is also necessary to improve the modularity of the system and integrate a standardized chip packaging device, because it can not only improve the convenience of upgrade, but also solve the problem of air bubbles caused by air leakage from the root cause. Last but not least, it is supposed to apply the platform for real Organ-On-Chip experiments and validate the system in all aspects.

It is worth mentioning that this system is the first version (Version 0) in the entire i-Microfluidic project, the final goal of this project is to create an integrated microsystem which can obtain similar function and performance to version 0. It might be realized by not only shrinking the size of off-the-shelf components to micro-scale by using micro-fabrication technology but also converting the bulky microcontroller and PCB board into microchips. This should be a promising research direction in the next few years.

5

Reflection

This chapter contains the details of the author's personal scientific pursuit while executing this thesis work, which is divided into five categories including 'Research goal and scheme selection', 'Component selection and purchase', 'Experimental concerns', 'COVID-19 related issue' and 'Acknowledgement'. A graph is also attached in the end to illustrate the timeline and milestones of this project.

5.1. Research Goal and Scheme Selection

Compared to most master projects, this project seems unique since it is hard to find a research focus on a typical scientific field, but concern more about the design, integration and test of a complete system. This makes me feel confused at the beginning when a research question was planned to be put forward. Perhaps it is because my thinking was bounded by the traditional academic research methodology. I put forward some research focus related to the subject, for example, 'the relation between system architecture and internal volume', 'PID control optimization of a flow control system', or ' optimization of microfluidic interconnections'. Nevertheless, I found that these topics are not realistic without the scheme design and prototyping of the basic version of the platform. In other words, as the start of a long-term project, it is significant to design and implement the first version of the system before detailed research in future work. After being instructed by my supervisors, I realized that I could focus on the design and implementation of the entire system and regarded it as a design project rather than a research project.

The final version of the system was decided in May. At the beginning (end of 2109), the plan was finishing the system design in 3 steps, including 'single-channel version design', 'multi-channel version design' and 'specific version design'. The specific version means that some extra functions such as cyclic vacuum or electrodes could be integrated to make the system more versatile. However, the application range was not decided since I would like to cover Organ-On-Chip applications as more as possible and finally I realized that it was too ambitious for a one-year master project. During that time, I did not give a proper evaluation of the lead time of Bronkhorst flow controller thus never finished the first version until I got the controllers in July. My supervisors and I realized this fact in May and made another schedule. At that point, single-channel version without flow controllers had been implemented, thus, we decided to skip the step of controller integration but went on to add more channels and cyclic vacuum functions before controllers arrived. The application range of this system has also changed from fuzzy to clear, which targets three kinds of popular Organ-On-Chip models including 'Lung-On-Chip', 'Gut-On-Chip, 'Tissue-On-Chip'.

Venturi pumping system was the scheme I decided to use right after the literature research presentation (end of 2019). This scheme has lots of unique advantages but what I did not realize at that time were the disadvantages which can be found in Section 2.6. Considering these disadvantages, I decided to drop this idea in February 2020 and decided to replace the Venturi pump with a normal centrifugal vacuum pump. This made me realize that I need to judge my ideas critically at all times, instead of deciding to use it just because of its shining advantages. Fortunately, I had prepared lots of alternatives in the design process, which is why I can find a solution quickly at that time.

5.2. Component Selection and Purchase

In this project, there is a type of work that I have never known before, that is, contacting the company in person and purchasing off-the-shelf experimental instruments and materials. At first, I did not realize the difficulty of this job, but after I started to purchase equipment, I realized that it was more complicated than my expectation. This job includes components selection, communication via suppliers, asking for quotations, purchasing with funds, after-sales service contact, etc., all of which require strong communication and planning ability. In addition, I purchased more than 10 sets of equipment and materials and spent nearly 7000 euros, which requires these abilities to ensure the smooth progress of the project.

Two components were given up during system design, including a proportional control valve from *Burkert* and a mini vacuum pump from *NITTO KOHKI*. The vacuum pump was dropped since a smaller and cheaper pump was used to compare with the NITTO pump and I found that the cheaper one is more suitable for my system even though it may have poorer quality. The Burkert valve was tested not suitable for liquid. Even though I wrote liquid in the quotation, the company did not deliver the proper one. I negotiated with them for several times but failed to replace with a new one eventually, which made me realize that I need to be 100 percent clear when choosing equipment and writing the quotation, and there should be no ambiguity to avoid unnecessary misunderstanding. Luckily, there is a PID controlled valve in Bronkhorst controller thus no external valves is needed in my system. This was not realized since I only considered using the sensor and would like to design a PID controller by myself. However, I found it is unnecessary work at present and it is a proper decision to use a flow controller rather than a flow sensor and an external valve.

5.3. Experimental Concerns

Safety concern is one of the most important thing during experiments. This is shown significantly during three procedures, which are pump selection, battery selection and electrical experiments. One reason that I gave up the Venturi idea is that gas tanks are needed to actuate the pump. Since only tiny tanks are allowed in my system, most commercial mini gas cylinders have thin walls with hundreds of bars of pressure inside, which means a small hit may break the cylinder and damage the lab or even hurt the researcher. As for battery selection, a NiMH battery was selected rather than Li-ion battery due to a better safety property even though Li-ion batteries has a smaller footprint. During prototyping procedure, since standard wires had not arrived, lab cables with clamps were used to connect different pins which means there were possibility to short the devices during tests. Now, I realize that it was a wrong way to do experiments since all safety issues should be got rid of during the experiments.

I found that I should use standardized interfaces as much as possible during the prototyping procedure. I was anxious to verify the feasibility of the idea, thus often could not wait to buy standardized connections to conduct experiments, which not only led to the above security problems but also greatly increased the workload of interface replacement in the later stage. After I purchased IDEX switch valve, I did not wait for purchased standard Molex interface as instructed, but directly soldered wires on 12 pins. My idea was that since it took at least one week to get a new interface, I could verify whether the equipment was feasible by this week. But it took me a long time to clean these pins when I needed to change to a standardized interface one month later. If I did not rush to verify the equipment but focus on other work at first, these unnecessary tasks would be omitted.

I sometimes spent time looking for components during experiments. This may be because I did not store the purchased components in an orderly way. Although I have classified different types of components, due to the limitation of storage boxes, there were too many small components in the same box, which were easy to confuse me. To sum up, I need to work more methodically in future research and pay great attention to the neatness of the experimental environment.

5.4. COVID-19 Related Issue

This project was influenced by COVID-19, which is mainly reflected in the following aspects.

(1) Due to the outbreak of the epidemic in Europe, students were restricted from entering the department. Due to the careful consideration of my tutor, I did not enter the laboratory for experiments from the beginning to the end of March but only did some simple online work such as component selection and scheme design, which delayed my project for several weeks.

(2) Meetings were changed to online, which made it more difficult to communicate with supervi-

sors. Moreover, due to public measures, meetings were reduced, and some milestones could not be determined, which indirectly led to the extension of components purchase duration.

(3) Lab restrictions were put forward and I had to register for the lab every day in order to keep the progress. Since some labs were very popular, I had to move my setup to the other room which was less crowded. Sometimes, I had to use instruments in the crowded room, therefore, I needed to carry my setup carefully through both rooms.

Fortunately, I overcame these challenges due to my flexible plan and self-encouragement.

5.5. Conclusion

Based on the above and the entire project, I have the following insights and have made significant improvements and upgrades in the following aspects:

(1) It is necessary to have clear design goals and pay attention to the design of milestones in the research process to make the planning and implementation of the project more orderly.

(2) Safety is a point that cannot be ignored in the process of the project. It is necessary to examine whether the experimental design and equipment selection are safe at all times.

(3) It is important to focus not only on design and experiment itself but also on the presentation, communication and negotiation abilities.

In this project, I have done the following excellently, leading to the success of this project.

(1) I never delayed my work, and always finished tasks before the deadline in strict accordance with the schedule.

(2) Flexible project planning makes my project less affected by COVID-19, even if it is an experimental based project.

(3) The active communication with my supervisors made me take fewer detours in design, which not only saved my time but also improved the results of the design.

5.6. Acknowledgement

First, I would like to be appreciated for my supervisors, Dr. Murali Ghatkesar, Gürhan Özkayar and Prof. Joost Lötters. During the project, they put forward lots of creative ideas and suggestions, which greatly contributes to the success of the project.

Second, I want to be grateful to Rob and all PME lab technicians since they have a lot of experience in the practical operation, and gave me many suggestions on the design and operation of the experiments.

Third, I want to thank my family, girlfriend and friends. They financially support my master project and have been encouraging me to overcome challenges during the epidemic and reduced my anxiety all the time.

Last but not least, thanks to TU Delft and Bronkhorst High-Tech B.V. for their financial support for this project.

5.7. Timeline

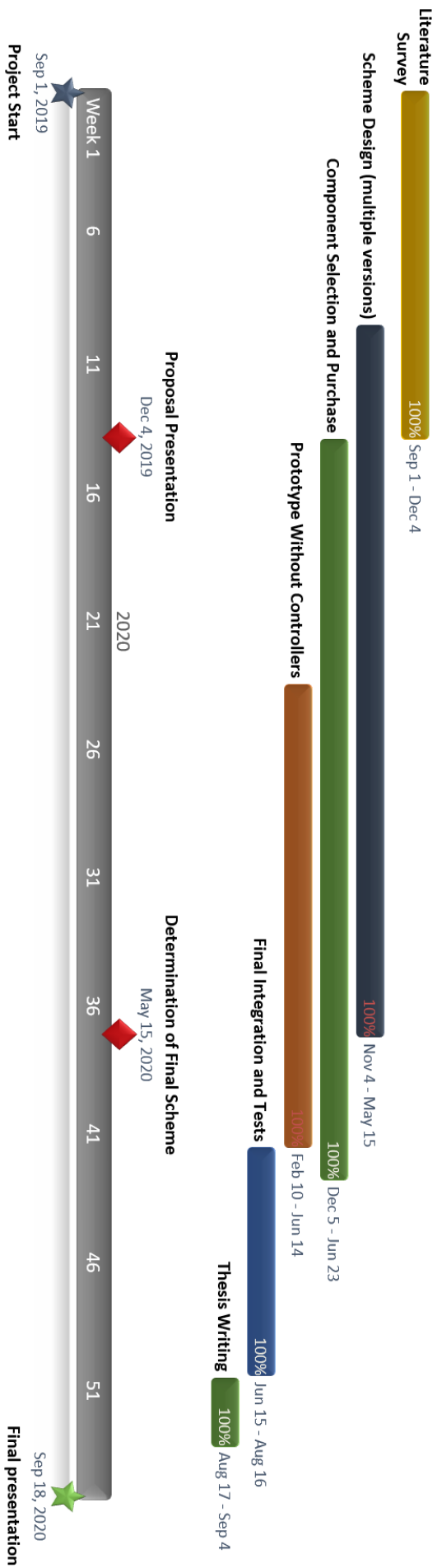The timeline and milestones of the project are shown clearly from the graph in the next page.

Figure 5.1: Timeline of the master project

Bibliography

[1] P. N. Joshi, "Cells and organs on chip—a revolutionary platform for biomedicine," in *Lab-on-a-Chip Fabrication and Application* (M. Stoytcheva and R. Zlatev, eds.), ch. 5, Rijeka: IntechOpen, 2016.

[2] K. Yum, S. G. Hong, K. E. Healy, and L. P. Lee, "Physiologically relevant organs on chips," *Biotechnology Journal*, vol. 9, no. 1, pp. 16–27, 2014.

[3] J. T. Morgan, J. A. Wood, N. M. Shah, M. L. Hughbanks, P. Russell, A. I. Barakat, and C. J. Murphy, "Integration of basal topographic cues and apical shear stress in vascular endothelial cells," *Biomaterials*, vol. 33, no. 16, pp. 4126 – 4135, 2012.

[4] J. Shemesh, I. Jalilian, A. Shi, G. Heng Yeoh, M. L. Knothe Tate, and M. Ebrahimi Warkiani, "Flow-induced stress on adherent cells in microfluidic devices," *Lab Chip*, vol. 15, pp. 4114–4127, 2015.

[5] W. Zheng, Z. Wang, W. Zhang, and X. Jiang, "A simple pdms-based microfluidic channel design that removes bubbles for long-term on-chip culture of mammalian cells," *Lab Chip*, vol. 10, pp. 2906–2910, 2010.

[6] D. Huh, H. Fujioka, Y.-C. Tung, N. Futai, R. Paine, J. B. Grotberg, and S. Takayama, "Acoustically detectable cellular-level lung injury induced by fluid mechanical stresses in microfluidic airway systems," *Proceedings of the National Academy of Sciences*, vol. 104, no. 48, pp. 18886–18891, 2007.

[7] K. Brower, R. Puccinelli, C. Markin, T. Shimko, S. Longwell, B. Cruz, R. Gomez-Sjoberg, and P. Fordyce, "An open-source, programmable pneumatic setup for operation and automated control of single- and multi-layer microfluidic devices," *HardwareX*, vol. 3, pp. 117–134, 2018. cited By 8.

[8] Elveflow, "Ob1 mk3 – microfluidic flow control system." `https://www.elveflow.com/microfluidic-flow-control-products/flow-control-system/pressure-controller/`.

[9] Fluigent, "Lineup™ series." `https://www.fluigent.com/product/microfluidic-components/lineup-series/`.

[10] Micronit, "Micronit has partnered with fluigent to design a compact platform for any organ-specific experiment.." `https://www.micronit.com/products/compact-organ-on-a-chip-platform.html`.

[11] C. K. Byun, K. Abi-Samra, Y.-K. Cho, and S. Takayama, "Pumps for microfluidic cell culture," *ELECTROPHORESIS*, vol. 35, no. 2-3, pp. 245–257, 2014.

[12] A. Kalantarifard, E. A. Haghighi, and C. Elbuken, "Damping hydrodynamic fluctuations in microfluidic systems," *Chemical Engineering Science*, vol. 178, pp. 238 – 247, 2018.

[13] SciTechDaily, "New organ on a chip lets researchers study effects of drugs and disease." `https://scitechdaily.com/organ-on-a-chip-lets-researchers-study-effects-of-drugs-and-disease/`.

[14] N. Convery and N. Gadegaard, "30 years of microfluidics," *Micro and Nano Engineering*, vol. 2, pp. 76 – 91, 2019.

[15] P. Nigam, *Cells and Organs on Chip—A Revolutionary Platform for Biomedicine*. 06 2016.

[16] T. Porkka-Heiskanen, "Sleep homeostasis," *Current Opinion in Neurobiology*, vol. 23, no. 5, pp. 799 – 805, 2013. Circadian rhythm and sleep.

[17] R.-C. K. e. a. Sosa-Hernández JE, Villalba-Rodríguez AM, "Organs-on-a-chip module: A review from the development and applications perspective.," *Micromachines (Basel)*, vol. 9, no. 10, p. 536, 2018.

[18] F. M. Y. X. Q. K. L. B. Aziz AUR, Geng C, ". the role of microfluidics for organ on chip simulations.," *Bioengineering (Basel)*, vol. 4, no. 2, p. 39, 2017.

[19] H. Avci, F. Doğan Güzel, S. Erol, and A. Akpek, "Recent advances in organ-on-a-chip technologies and future challenges: A review," *Turkish Journal of Chemistry*, vol. 42, pp. 587–610, 05 2017.

[20] A. Grosberg, P. W. Alford, M. L. McCain, and K. K. Parker, "Ensembles of engineered cardiac tissues for physiological and pharmacological study: Heart on a chip," *Lab Chip*, vol. 11, pp. 4165–4173, 2011.

[21] S. Vassanelli, "Brain-chip interfaces: The present and the future," *Procedia Computer Science*, vol. 7, pp. 61 – 64, 2011. Proceedings of the 2nd European Future Technologies Conference and Exhibition 2011 (FET 11).

[22] M. Mastrangeli, S. Millet, T. ORCHID partners, and J. van den Eijnden-van Raaij, "Organ-on-chip in development: Towards a roadmap for organs-on-chip," *ALTEX - Alternatives to animal experimentation*, vol. 36, pp. 650–668, Oct. 2019.

[23] A. Carraro, W.-M. Hsu, K. M. Kulig, W. S. Cheung, M. L. Miller, E. J. Weinberg, E. F. Swart, M. Kaazempur-Mofrad, J. T. Borenstein, J. P. Vacanti, and C. Neville, "In vitro analysis of a hepatic device with intrinsic microvascular-based channels," *Biomedical Microdevices*, vol. 10, pp. 795–805, Dec 2008.

[24] K. Viravaidya and M. L. Shuler, "Incorporation of 3t3-l1 cells to mimic bioaccumulation in a microscale cell culture analog device for toxicity studies," *Biotechnology Progress*, vol. 20, no. 2, pp. 590–597, 2004.

[25] A. Sin, K. C. Chin, M. F. Jamil, Y. Kostov, G. Rao, and M. L. Shuler, "The design and fabrication of three-chamber microscale cell culture analog devices with integrated dissolved oxygen sensors," *Biotechnology Progress*, vol. 20, no. 1, pp. 338–345, 2004.

[26] G. J. Mahler, M. B. Esch, R. P. Glahn, and M. L. Shuler, "Characterization of a gastrointestinal tract microscale cell culture analog used to predict drug toxicity," *Biotechnology and Bioengineering*, vol. 104, no. 1, pp. 193–205, 2009.

[27] D. A. Tatosian and M. L. Shuler, "A novel system for evaluation of drug mixtures for potential efficacy in treating multidrug resistant cancers," *Biotechnology and Bioengineering*, vol. 103, no. 1, pp. 187–198, 2009.

[28] J. H. Sung and M. L. Shuler, "A micro cell culture analog (µcca) with 3-d hydrogel culture of multiple cell lines to assess metabolism-dependent cytotoxicity of anti-cancer drugs," *Lab Chip*, vol. 9, pp. 1385–1394, 2009.

[29] S. N. B. . D. E. Ingber, "Microfluidic organs-on-chips," *Nature Biotechnology*, vol. 32, pp. 760–772, 2014.

[30] Fluigent, "Comparison between peristaltic, syringe and pressure pumps for microfluidic applications." `https://www.fluigent.com/microfluidic-expertise/advantages-of-pressure-based-microfluidic/system-comparison-for-microfluidic-applications/`.

[31] Wikipedia, "Growth medium." `https://en.wikipedia.org/wiki/Growth_medium`.

[32] B. Zhang and M. Radisic, "Organ-on-a-chip devices advance to market," *Lab Chip*, vol. 17, pp. 2395–2420, 2017.

[33] D. D. Nalayanda, C. Puleo, W. B. Fulton, L. M. Sharpe, T.-H. Wang, and F. Abdullah, "An open-access microfluidic model for lung-specific functional studies at an air-liquid interface," *Biomedical Microdevices*, vol. 11, p. 1081, May 2009.

[34] S. G. M. Uzel, R. J. Platt, V. Subramanian, T. M. Pearl, C. J. Rowlands, V. Chan, L. A. Boyer, P. T. C. So, and R. D. Kamm, "Microfluidic device for the formation of optically excitable, three-dimensional, compartmentalized motor units," *Science Advances*, vol. 2, no. 8, 2016.

[35] D. Huh, B. D. Matthews, A. Mammoto, M. Montoya-Zavala, H. Y. Hsin, and D. E. Ingber, "Reconstituting organ-level lung functions on a chip," *Science*, vol. 328, no. 5986, pp. 1662–1668, 2010.

[36] D. Huh, "A human breathing lung-on-a-chip," *Annals of the American Thoracic Society*, vol. 12 Suppl 1, pp. S42–4, 03 2015.

[37] "Dedication," in *Laminar Flow Forced Convection in Ducts* (R. Shah and A. London, eds.), p. v, Academic Press, 1978.

[38] E. Gutierrez, B. G. Petrich, S. J. Shattil, M. H. Ginsberg, A. Groisman, and A. Kasirer-Friede, "Microfluidic devices for studies of shear-dependent platelet adhesion," *Lab Chip*, vol. 8, pp. 1486–1495, 2008.

[39] G. M. Walker, J. Sai, A. Richmond, M. Stremler, C. Y. Chung, and J. P. Wikswo, "Effects of flow and diffusion on chemotaxis studies in a microfabricated gradient generator," *Lab Chip*, vol. 5, pp. 611–618, 2005.

[40] N. Langerak, "Optimization of fluid flow in a novel organ chip," *M.Sc Thesis, Utrecht University*, 2019.

[41] E. W. K. Young, A. R. Wheeler, and C. A. Simmons, "Matrix-dependent adhesion of vascular and valvular endothelial cells in microfluidic channels," *Lab Chip*, vol. 7, pp. 1759–1766, 2007.

[42] P. de Haan, M. A. Ianovska, K. Mathwig, G. A. A. van Lieshout, V. Triantis, H. Bouwmeester, and E. Verpoorte, "Digestion-on-a-chip: a continuous-flow modular microsystem recreating enzymatic digestion in the gastrointestinal tract," *Lab Chip*, vol. 19, pp. 1599–1609, 2019.

[43] S. Wang, E. Li, Y. Gao, Y. Wang, Z. Guo, J. He, J. Zhang, Z. Gao, and Q. Wang, "Study on invadopodia formation for lung carcinoma invasion with a microfluidic 3d culture device," *PLoS ONE*, vol. 8, no. 2, 2013. cited By 31.

[44] K. Benam, R. Villenave, C. Lucchesi, A. Varone, C. Hubeau, H.-H. Lee, S. Alves, M. Salmon, T. Ferrante, J. Weaver, A. Bahinski, G. Hamilton, and D. Ingber, "Small airway-on-a-chip enables analysis of human lung inflammation and drug responses in vitro," *Nature Methods*, vol. 13, no. 2, pp. 151–157, 2016. cited By 154.

[45] D. Huh, D. Leslie, B. Matthews, J. Fraser, S. Jurek, G. Hamilton, K. Thorneloe, M. McAlexander, and D. Ingber, "Erratum: A human disease model of drug toxicity-induced pulmonary edema in a lung-on-a-chip microdevice (science translational medicine doi: 10.1126/scitranslmed.3004249)," *Science Translational Medicine*, vol. 10, no. 449, 2012. cited By 0.

[46] H. Kim, D. Huh, G. Hamilton, and D. Ingber, "Human gut-on-a-chip inhabited by microbial flora that experiences intestinal peristalsis-like motions and flow," *Lab on a Chip*, vol. 12, no. 12, pp. 2165–2174, 2012. cited By 554.

[47] H. Kim, H. Li, J. Collins, and D. Ingber, "Contributions of microbiome and mechanical deformation to intestinal bacterial overgrowth and inflammation in a human gut-on-a-chip," *Proceedings of the National Academy of Sciences of the United States of America*, vol. 113, no. 1, pp. E7–E15, 2016. cited By 212.

[48] H. Kim and D. Ingber, "Gut-on-a-chip microenvironment induces human intestinal cells to undergo villus differentiation," *Integrative Biology (United Kingdom)*, vol. 5, no. 9, pp. 1130–1140, 2013. cited By 225.

[49] H. Takeuchi, J. Thongborisute, Y. Matsui, H. Sugihara, H. Yamamoto, and Y. Kawashima, "Novel mucoadhesion tests for polymers and polymer-coated particles to design optimal mucoadhesive drug delivery systems," *Advanced Drug Delivery Reviews*, vol. 57, no. 11, pp. 1583–1594, 2005. cited By 218.

[50] Y.-C. Toh, T. Lim, D. Tai, G. Xiao, D. Van Noort, and H. Yu, "A microfluidic 3d hepatocyte chip for drug toxicity testing," *Lab on a Chip*, vol. 9, no. 14, pp. 2026–2035, 2009. cited By 257.

[51] O. Farokhzad, A. Khademhosseini, S. Jon, A. Hermmann, J. Cheng, C. Chin, A. Kiselyuk, B. Teply, G. Eng, and R. Langer, "Microfluidic system for studying the interaction of nanoparticles and microparticles with cells," *Analytical Chemistry*, vol. 77, no. 17, pp. 5453–5459, 2005. cited By 134.

[52] P. Van Midwoud, M. Merema, E. Verpoorte, and G. Groothuis, "A microfluidic approach for in vitro assessment of interorgan interactions in drug metabolism using intestinal and liver slices," *Lab on a Chip*, vol. 10, no. 20, pp. 2778–2786, 2010. cited By 113.

[53] C.-T. Ho, R.-Z. Lin, W.-Y. Chang, H.-Y. Chang, and C.-H. Liu, "Rapid heterogeneous liver-cell on-chip patterning via the enhanced field-induced dielectrophoresis trap," *Lab on a Chip*, vol. 6, no. 6, pp. 724–734, 2006. cited By 221.

[54] M. Esch, G. Mahler, T. Stokol, and M. Shuler, "Body-on-a-chip simulation with gastrointestinal tract and liver tissues suggests that ingested nanoparticles have the potential to cause liver injury," *Lab on a Chip*, vol. 14, no. 16, pp. 3081–3092, 2014. cited By 107.

[55] K.-J. Jang, A. Mehr, G. Hamilton, L. McPartlin, S. Chung, K.-Y. Suh, and D. Ingber, "Human kidney proximal tubule-on-a-chip for drug transport and nephrotoxicity assessment," *Integrative Biology (United Kingdom)*, vol. 5, no. 9, pp. 1119–1129, 2013. cited By 294.

[56] K.-J. Jang and K.-Y. Suh, "A multi-layer microfluidic device for efficient culture and analysis of renal tubular cells," *Lab on a Chip*, vol. 10, no. 1, pp. 36–42, 2010. cited By 273.

[57] E. Weinberg, M. Kaazempur-Mofrad, and J. Borenstein, "Concept and computational design for a bioartificial nephron-on-a-chip," *International Journal of Artificial Organs*, vol. 31, no. 6, pp. 508–514, 2008. cited By 22.

[58] U. Marx, H. Walles, S. Hoffmann, G. Lindner, R. Horland, F. Sonntag, U. Klotzbach, D. Sakharov, A. Tonevitsky, and R. Lauster, "'human-on-a-chip' developments: A translational cutting-edge alternative to systemic safety assessment and efficiency evaluation of substances in laboratory animals and man?," *Alternatives to Laboratory Animals*, vol. 40, no. 5, pp. 235–257, 2012. PMID: 23215661.

[59] S. Kim, H. Lee, M. Chung, and N. Jeon, "Engineering of functional, perfusable 3d microvascular networks on a chip," *Lab on a Chip*, vol. 13, no. 8, pp. 1489–1500, 2013. cited By 323.

[60] J. Song and L. Munn, "Fluid forces control endothelial sprouting," *Proceedings of the National Academy of Sciences of the United States of America*, vol. 108, no. 37, pp. 15342–15347, 2011. cited By 234.

[61] Y. S. Zhang, A. Arneri, S. Bersini, S.-R. Shin, K. Zhu, Z. Goli-Malekabadi, J. Aleman, C. Colosi, F. Busignani, V. Dell'Erba, C. Bishop, T. Shupe, D. Demarchi, M. Moretti, M. Rasponi, M. R. Dokmeci, A. Atala, and A. Khademhosseini, "Bioprinting 3d microfibrous scaffolds for engineering endothelialized myocardium and heart-on-a-chip," *Biomaterials*, vol. 110, pp. 45 – 59, 2016.

[62] A. Sin, K. Chin, M. Jamil, Y. Kostov, G. Rao, and M. Shuler, "The design and fabrication of three-chamber microscale cell culture analog devices with integrated dissolved oxygen sensors," *Biotechnology Progress*, vol. 20, no. 1, pp. 338–345, 2004. cited By 210.

[63] C. Zhang, Z. Zhao, N. Abdul Rahim, D. Van Noort, and H. Yu, "Towards a human-on-chip: Culturing multiple cell types on a chip with compartmentalized microenvironments," *Lab on a Chip*, vol. 9, no. 22, pp. 3185–3192, 2009. cited By 186.

[64] I. Maschmeyer, A. Lorenz, K. Schimek, T. Hasenberg, A. Ramme, J. Hübner, M. Lindner, C. Drewell, S. Bauer, A. Thomas, N. Sambo, F. Sonntag, R. Lauster, and U. Marx, "A four-organ-chip for interconnected long-term co-culture of human intestine, liver, skin and kidney equivalents," *Lab on a Chip*, vol. 15, no. 12, pp. 2688–2699, 2015. cited By 263.

[65] S. Stott, C.-H. Hsu, D. Tsukrov, M. Yu, D. Miyamoto, B. Waltman, S. Michael Rothenberg, A. Shah, M. Smas, G. Korir, F. Floyd Jr., A. Gilman, J. Lord, D. Winokur, S. Springer, D. Irimia, S. Nagrath, L. Sequist, R. Lee, K. Isselbacher, S. Maheswaran, D. Haber, and M. Toner, "Isolation of circulating tumor cells using a microvortex-generating herringbone-chip," *Proceedings of the National Academy of Sciences of the United States of America*, vol. 107, no. 43, pp. 18392–18397, 2010. cited By 990.

[66] E. Sollier, D. Go, J. Che, D. Gossett, S. O'Byrne, W. Weaver, N. Kummer, M. Rettig, J. Goldman, N. Nickols, S. McCloskey, R. Kulkarni, and D. Di Carlo, "Size-selective collection of circulating tumor cells using vortex technology," *Lab on a Chip*, vol. 14, no. 1, pp. 63–77, 2014. cited By 253.

[67] C. Ericson, J. Holm, T. Ericson, and S. Hjerté, "Electroosmosis- and pressure-driven chromatography in chips using continuous beds," *Analytical Chemistry*, vol. 72, no. 1, pp. 81–87, 2000. cited By 214.

[68] C. L. A. V. C. H. H.-H. L. S. E. A. M. S. T. C. F. J. C. W. A. B. G. A. H. . D. E. I. Kambez H Benam, Remi Villenave, "Small airway-on-a-chip enables analysis of human lung inflammation and drug responses *in vitro*," *Nature Methods*, vol. 13, pp. 151–157, 2016.

[69] Z. Jiao, J. Zhao, Z. Chao, Z. You, and J. Zhao, "An air-chamber-based microfluidic stabilizer for attenuating syringe-pump-induced fluctuations," *Microfluidics and Nanofluidics*, vol. 23, p. 26, Jan 2019.

[70] Elveflow, "Air bubbles and microfluidics: Tips and tricks to remove them." `https://www.elveflow.com/microfluidic-tutorials/microfluidic-reviews-and-tutorials/air-bubbles-and-microfluidics/`.

[71] Y. Wang, D. Lee, L. Zhang, H. Jeon, J. Mendoza-Elias, T. Harvat, S. Hassan, A. Zhou, D. Eddington, and J. Oberholzer, "Systematic prevention of bubble formation and accumulation for long-term culture of pancreatic islet cells in microfluidic device," *Biomedical microdevices*, vol. 14, pp. 419–26, 01 2012.

[72] D. W. Lee, N. Choi, and J. H. Sung, "A microfluidic chip with gravity-induced unidirectional flow for perfusion cell culture," *Biotechnology Progress*, vol. 35, no. 1, p. e2701, 2019.

[73] Elveflow, "How to choose a microfluidic tubing?." `https://www.elveflow.com/microfluidic-tutorials/microfluidic-reviews-and-tutorials/microfluidic-fittings-and-tubing-resources/how-to-choose-a-microfluidic-tubing/`.

[74] A. K. Sen, J. Darabi, and D. R. Knapp, "A fluidic interconnection system for polymer-based microfluidic devices," *Microsystem Technologies*, vol. 16, pp. 617–623, Apr 2010.

[75] D. Sabourin, D. Snakenborg, and M. Dufva, "Interconnection blocks with minimal dead volumes permitting planar interconnection to thin microfluidic devices," *Microfluidics and Nanofluidics*, vol. 9, pp. 87–93, Jul 2010.

[76] T. Jangnoi and U. Pinsopon, "Velocity control of electro-hydraulic pump control system using gear pump," *International Journal of Innovative Computing, Information and Control*, vol. 14, pp. 2307–2323, 12 2018.

[77] Corsolution, "Pneuwave pump." `https://www.mycorsolutions.com/pneuwave.html`.

[78] Corsolution, "Periwave pump." `https://www.mycorsolutions.com/periwave.html`.

[79] C. Watson and S. Senyo, "All-in-one automated microfluidics control system," *HardwareX*, vol. 5, 2019. cited By 1.

[80] B. Li, L. Li, A. Guan, Q. Dong, K. Ruan, R. Hu, and Z. Li, "A smartphone controlled handheld microfluidic liquid handling system," *Lab on a Chip*, vol. 14, no. 20, pp. 4085–4092, 2014. cited By 30.

[81] Y.-D. Ma, K.-H. Li, Y.-H. Chen, Y.-M. Lee, S.-T. Chou, Y.-Y. Lai, P.-C. Huang, H.-P. Ma, and G.-B. Lee, "A sample-to-answer, portable platform for rapid detection of pathogens with a smartphone interface," *Lab Chip*, pp. –, 2019.

[82] Bartels, "Bartels micropump." `https://www.bartels-mikrotechnik.de/index.php/en/products/micropumps`.

[83] Takasago, "Tfs micro needle valve, mnv series," Sep. 2012.

[84] Takasago, "Small syringe pumps sbp series." `https://www.takasago-fluidics.com/p/pump/s/syringe/SBP/`.

[85] Leland, "Mini cartridges." `http://www.lelandgas.com/mini_cartridges.htm`.

[86] Takasago, "Diaphragm isolation valves nv series." `https://www.takasago-fluidics.com/p/valve/s/diaphragm/NV`.

[87] A. Gunda, "A proportionally controlled microvalve using a piezoelectric unimorph microactuator," *Master thesis, TU Delft*, vol. 51, Sep. 2019.

[88] X. Zhu, L. Yi Chu, B.-h. Chueh, M. Shen, B. Hazarika, N. Phadke, and S. Takayama, "Arrays of horizontally-oriented mini-reservoirs generate steady microfluidic flows for continuous perfusion cell culture and gradient generation," *Analyst*, vol. 129, pp. 1026–1031, 2004.

[89] H. Ota, R. Yamamoto, K. Deguchi, Y. Tanaka, Y. Kazoe, Y. Sato, and N. Miki, "Three-dimensional spheroid-forming lab-on-a-chip using micro-rotational flow," *Sensors and Actuators B: Chemical*, vol. 147, no. 1, pp. 359 – 365, 2010.

[90] M.-H. Wu, S.-B. Huang, Z. Cui, Z. Cui, and G.-B. Lee, "A high throughput perfusion-based microbioreactor platform integrated with pneumatic micropumps for three-dimensional cell culture," *Biomedical Microdevices*, vol. 10, pp. 309–319, Apr 2008.

[91] W. Gu, X. Zhu, N. Futai, B. S. Cho, and S. Takayama, "Computerized microfluidic cell culture using elastomeric channels and braille displays," *Proceedings of the National Academy of Sciences*, vol. 101, no. 45, pp. 15861–15866, 2004.

[92] K. Kaarj and Yoon, "Methods of delivering mechanical stimuli to organ-on-a-chip," *Micromachines*, vol. 10, p. 700, 10 2019.

[93] Fluigent, "L-switch™." `https://www.fluigent.com/product/microfluidic-components/l-switch/`.

[94] Bronkhorst, "Instruction manual: mini cori-flow™ m1x series, compact coriolis mass flow, meters/controllers for liquids and gases," Jul. 2018.

[95] Bürkert, *Product Overview: Proportional Valves*. 04 2019.

[96] K. W. Oh, K. Lee, B. Ahn, and E. P. Furlani, "Design of pressure-driven microfluidic networks using electric circuit analogy," *Lab Chip*, vol. 12, pp. 515–545, 2012.

[97] R. Schmidt, *The design of high performance mechatronics*, p. 25. 2nd ed. 2014.

A
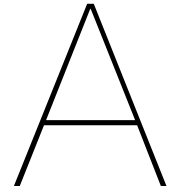
System Integration

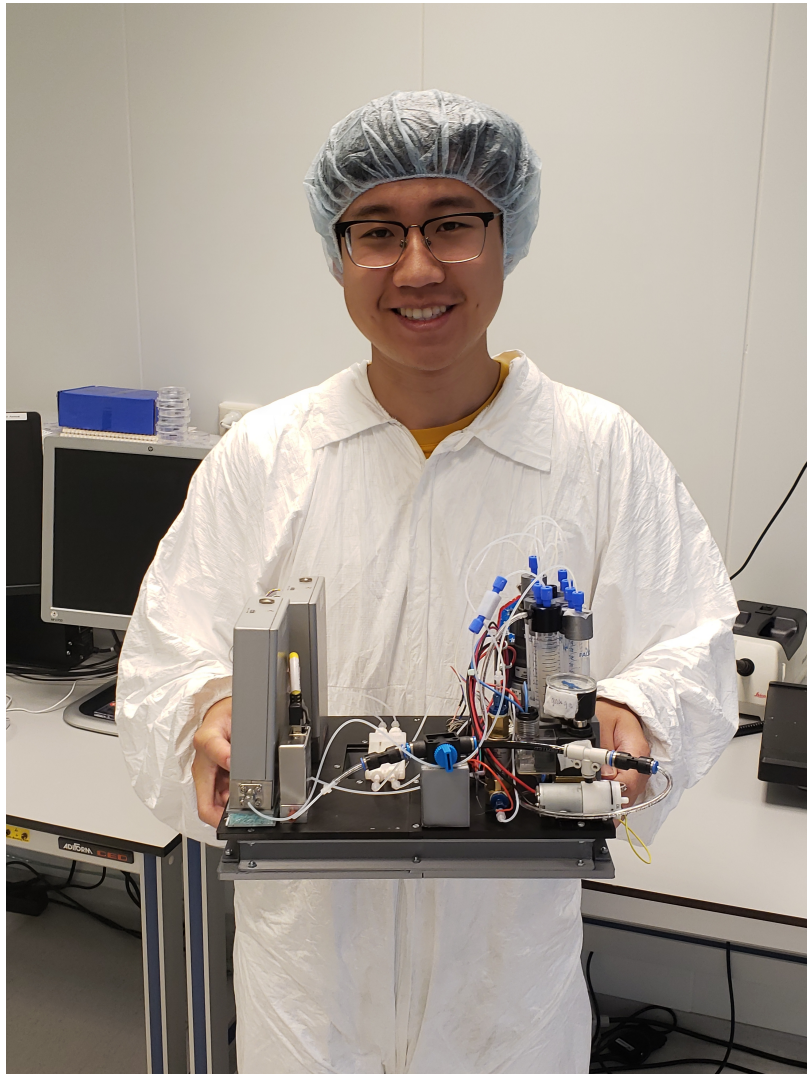## A.1. Author Holding the Portable OOC Platform

Figure A.1: Photo of platform held by the author. The platform is lightweight enough for a person to carry in the lab.

A.2. List of Components

Name	Brand	Model Key	Link of Manual/Website	Page	Unit Price	Total Price	Way of Obtaining
Vacuum Pump	SURGEFLO	-	https://nl.aliexpress.com/item/33006096807.html?spm=a2g0s.9042311.0.0.4e144c4dlqjenH	-	1.39	1.39	Purchase from Aliexpress
Shut-off Valve	-	-	-	-	-	-	Supported by PME Department
Vacuum Gauge	Festo	VAM-63-V1/0-R1/4-EN	https://www.festo.com/us/en/a/download-document/datasheet/537811/	-	26.36	26.36	Supported by PME Department
Manual Valve	Festo	HE-2-QS-6	https://docs.rs-online.com/94e1/0900766b816a12cc.pdf	-	18.34	18.34	Supported by PME Department
Switch Valve	IDEX	MHP7970-500-4	https://www.idex-hs.com/store/pub/media/productattachments/files/downloads/File-1469551785.pdf	-	2075.11	2075.11	Purchase form Inacom
Three-way Valve	SMC	VDW-250-1-G-2-01F-A-Q	https://www.smcworld.com/discon/en/oldpdf/vdw-old-e.pdf	402-406	22.21	22.21	Purchase form RS online
Flow Controller	Bronkhorst	ML120V21-BAD-CC-K-S-DA-A0V	https://www.bronkhorst.com/getmedia/84f1ce1f-9a10-4007-b89d-873031f9ad9f/917097-Manual-mini-CORI-FLOW-ML120.pdf	-	1516.95	3033.9	Supported by Bronkhorst
Pressure Controller	Bronkhorst	IQP-600C-1K5A-AAD-00-V-A	https://www.bronkhorst.com/getmedia/aef32966-8264-45d8-8478-b40df22290ab/917045-Manual-IQ-FLOW.pdf	-	233.3	233.3	Supported by Bronkhorst
						5410.61	

Figure A.2: List of components
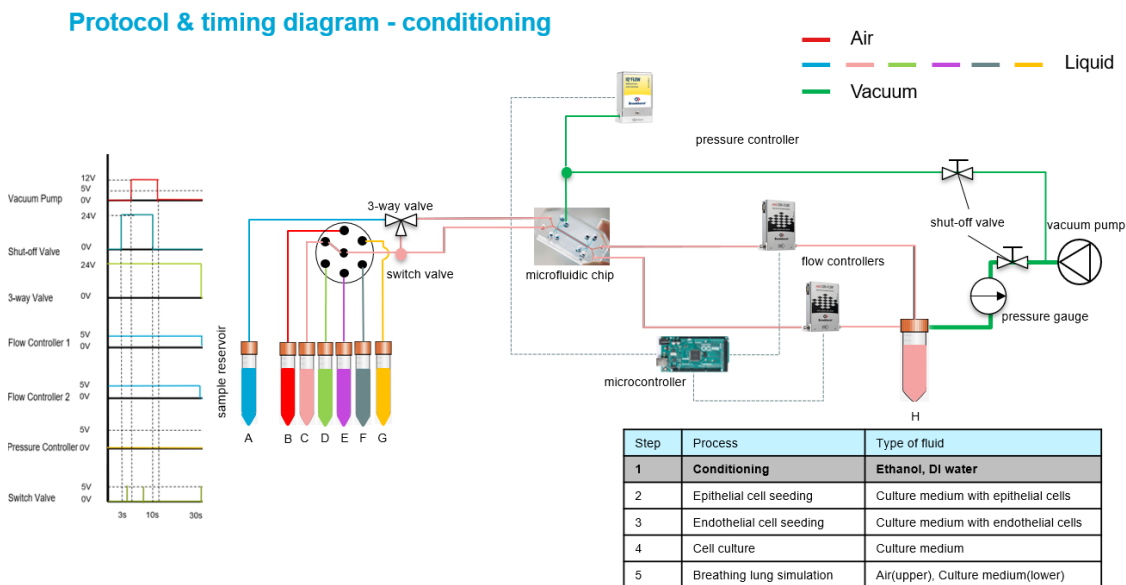
A.3. Protocol with System Schematic

Figure A.3: Protocol of Lung-On-Chip experiments - conditioning process.

Protocol & timing diagram - epithelial cell seeding
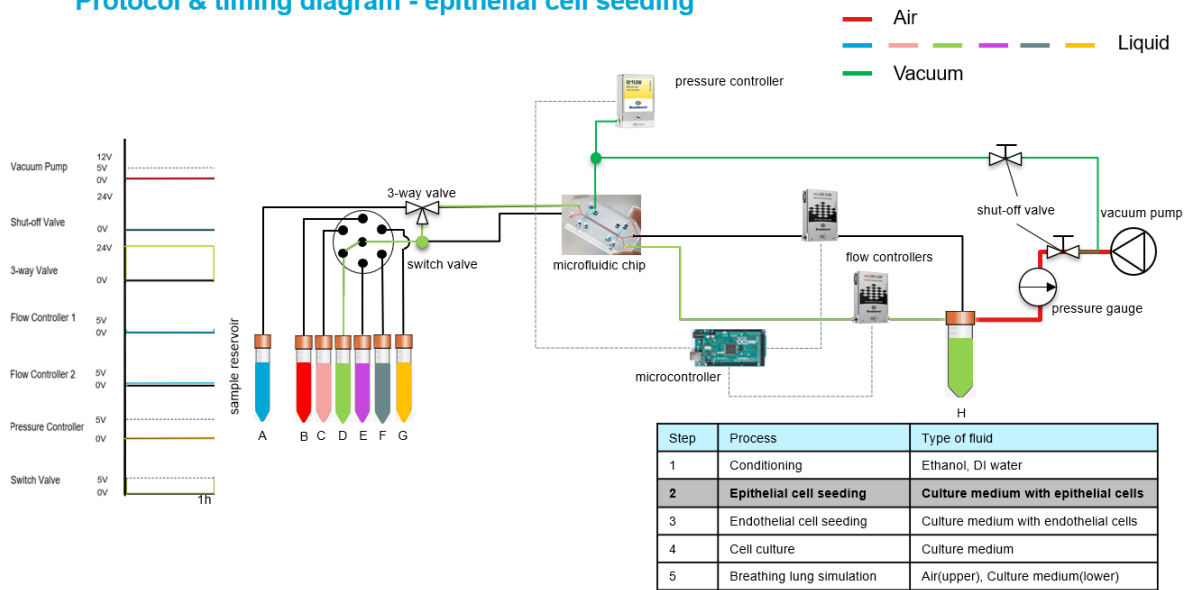
Figure A.4: Protocol of Lung-On-Chip experiments - epithelial cell seeding process.

Step	Process	Type of fluid
1	Conditioning	Ethanol, DI water
2	**Epithelial cell seeding**	**Culture medium with epithelial cells**
3	Endothelial cell seeding	Culture medium with endothelial cells
4	Cell culture	Culture medium
5	Breathing lung simulation	Air(upper), Culture medium(lower)

Protocol & timing diagram - endothelial cell seeding
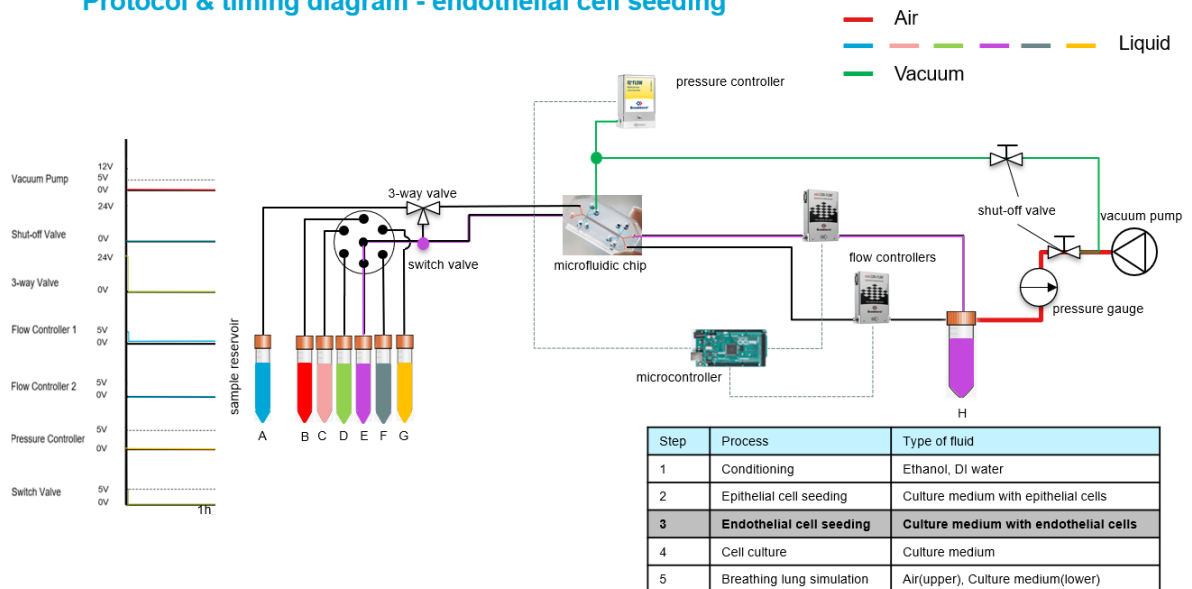
Figure A.5: Protocol of Lung-On-Chip experiments - endothelial cell seeding process.

Step	Process	Type of fluid
1	Conditioning	Ethanol, DI water
2	Epithelial cell seeding	Culture medium with epithelial cells
3	**Endothelial cell seeding**	**Culture medium with endothelial cells**
4	Cell culture	Culture medium
5	Breathing lung simulation	Air(upper), Culture medium(lower)

Protocol & timing diagram – cell culture

Step	Process	Type of fluid
1	Conditioning	Ethanol, DI water
2	Epithelial cell seeding	Culture medium with epithelial cells
3	Endothelial cell seeding	Culture medium with endothelial cells
4	**Cell culture**	**Culture medium**
5	Breathing lung simulation	Air(upper), Culture medium(lower)

Figure A.6: Protocol of Lung-On-Chip experiments - cell culture process.

Protocol & timing diagram – breathing lung simulation

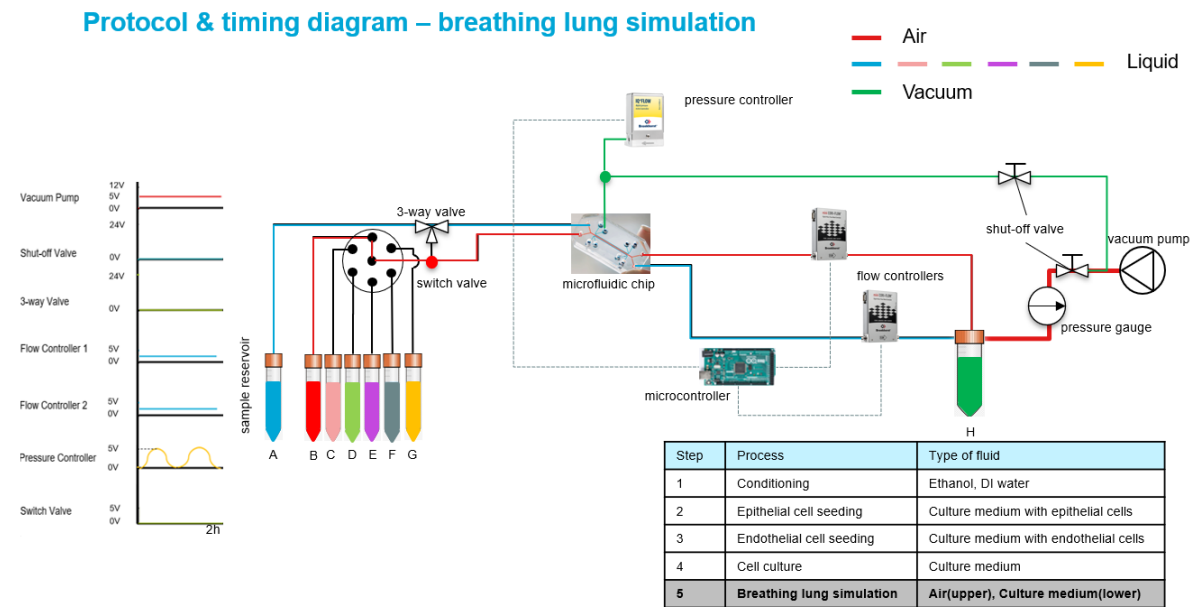| Step	Process	Type of fluid
1	Conditioning	Ethanol, DI water
2	Epithelial cell seeding	Culture medium with epithelial cells
3	Endothelial cell seeding	Culture medium with endothelial cells
4	Cell culture	Culture medium
5	**Breathing lung simulation**	**Air(upper), Culture medium(lower)**

Figure A.7: Protocol of Lung-On-Chip experiments - breathing lung simulation.

A.4. Work required for system upgrade

Number of channels	Has it been realized?	Extra components to be added	Extra work for upgrading
1	Yes	-	-
2	Yes	-	-
3	No	flow controller with vibration isolation plate * 1, source reservoir *1, 32" ID, 16" OD Teflon tubing and connectors	1. Extend the surface of the platform and fix the extra controller. 2. Create an extra electrical interface for the extra controller. 3. Remove the block on the third thread hole of the cap on waste reservoir. 4. Connect tubings and integrate everything.
4	No	flow controller with vibration isolation plate * 2, source reservoir * 2, new cap for waste reservoir with four thread holes * 1, 32" ID, 16" OD Teflon tubing and connectors	1. Extend the surface of the platform and fix the extra controllers. 2. Create extra electrical interfaces for the extra controllers respectively. 3. Replace the original cap with the new cap for waste reservoir. 4. Connect tubings and integrate everything.
…	No	…	…

Figure A.8: Work required for system upgrade. According to the above table, there are several points to be explained. (1) The number of channels can be simply added by adding splitters and extra tubings if no specific flow control for each channel is required. (2) Adding new controllers can control the flow in each channel separately but only one extra controller may make the system not portable anymore. If portability is not necessary, fixing the controller is more convenient and the electrical interface can be created without the connection with the original Arduino and circuit but off-the-shelf connectors. (3) Upgrading the system may take several days if new controllers are connected to the original Arduino and circuit. If not, the procedure may cost less than one day. (4) Ellipsis indicates that more channels can be integrated into the setup, and the steps are similar to those when adding to four channels, but the number of components needs to be increased.

B

System Architecture

B.1. List of Architecture Accessories

Name	Quantity	Parameter	Way of Obtaining
Reservoir	8	10ml	Supported by PME Department
Leak tight cap	1	-	Supported by PME Department
PTFE tubing	-	1/16" X 1/32"	Supported by PME Department
PU tubing	-	4mm X 2.5mm	Supported by PME Department
PU tubing	-	6mm X 4mm	Supported by PME Department
Plastic thread fitting and Ferrule	10	1/4"-28 to 1/16" OD	Supported by PME Department
Plastic fitting	1	1/4"-28 to 2.5mm ID	Supported by PME Department
Metal thread fitting and Ferrule	7	1/4"-28 to 1/16" OD	Purchase from Inacom
Barbed adapter	7	1/4"-28 to 1/16" OD	Supported by PME Department
Syringe needle	4	0.25mm	Supported by PME Department
Screw	34	M3 X 12	Supported by PME Department
Screw	4	M3 X 16	Supported by PME Department
Screw	2	M4 X 12	Supported by PME Department
Screw	4	M5 X 12	Supported by PME Department
Screw	2	UNC 4-40	Purchase from RS online
Nut	38	M3	Supported by PME Department

Figure B.1: List of architecture accessories
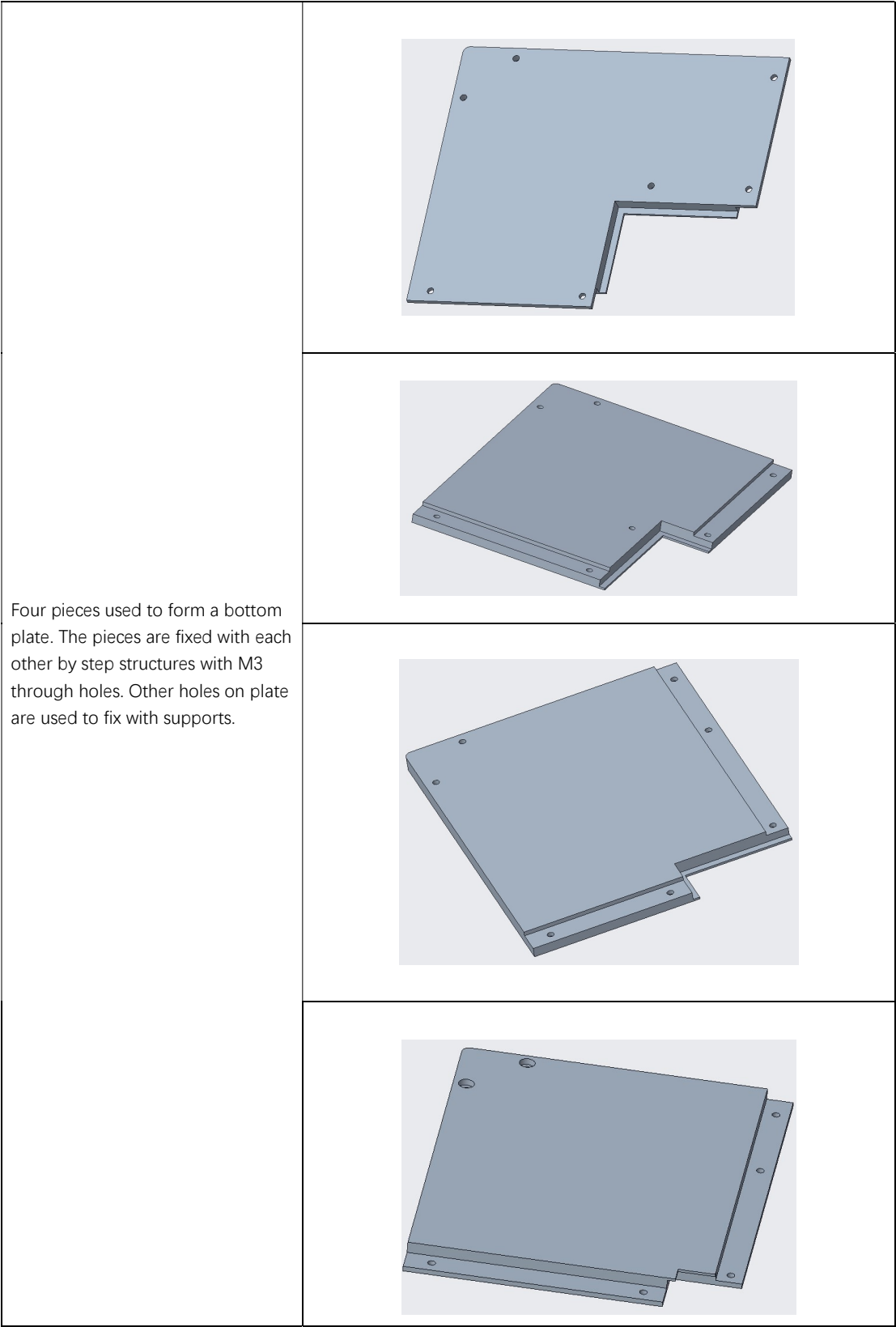
B.2. CAD Model of Platform Components

Four pieces used to form a bottom plate. The pieces are fixed with each other by step structures with M3 through holes. Other holes on plate are used to fix with supports.

Figure B.2: CAD model of components for bottom plate

Four pieces used to form a top plate. The pieces are fixed with each other by step structures with M3 through holes. Other holes on plate are used to fix with supports and other fluidic components such as pumps, vlaves and their frames. The square holes are used to connect fluidic components with electronic interfaces by D-sub, RJ45, Molex 12pin, and general PCB headers.	

Figure B.3: CAD model of components for top plate

Supports used to separate top and bottom plates. The third picture shows the middle support which is also used to form a window for chip accommodation. The square hole in first picture is used to connect Arduino microcontroller to outside laptop and make room for battery connection and its switch. The circle hole is used to accommodate the switch for the entire system.
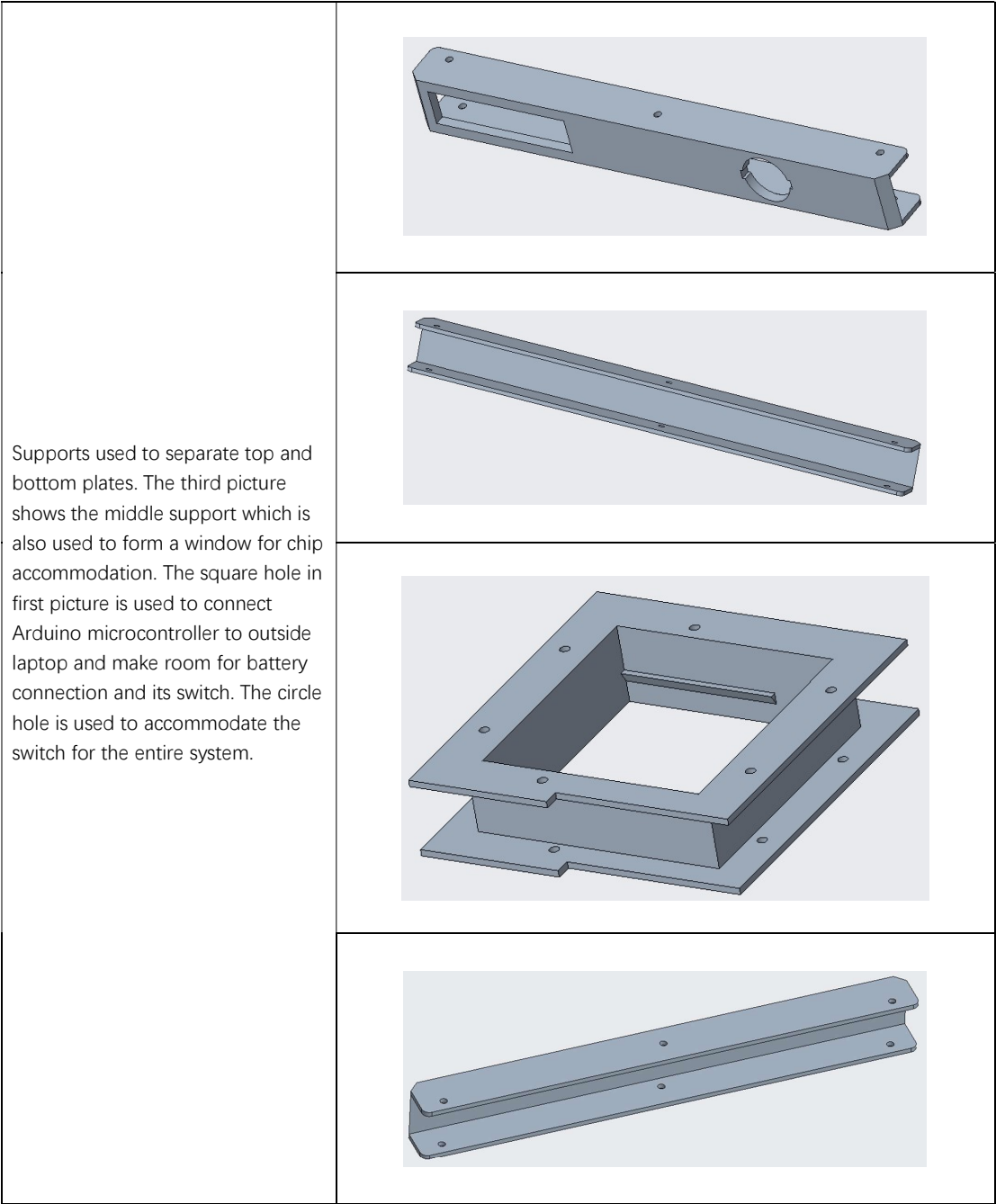

Figure B.4: CAD model of supports in sandwich structure.
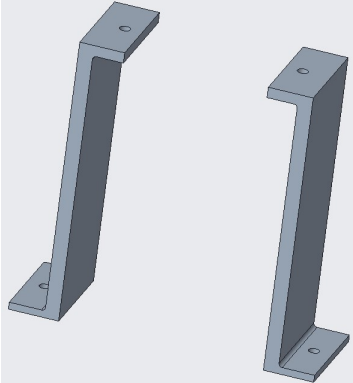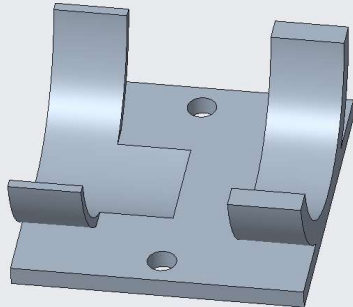
Support frame for fixing the gauge. The curve part is used to fit the splitter connected to gauge and the structure is fixed by double-side tape in curvature.	
The frame used to fix switch valve. The valve is vertically placed and two UNC 4-40 screws are used to fix the switch valve through the holes on top of the frame.	
The frame used to fix vacuum pump. The pump has a cylinder structure thus can be fixed by double-side types in the curvature part. Holes are used to fix the frame on top of the top plate.	
The support used to place the manual valve at higher location to decrease the stress in vacuum tubes. The structure are all connected by double-side types.	
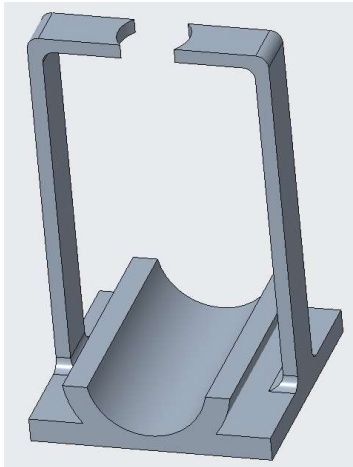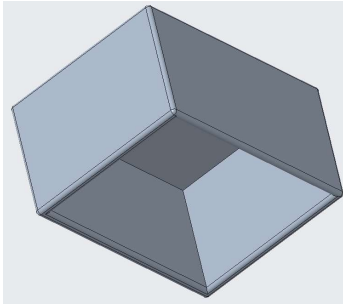
Figure B.5: CAD model of frames to support components on top of the platform.

Electronics Design
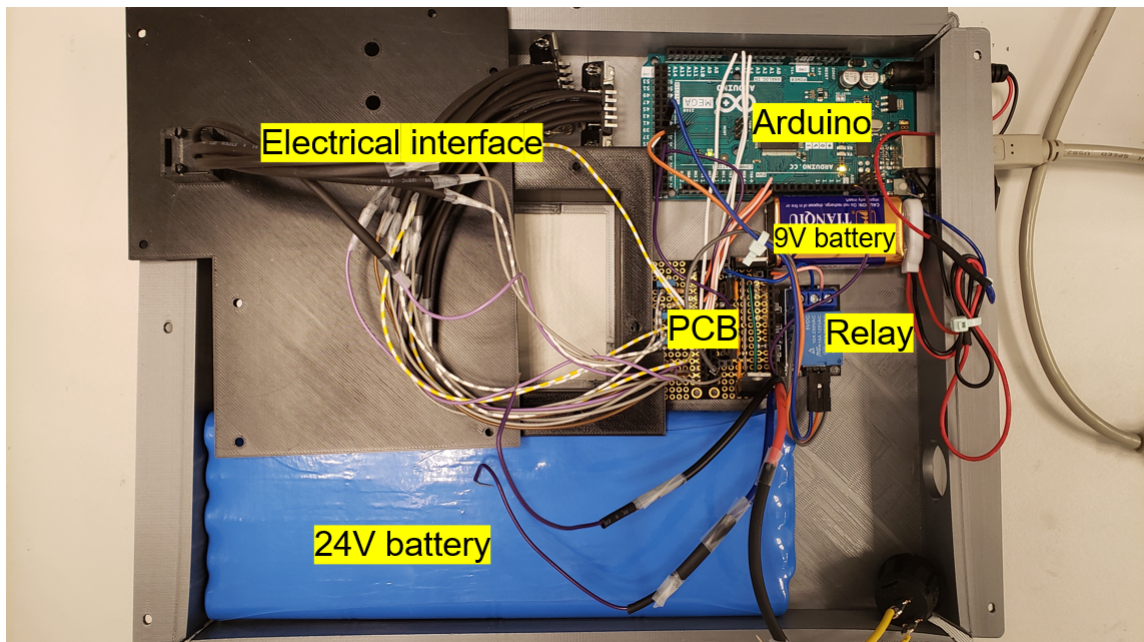
C.1. Photo of Located Electronics

Figure C.1: Photo of electronics placed in the base of platform.

C.2. List of electronics

Name	Brand	Quantity	Link of Manual/Website	Parameter	Unit Price	Total Price	Way of Obtaining
Arduino Mega 2560	Arduino	1	https://docs.rs-online.com/9ab3/0900766b80e8ba22.pdf	-	46.94	46.94	Purchase from RS online
Battery 1	HENSENS	1	https://www.123accu.nl/Soundcast-20S-1P-accu-24V-2000-mAh-123accu-huismerk-i27294.html?mkwid=sGugb8Byg_dc%7Cpcrid%7C171663098801%7Cpkw%7C%7Cpmt%7C%7Cslid%7C%7Cprid%7CASO00611_4894128104582&pgrid=40095430284&ptaid=pla-297471473451&gclid=EAIaIQobChMI9LD_lYKx6QIVlrt3Ch0RTQapEAQYBSABEgKxpPD_BwE	24VDC	47.5	47.5	Purchase from 123accu
Battery 2	TIANQIU	1	https://tianqiu.en.made-in-china.com/product/KvtmsGnHaYkb/China-6f22-9V-Tianqiu-Super-Heavy-Duty-Carbon-Dry-Battery.html	9VDC	1.1	1.1	Purchase from Aliexpress
Cooling fan	ebm-papst	1	https://docs.rs-online.com/d403/0900766b816d6d50.pdf	5V,0.4W	24.9	24.9	Purchase from RS online
Resistor	-	1	-	220Ω	-	-	Supported by PME Department
Resistor	-	2	-	4.7kΩ	-	-	Supported by PME Department
Resistor	-	3	-	8.5kΩ	-	-	Supported by PME Department
Transistor	STMicroelectronics	3	https://docs.rs-online.com/d061/0900766b8135f82f.pdf	80V,3A	2.69	2.69	Purchase from RS online
Voltage regulator	STMicroelectronics	1	https://docs.rs-online.com/9aaa/0900766b814b2420.pdf	12V,1.5A	0.417	0.417	Purchase from RS online
Voltage regulator	STMicroelectronics	1	https://docs.rs-online.com/61d4/0900766b813d3857.pdf	5V,1.5A	0.559	0.559	Purchase from RS online
Capacitor	EPCOS	3	https://nl.rs-online.com/web/p/polyester-film-capacitors/0334221/	100nF	0.15	0.45	Purchase from RS online
General purpose PCB	ADAFRUIT INDUSTRIES	1	https://docs.rs-online.com/82cc/0900766b8153435e.pdf	-	8.05	8.05	Purchase from RS online
Internet cable	Omron	1	https://docs.rs-online.com/504e/0900766b815165a2.pdf	-	11.4	11.4	Purchase from RS online
RJ45 connector	MH Connectors	1	https://docs.rs-online.com/9abe/0900766b813030b5.pdf	-	1.26	1.26	Purchase from RS online
9 pin D sub connector Male	TE Connectivity	2	https://docs.rs-online.com/6181/0900766b804c485c.pdf	-	4.302	4.302	Purchase from RS online
9 pin D sub connector Female	RS PRO	4	https://docs.rs-online.com/20e6/0900766b815860ec.pdf	-	0.929	0.929	Purchase from RS online
SPST Switch	Arcolectric	2	https://docs.rs-online.com/af05/0900766b808a97c8.pdf	-	2.2	2.2	Purchase from RS online
Relay	TONGLING	1	https://www.generationrobots.com/media/JQC-3FF-v1.pdf	5VDC	0.61	0.61	Purchase from Aliexpress
						153.307	

Figure C.2: List of electronics
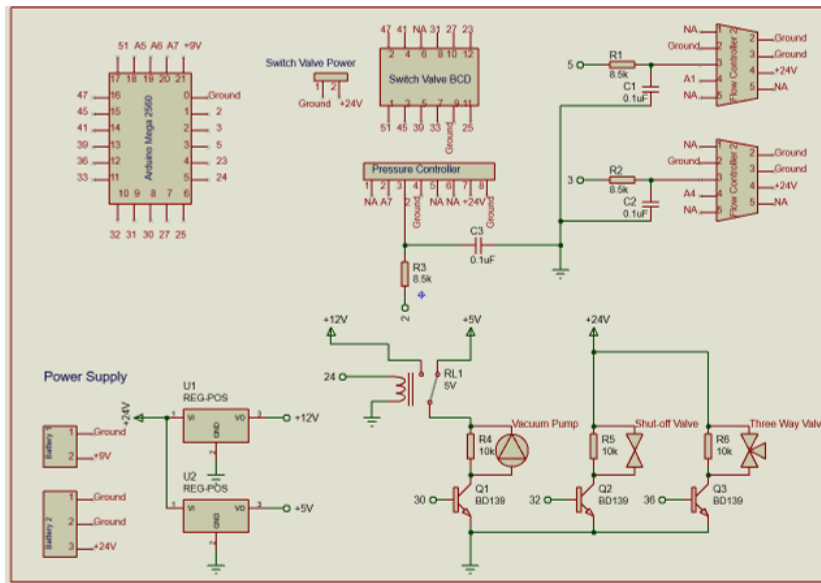
C.3. Schematic Diagram of Electronics

Figure C.3: Schematic diagram of electronics. The power supply are placed at bottom left with two regulators (5 V and 12 V). All transistor controlled devices are placed at bottom right while electronic interfaces with flow controllers, switch valve and pressure controller are at upper right. The Arduino is placed at upper left side. Only the pins in use are indicated in the figure.

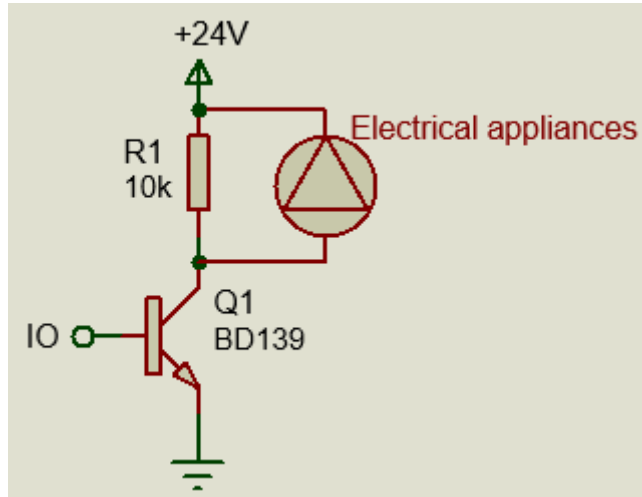# C.4. Self-made Electronic Modules

C.4.1. Transistor switch

Figure C.4: Schematic diagram of transistor switch.

The vacuum pump, shut-off valve and 3-way valve should be controller logically by 3 transistor switches respectively.

Each transistor switch consists of a transistor and a 10 kΩ resistor. The collector of the transistor is connected in series with the resistor and 24V power supply, the emitter is connected to the ground, and the base is connected to the digital output port of Arduino. The electrical appliance is connected parallel to resistor so that the port connected to collector can have selected potential level (0/24V) triggered by IO port from Arduino. While the potential level is 0V, a potential difference appears and starts to power the electrical appliance.
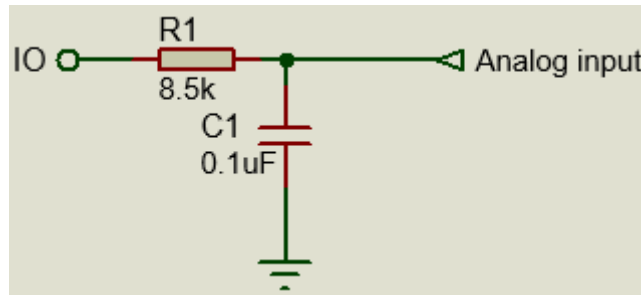
C.4.2. Low-pass filter

Figure C.5: Schematic diagram of low pass filter

The low pass filters are used to transform PWM signal to pure analog signal. Since the PWM signal is a square wave signal consisting of sin wave signals in different frequencies. The principle is to filter out all high-frequency signals and only remain low-frequency signals. Using the resistor with 8.5 kΩ resistance and capacitor with 0.1 μF capacitance, the cut-off frequency can be calculated as follows.

$$\omega_0 = \frac{1}{2\pi RC} = 187.24 Hz$$

In order to get a signal without fluctuations, the frequency of PWM signal should be set to at least 100 times of the cut-off frequency. Thus, the clock in Arduino is programmed to increase to 31 kHz.
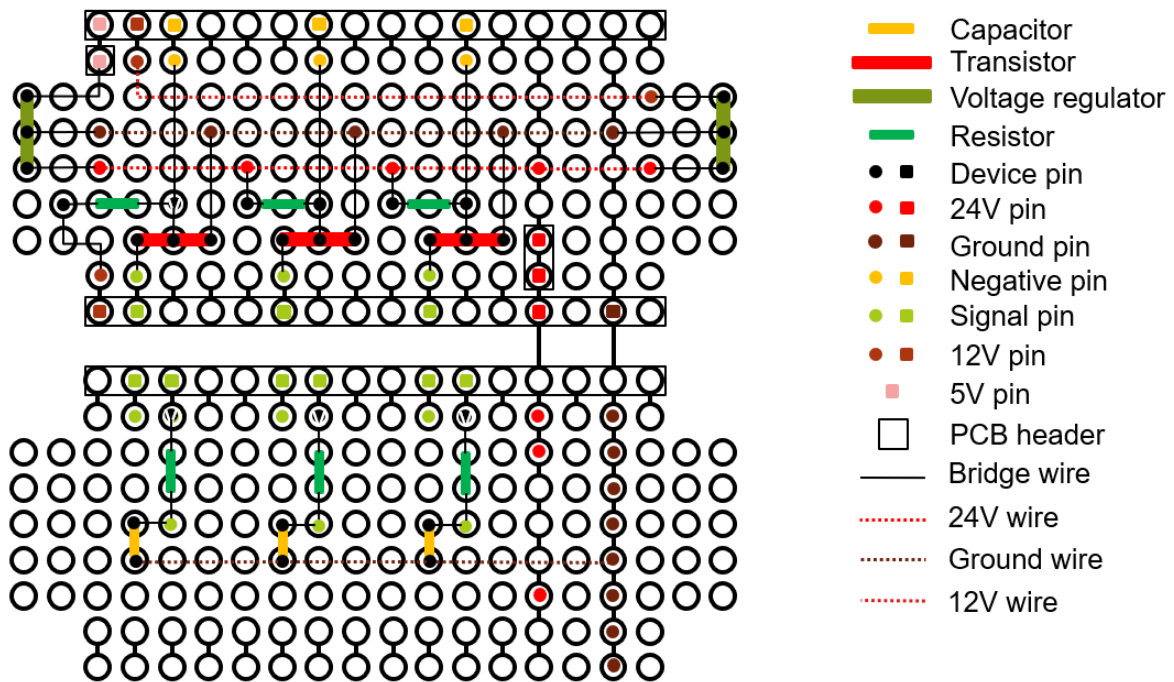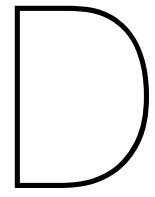
C.5. PCB Layout

Figure C.6: Layout of general purpose PCB. The dash lines represent wires in the back side while other devices are placed at the front side. Most connections are formed by deflecting pins of devices and solder them with pins of other devices, thus no extra wires are used.

D

Arduino Programme

```
#include <SCoop.h> //Multitask function is used in this
program, so the library is necessary.

//The default settings of the program, including setting up 6
tesks, the pin code of switch valves and arduino ports for
transistor switches and controllers. It is not spposed to
change the pin codes in this part.//

//Multi-task setting
defineTask(TaskTest1);
defineTask(TaskTest2);
defineTask(TaskTest3);
defineTask(TaskTest4);
defineTask(TaskTest5);
defineTask(TaskTest6);

//Set pin code of switch valve BCD control, The location of
the pins can be found by a triangle note on interface.//

int Pin1 = 51;
int Pin2 = 47;
int Pin3 = 45;
int Pin4 = 41;
int Pin5 = 39;
int Pin7 = 33;
int Pin8 = 31;
int Pin10 = 27;
int Pin11 = 25;
int Pin12 = 23;

//Default feedback pins of switch valve BCD control. The
first four pins reflects the poistion of motor. Error and
Done pins shows use 0/1 to show if the motion is finished
successfully. If it has rotated successfully, 1 will be shown
on serial chart of Arduino (The last number of 6 numbers in
series).//

int FB_0;
int FB_1;
int FB_2;
int FB_3;
```

```
int Error;
int Done;

//Set pin code of transistor switch. The numbers are the same
number of Arduino IO. All are diginal IO thus can only output
0/5V to turn off/on the transistors.//

int Threeway = 36; //three-way valve
int AV = 32; //shut-off valve
int VP = 30; //vacuum pump
int Relay  = 24; //relay of vacuum pump
int Fan  = 53; //Fan control

//Pin code of setpoint and readout of controllers. The
numbers are the same number of Arduino IO. 'A' means the IO
is analog input which can readout the analog signal from
controller outputs. Digital IO are used as analog output
here. However, the analog output signals are in PWM form thus
need to be filtered to pure analog signal.//

int cori1in = 5; //setpoint of flow controller 1
int cori1out = A1; //readout of flow controller 1
int cori2in = 3; //setpoint of flow controller 2
int cori2out = A4; //readout of flow controller 2
int pressin = 2; //setpoint of pressure controller
int pressout = A7; //readout of flow pressure controller

//Analogwrite setting. They are used as intermediate variable
to show the real value from controllers.//

int val1;
int val2;
int val3;
int Val1;
int Val2;
int Val3;

//Task 1: Switch valve control. Ten pins need to be
```

controlled by diginal IO from Arduino. Among them, Pin1,2,3,4,5,7 send out signals from the valve thus Arduino need to set 'INPUT' function to readout values from them. Pin8,10,11,12 are BCD control pins which need to apply the values from Arduino IO. Thus, Arduino needs to send out signals to these pins in order to control the motor of valve in a digital way. Pin9 is a ground pin thus do not need to be controlled here.//

```
void TaskTest1::setup() //Default setting of BCD control
{
  pinMode(Pin1,INPUT);
  pinMode(Pin2,INPUT);
  pinMode(Pin3,INPUT);
  pinMode(Pin4,INPUT);
  pinMode(Pin5,INPUT);
  pinMode(Pin7,INPUT);
  pinMode(Pin8,OUTPUT);
  pinMode(Pin10,OUTPUT);
  pinMode(Pin11,OUTPUT);
  pinMode(Pin12,OUTPUT);
}
```

//This part is the implementation of switch valve control. It is a loop thus all commands will be Implement every 40ms (default). Since there is a conflict if the feedback is printed as well as the sensed flow rates and pressure from controller, in most cases, the print part will be regarded as comments. BCD control are implemented by Pin8,10,11,12. Pin 12 represents the first digits, 11 is the second, 10 is the third and 8 is the fourth. For example, If 12 is 'HIGH', 11 is 'LOW', 10 is 'HIGH', 8 is 'LOW', the 5th port will be opened up since 1010 is the binary form of 5. Since the valve only has 6 ports, 0110 is the largest binary it can reach.//

```
void TaskTest1::loop() //Switch valve control implementation
{
  FB_0 = digitalRead(Pin1); //Readout feedback control state
  FB_1 = digitalRead(Pin2);
  FB_2 = digitalRead(Pin3);
  FB_3 = digitalRead(Pin4);
```

```
  Error = digitalRead(Pin5);
  Done = digitalRead(Pin7);
  digitalWrite(Pin8,LOW); // Motor control
  digitalWrite(Pin10,HIGH);
  digitalWrite(Pin11,LOW);
  digitalWrite(Pin12,HIGH);
  //Serial.println(FB_0); //Print feedback control state
  //Serial.println(FB_1);
  //Serial.println(FB_2);
  //Serial.println(FB_3);
  //Serial.println(Error);
  //Serial.println(Done);
}
```

//Three transistor switches and one relay is controlled in this section. The transistor can be triggered by digital siganls from Arduino, each of them control vacuum pump(VP), Shut-off valve (AV) and 3-way valve (Threeway) repectively. In the loop part, HIGH means a 5V signal is sent to the transistor thus the component is powered by the outside battery. Otherwise it is turned off. The process starts from up to down in loop part, in each step, a 'sleep' command is used to make a interval between each action. The value behind 'sleep' is in unit of miliseconds thus 'sleep(2000)' means the second action after sleep will be 2 seconds after the previous action.//

```
void TaskTest2::setup() //Default setting of Components control
{
  pinMode(VP,OUTPUT);
  pinMode(AV,OUTPUT);
  pinMode(Threeway,OUTPUT);
  pinMode(Relay,OUTPUT);
}

void TaskTest2::loop() //Control of the pumping and valve system
```

```
{
  digitalWrite(Relay,HIGH); //Connect pump to 12V power
  digitalWrite(Threeway,LOW); //
  sleep(2000);
  digitalWrite(AV,HIGH); //Turn on shut-off valve
  sleep(2000);
  digitalWrite(VP,HIGH); //Turn on vacuum pump
  sleep(5000);
  digitalWrite(AV,LOW); //Turn off shut-off valve
  sleep(1000);
  //digitalWrite(VP,LOW); //Turn off vacuum pump
  digitalWrite(Relay,LOW); //Turn off relay and connect pump
to 5V power
  sleep(5000000);
}
```

```
//Flow controller of flow path 1 is controlled in this
section. Fan is also controlled here by digital IO of
Arduino. The settings of IO1,4,6,7,8,9,10,11,12 are default
settings and should not be modified The clock of Arduino is
modified to form a high-frequency PWM. The setpoint from
Cori1in pin ranges from 17 to 255. 255 means the desired flow
rate in flow path 1 should be the maximum rate while 17
represents the minimum rate in path 1. Please refer to the
paper (Section 3.1.1) and relation diagram for exact value of
different fluids. The way to convert the relation of DI water
to other fluids is: (1)Put desired volumetric flow rate and
density of fluid into equation(3) and get desired mass flow
rate (2)Put the mass flow rate and density of DI water into
equation(3) and get equivalent volumetric flow rate of DI
water. (3)Use the relation diagram (liquid OR gas) to find
the matched applied voltage. (4)Use equation(4) to get the
setpoint that needs to be input into Arduino program, so that
a desired volumetric flow rate of typical fluids can be
reached.//
```

```
void TaskTest3::setup() // Default settings of controller 1
```

```
setpoints
{
   TCCR3B = TCCR3B & 0b11111000 | 0x01; //Clock setting of
Arduino, Increase the frequency of PWM output
   TCCR2B = TCCR3B & 0b11111000 | 0x01;
   TCCR4B = TCCR3B & 0b11111000 | 0x01;
  pinMode(cori1in, OUTPUT);
  pinMode(Fan, OUTPUT);
}

void TaskTest3::loop() // Setpoint input
{
   analogWrite(1,100);
   analogWrite(cori1in,30);
   //sleep(10000);
   //analogWrite(cori1in,200);
   //sleep(10000);
   analogWrite(4,100);
   analogWrite(6,100);
   analogWrite(7,100);
   analogWrite(8,100);
   analogWrite(9,100);
   analogWrite(10,100);
   analogWrite(11,200);
   analogWrite(12,100);
   digitalWrite(Fan,HIGH); //turn on and turn off the cooling
fan
   sleep(5);
}




//This section controls flow controller of flow path 2. The
way to decide the setpoint and program are the same as task3.
//

void TaskTest4::setup() // Default settings of controller 2
setpoints
{
```

```
  TCCR3B = TCCR3B & 0b11111000 | 0x01; //Clock setting of
Arduino, Increase the frequency of PWM output
  TCCR2B = TCCR3B & 0b11111000 | 0x01;
  TCCR4B = TCCR3B & 0b11111000 | 0x01;
  pinMode(cori2in, OUTPUT);
}

void TaskTest4::loop() // Setpoint input
{
   analogWrite(1,100);
 //analogWrite(cori2in,255);
   //sleep(39500);
   analogWrite(cori2in,50);
   //sleep(5000000);
   analogWrite(4,100);
   analogWrite(6,100);
   analogWrite(7,100);
   analogWrite(8,100);
   analogWrite(9,100);
   analogWrite(10,100);
   analogWrite(11,200);
   analogWrite(12,100);
}
```

//Pressure controller is controlled in this section. The
value of setpoint should refer to paper (section 3.1.1) The
controllable range is from 140 to 255. The input shaping can
be added refer to paper (appendix).//

```
void TaskTest5::setup() // Default settings of controller
setpoints
{

}

void TaskTest5::loop() // Setpoint input
{
  //analogWrite(pressin,230);
```

```
  //sleep(10); // Input shaping
  //analogWrite(pressin,255); //The upper bound of step
response
  //sleep(10000);
  analogWrite(pressin,210); //The lower bound of step response
  //sleep(10000);
}
```

//The sensed flow rates and pressure level will be displayed
by this section. The graphs can be shown by clicking 'tools'
- 'serial plot' so that the graphs of all values can be shown
in a same window. According to applications, several plots
can be deleted by changing them into comments.//

```
void TaskTest6::setup() //Default settings controller readout
{
  Serial.begin(9600); //Baud rate. Do not change it only if
necessary.
}

void TaskTest6::loop() //Readout and print of sensed value
{
  val1 = analogRead(cori1out); //Readoout the values from
controllers
  val2 = analogRead(cori2out);
  val3 = analogRead(pressout);
  Val1 = val1;
  Val2 = val2;
  Val3 = 1024 - val3; //To make the plot more intuitive, high
vacuum should be shown with a larger value
  Serial.print("X: "); Serial.print(Val1); Serial.print("  ");
//Plot the value of flow controller 1
  Serial.print("Y: "); Serial.print(Val2); Serial.print("  ");
//Plot the value of flow controller 2
  Serial.print("Z: "); Serial.print(Val3); Serial.print("  ");
//Plot the value of pressure controller
  Serial.println("uT"); //Necessary code to get show all
```

```
plots in a single window
  delay(100); //Sampling interval. This can be changed
according to requirements
}




//Necessary code to implement 'multitask' function. Never
change or delete it.//

void setup() {
  mySCoop.start();
}

void loop()
{
  yield();
}
```

E

Other Tests and Supplement
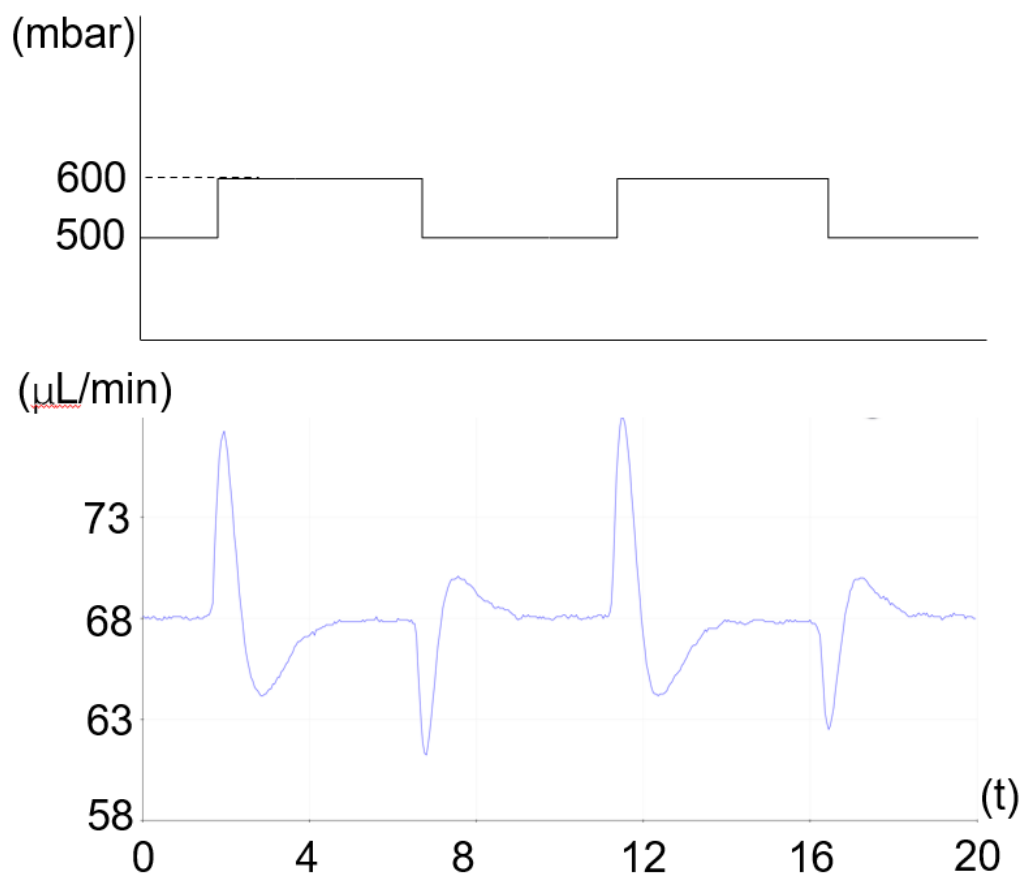
E.1. Robustness Test of Cori-FLOW

Figure E.1: Robustness test of flow controller. DI water was used in this test. The controller was connected to a waste reservoir which was connected to a pressure controller to form changing vacuum inside the waste reservoir. The vacuum was in the form of a square wave form -500 mbar to -600 mbar in a period of 10 s. Thus, the scale value of y-axis in first figure represents the pressure difference. In Figure E.1, upper figure shows the changing vacuum while the lower shows the flow response under a maximum setpoint of flow controller. The figure shows that the controller can maintain a stable flow rate under changing environment, but the settling time is around 3 seconds. Thus, the controller is not fast, but considering the application of flow rate which has suggested sampling interval of 4 seconds, it is still satisfactory.

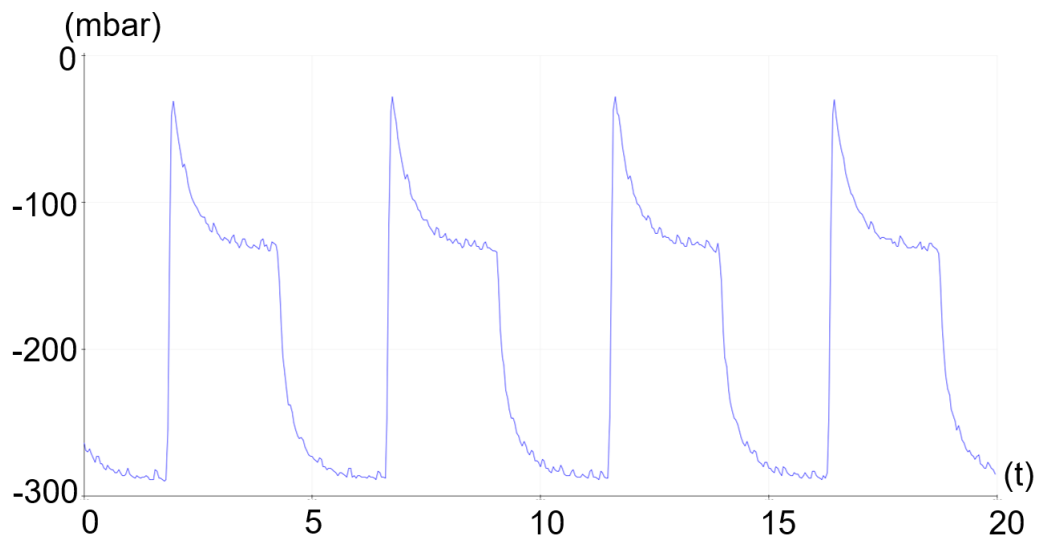## E.2. Cyclic Vacuum Test Without Input Shaping

Figure E.2: Vacuum curve without input shaping. Input shaping can be implemented by adding a 10 ms step at the middle of the upper and lower bound of the setpoint in a step response. This leads to a slower response but without overshoot and a more stable system.

E.3. Photo of Bubble Test

Figure E.3: Photo of bubble test experiment. The Arduino program is on laptop while the screen at upper-left is used to monitor the bubbles in microchannels. The platform is put beside the microscope because the equivalent chip is too bulky to keep sufficient distance for focusing. It will not be a problem in real-chip experiments since real chips are small enough to be put into the window.

F

Videos of Working System

F.1. 360-degree view of the assembled setup

The video shows the entire setup from 360-degree perspective.
https://youtu.be/wKV3z2K3R0Q

F.2. Placing the setup under a microscope

The video shows that the author is placing the setup under the microscope for further tests. There is no conflict between both instruments and the procedure is smooth and easy to be implemented.
https://youtu.be/Hnwtex899xQ

F.3. Microscope compatibility

The video shows how the setup is compatible with the microscope in detail by inserting it onto the plate under the microscope.
https://www.youtube.com/watch?v=qEe9MO0er-k

F.4. Flow actuation

This video shows that the flow can be actuated through the flow path without fluctuation.
https://youtu.be/KyDqRGHJH88

F.5. Flow manipulation

The video below shows that the sample can be input into the system in different flow rates and different samples can be switched automatically. The display on upper-right shows the flow rate of liquids in both channels.
https://youtu.be/qWxZb1IXWQs

F.6. Bubble test

The video shows that there is no bubble formed during the 140s experiments in equivalent chip under microscope. The flow rate shown on upper-right indicates that there is flow inside the channel. In next phase, microbeads can be added into the sample so that flow can be monitored in real-time without the display from controller.
https://youtu.be/tp4KS4O5Rf4